ENHANCING THE BIT ERROR RATE PERFORMANCE OF ULTRA WIDEBAND SYSTEMS USING TIME-HOPPING PULSE POSITION MODULATION IN MULTIPLE ACCESS ENVIRONMENTS

HASAN HATEM HASAN MOSA

PhD. Thesis **2017**

ENHANCING THE BIT ERROR RATE PERFORMANCE OF ULTRA WIDEBAND SYSTEMS USING TIME-HOPPING PULSE POSITION MODULATION IN MULTIPLE ACCESS ENVIRONMENTS

HASAN HATEM HASAN MOSA

School of Computing, Science and Engineering

College of Science and Technology

The University of Salford, Salford, UK

Submitted in Partial Fulfilment of the Requirements of the Degree of Doctor of Philosophy, 2017

TABLE OF CONTENTS

LIST OF ABBREVIATIONS

ADSL	Asymmetric Digital Subscriber Line
ANSI	American National Standards Institute
AWGN	Additive White Gaussian Noise
BER	Bit Error Rate
BPSK	Binary Phase Shift Keying
cdf	cumulative density function
CF	Characteristic Function
CW	Carrier-Wave
DAB	Digital Audio Broadcast
DC	Direct Current
DS/SS	Direct Sequence Spread Spectrum
EIRP	Effective Isotropic Radiated Power
ETSI	European Technical Standards Institute
FCC	Federal Communications Commission
FDD	Frequency Division Duplex
FFT	Fast Fourier Transform
FH/SS	Frequency-Hopping Spread Spectrum
FWA	Fixed Wireless Access
GA	Gaussian Approximation

GPR	Ground Penetration Radar
GPS	Global Positioning System
HF	High-Frequency
IEEE	Institute of Electrical and Electronic Engineers
IF	Intermediate Frequency
IRCC	International Radio Consultative Committee
ISDB	Integrated Services Digital Broadcasting
ISI	Inter Symbol Interference
ISO	International Standards Organisation
ISM	Industrial, Scientific and Medical
ITU	International Telecommunication Union
I-UWB	Impulse - Ultra Wide Band
LANs	Local Area Networks
LMS	Land Mobile Satellite
LOS	Line-Of-Sight
LP-WPAN	Low Power WPAN
MAC	Media Access Control
MAI	Multiple Access Interference
MAN	Metropolitan Area Network
MC-UWB	Multi Carrier-Ultra Wide Band
MED	Maximum Excess Delay

MPCs	Multi-Path components
NB	Narrower Band
NLOS	Non-Line-Of-Sight
NOCs	Network & Optical Communication (research group)
OFDM	Orthogonal Frequency Division Multiplexing
OOK	On-Off Keying
PAM	Pulse Amplitude Modulation
PANs	Personal Area Networks
PCS	Personal Communication Services
pdf	probability density function
PDP	Power-Delay Profiles
PN	Pseudo-random Noise
PPM	Pulse Position Modulation
PRI	Pulse Repetition Interval
PSD	Power spectral density
PTM	Pulse Time Modulation
RF	Radio Frequency
RMS	Root Mean Square
RS	Rician shadowed
RV	Random Variable
SNR	Signal-to-Noise Ratio

TDC	Time Domain Corporation
TH	Time Hopping
TH-PPM	Time Hopping- Pulse Position Modulation
THSS	Time Hopping Spread Spectrum
TM-UWB	Time Modulated- Ultra Wide Band
UHF	Ultra High Frequency
UMTS	Universal Mobile Telecommunication System
UWB	Ultra-Wide Band
VHF	Very High Frequency
WLAN	Wireless Local Area Networks
WPAN	Wireless Personal Area Network

LIST OF SYMBOLS

A_k	Attenuation associated to the k^{th} transmitter.
B	Channel bandwidth.
b_j	Modulation date bit.
C	Channel capacity.
c_j	Pulse shift pattern represents a distinctive time-hopping sequence (Decimal PN code assigned for the j^{th} monocycle).
$c_j^{(k)}$	Decimal PN code assigned for the j^{th} monocycle for the k^{th} user that determines the time hopping sequence.
$d_i^{(k)}$	The i^{th} binary data bit transmitted by the k^{th} source.
E_b	Bit energy.
F	Fourier transform.
f_C	The center frequency.
f_H	The upper frequency of the -10 dB emission point.
f_L	The lower frequency of the -10 dB emission point.
I	The total MAI due to all N_u-1 interfering signals.
N	Noise Power.
N_h	The number of time slots per frame (number of chip "hops" per frame).
N_0	Noise energy.
N_s	Repetition code length (the number of pulses per bit).
N_u	Number of users.

$n_{tot}(t)$	The overall interference and noise.
P_e	Probability of error.
$p(t)$	The UWB pulse shape.
$P_0(t)$	The Gaussian pulse.
$P_G(t)$	Gaussian function.
$P_{G0}(t)$	Zero order Gaussian pulse in time domain.
$P_{Gn}(t)$	*n* order Gaussian pulse in time domain.
$P_n(t)$	The n^{th}-order Gaussian monocycle.
R_b	The bit rate.
$R(x)$	Autocorrelation function.
$R_t(x)$	Cross correlation function.
$R_t(\Theta_{0,j}^{(k)})$	The value of the cross correlation at the time when the first data bit of the k^{th} user is sent, for the j^{th} pulse.
$R_t(\Theta_{1,j}^{(k)})$	The value of the cross correlation at the time when the second data bit of the k^{th} user is sent, for the j^{th} pulse.
$r(t)$	The received signal.
S	Signal power.
$s(t)$	The transmitted signal.
$S^{(k)}(t)$	The transmitted signal of TH-IR system from the k^{th} user.
$s^{(k)}(t,i)$	Typical format of the k^{th} user's transmitted signal conveying the i^{th} data bit.

$SNR_{out}(N_u)$	Average output signal-to-interference-plus-noise ratio of impulse radio for randomly selected time-hopping sequences as a function of the number of users.
T_b	Bit duration.
T_c	Time hopping chip width.
T_f	Frame width.
T_p	Impulse width (pulse length).
$t^{(k)}$	The k^{th} transmitter clock time.
v(t)	Template wave.
α_j	Single correlation process of each pulse.
β_k	Uniformly distributed over $[0, N_s - 1]$.
γ	Correlation receiver decision statistic.
δ	The time shift associated with PPM.
δ_{opt}	The optimum value of δ determined from the autocorrelation properties of the Gaussian pulses.
$\delta_D(.)$	The Dirac delta function which decides the clock timing of the pulses.
ε_n	Energy normalisation factor assigned for the Gaussian pulses.
η	The fractional bandwidth.
Λ	Total noise-interference parameter.
σ^2	Variance of the Gaussian distribution.

σ_{rec}^2	Variance of the receiver noise component at the pulse train integrator output.
τ_k	Time delay shifts associated to propagation and synchronism between the number of users clocks of the transmitted signals.
τ_p	Time normalisation factor or (impulse width parameter) to make $P_n(t)$ independent of a specific impulse duration.
$\Phi_{X^{(k)}\|\alpha,\beta}(\omega)$	The characteristic function of $X^{(k)}$ condition on α_k and β_k.
$\Phi_{Y^{(k)}\|\alpha,\beta}(\omega)$	The characteristic function of $Y^{(k)}$ condition on α_k and β_k.
$\Phi_{I^{(k)}\|\alpha}(\omega)$	The characteristic function of $I^{(k)}$ condition on α_k.
$\Phi_I(\omega)$	The characteristic function of the total interference.
$\Phi_n(\omega)$	The characteristic function of the noise term n.
$\Phi_\Lambda(\omega)$	The characteristic function of the total interference parameter.
ω	Angular frequency.

LIST OF FIGURES

LIST OF TABLES

ACKNOWLEDGEMENTS

The author would like to express his special thanks to **Dr. Martin Hope** for his supervision, help and enthusiasm over the past four years. I also would like to thank my parents, my wife, my sons, my brothers and sisters for their support and encouragement. Last, but not least, to the School of Computer Science and Engineering, University of Salford for the use of their facilities.

DEDICATION

I would like to dedicate this work to the soul of my father **Prof. Dr. HATEM BAKKAR** who opened the way for me to complete my studies until I reached this stage.

ABSTRACT

Ultra-Wide Band (UWB) technology is one of the possible solutions for future short-range indoor data communication with uniquely attractive features inviting major advances in wireless communications, networking, radar, imaging, and positioning systems.

A major challenge when designing UWB systems is choosing a suitable modulation technique. Data rate, transceiver complexity, and BER performance of the transmitted signal are all related to the employed modulation scheme. Several classical modulation schemes can be used to create UWB signals, some are more efficient than others. These schemes are namely, Pulse Position Modulation (PPM), Pulse Amplitude Modulation (PAM), Binary Phase Shift Keying (BPSK), and On-Off Keying (OOK) are reviewed.

In the thesis, the performance of PPM system, combined with Time Hopping Spread Spectrum (THSS) multiple access technique is evaluated in an asynchronous multiple access free space environment. The multiple access interference is first assumed to be a zero mean Gaussian random process to simulate the scenario of a multi user environment. An exact BER calculation is then evaluated based on the characteristic function (CF) method, for Time Hopping-Pulse Position Modulation Ultra Wide Band (TH-PPM UWB) systems with multiple access interference (MAI) in AWGN environment. The resulting analytical expression is then used to assess the accuracy of the MAI Gaussian Approximation (GA) first assumed. The GA is shown to be inaccurate for predicting BERs for medium and large signal-to-noise ratio (SNR) values.

Furthermore, the analysis of TH-PPM system is further extended to evaluate the influence of changing and optimising some of the system or signal parameters. It can be shown how the system is greatly sensitive to variations in some signal parameters, like the pulse shape, the time-shift parameter associated with PPM, and the pulse length. In addition, the system performance can be greatly improved by optimising other system parameters like the number of pulses per bit, Ns, and the number of time slots per frame, N_h. All these evaluation are addressed through numerical examples. Then, we can say that, by improving signal or system parameters, the BER performance of the system is greatly enhanced. This is achieved without imposing exact complexity to the transceiver and with moderate computational calculations.

CHAPTER 1

1 INTRODUCTION

1.1 Overview

High data rate wireless communication has been one of the major drivers in the development of communications in last 20 years. The great popularity of cellular phones, radio paging, mobile computing devices and other Personal Communication Services (PCS) demonstrates the rising demand for high speed data communication [1]. Rapid growth in mobile computing and other wireless data services are stimulating many proposals for high-speed data services up to 2 Mb/s for diversified applications. In addition to mobile applications, Fixed Wireless Access (FWA) technologies bring high quality telephony, internet access, and multimedia service to the home over wireless links. Research challenges for high data rate wireless communications include the development of efficient coding and modulation schemes, smart signal processing techniques to improve the quality of service, enhanced spectral efficiency of the wireless system, and better techniques for sharing the limited spectrum among different high capacity users [1]. Remarkable technologies have been proposed to deal with these challenges, such as multiple antenna system, space time processing, Orthogonal Frequency Division Multiplexing (OFDM), UWB radio systems, beam forming, and so on. UWB technology is defined as any wireless transmission scheme that occupies a bandwidth of more than 25% of a centre frequency, or more than 500 MHz. During the last decade UWB has been one of the most researched wireless communication technologies. This is mainly due to some of its unique properties such as high data rate, robustness to multipath fading, low power requirements, low implementation costs, and simple design [2]. UWB is a viable candidate for short range communications in dense multipath environments, especially indoor wireless and home entertainment systems.

The basic concept of UWB is to transmit and receive an extremely short duration radio frequency (RF) energy pulses over a very wide range of frequencies. This is in contrast to the conventional bandpass (or “narrowband”) systems such as global system for mobile

(GSM), 3G mobile networks, IEEE 802.11 and so on. It allows coexistence with already licensed operators in the radio spectrum. The rapidly growing wireless technology industry is leading to introduction of always-on wireless systems for both domestic and commercial use. The main objective the fourth-generation (4G) wireless technologies aim to achieve is the facilitation of these ubiquitous wireless systems globally. The wireless personal area networks (WPAN), wireless local area networks (WLAN), cellular, WiMAX, and satellite systems and other systems will be transformed into 4G technologies [3]. In addition, UWB has other useful characteristics such as low fading, the ability to carry signals through obstacles, carrier-free modulation, and low-cost implementation. These characteristics, therefore, give this technology the potential to be utilised for high speed, short-range indoor wireless communications, such as WLANs [4]. Unlike conventional communication systems, UWB systems operate at baseband, and thus involve no intermediate frequency (IF) stages and no carrier synchronisation. It theoretically promises a very high data rate by employing a large signal bandwidth. As the capacity of the channel is directly related to its bandwidth, UWB technologies are advantageous for use in a number of wireless applications, especially in short range and high bit rate networking.

UWB is not only confined to potential applications. The potential classes of UWB devices, as indicated by the FCC, are many [5], ranging from imaging systems (ground penetrating radar, wall-imaging systems, medical systems, and surveillance systems) to vehicular radar systems, communication and measurement systems. They all have spectrum efficiency potential in common. With the FCC acceptance for the operation of UWB, the development of UWB technology for application in communication systems has been greatly accelerated.

Several classical modulation schemes have been originally proposed to create a UWB signal, some are more efficient than others. These schemes are binary phase shift keying (BPSK), on-off Keying (OOK), N-ary pulse position modulation (N-PPM), and M-ary pulse amplitude modulation (M-PAM). A major challenge when designing UWB systems is choosing the right modulation type. Data rate, transceiver complexity, bit error rate (BER) performance, and spectral characteristics of the transmitted signal are all related to the employed modulation scheme. Determining the right modulation scheme for the right application is thus essential. The desired modulation technique needs to provide the best

error performance for a given energy per bit. The function of the transceiver is to extract the information bit sequence, modulated on the pulse train, from the desired and corrupted receiving waveforms with a high accuracy. Having generated a signal with minimal spectral features, it is also necessary to have an optimal receiving system. The optimal receive technique is a correlation receiver "correlator". A correlator multiplies the received RF signal with a "template" waveform and then integrates the output of that process to yield a single DC voltage upon which it decides whether the received bit is logic "1" or logic "0".

1.2 The Main Research Question

The research presented in this thesis answer this question:

- How can a modified analytic analysis of an UWB TH-PPM system provide an optimised selection of system parameters that enhances the BERs of the overall system?

1.3 Research Aim and Objectives

Ultra-Wide Band (UWB) technology is one of the possible solutions for future short-range indoor data communication with uniquely attractive features inviting major advances in wireless communications, networking, radar, imaging, and positioning systems. The Federal Communications Commission (FCC) has allocated 7, 500 MHz of spectrum for unlicensed use of ultra-wideband devices (UWB) in the 3.1 to 10.6 GHz frequency band to transmit low-powered (below - 41.3 dBm/MHz), ultra-short radio pulses (commonly monocycle pulses from 0.2 to 1.5 nanoseconds) through the air, and is capable of transmitting data at several hundred Mb/s (above 110 Mb/s) typically over short distances (10 meter) under restricted power. These systems are therefore considered suitable for high-data-rate applications, such as Wireless Local Area Networks (WLAN), streaming media, and for use in battery-powered wireless data devices [6].

Ultra-short impulses spreading the energy of the signal typically from near Direct Current (DC) to some GHz are used to transmit information in an Ultra-Wide Band (UWB) [5] communication system. UWB systems are different from the traditional communication systems, as they operate at baseband, and no intermediate frequency and no carrier

synchronisation is required. UWB has the potential to offer a very high data rate as it uses a large signal bandwidth. However, there are certain power spectrum density disadvantages including Federal Communications Commission (FCC) part 15, which would limit the capability of the system [7], [5].

Table 1-1 shows various wireless standards and approximate specifications.

Technology	Data Rate	Range	Power	Spectrum
UWB	110-480 Mb/s	10 meter	Low	7.5 GHz
Bluetooth	1 Mb/s	10 meter	Low	2.4 GHz
802.11a	54 Mb/s	100 meter	High	5.0 GHz
802.11b	11 Mb/s	100 meter	Medium	2.4 GHz
802.11ac	1300 Mb/s	100 meter	High	5 GHz
802.11n	300 Mb/s	100 meter	High	2.4- 5 GHz
Hyper LAN	25 Mb/s	30 meter	High	2.4 GHz
Home RF	11 Mb/s	45 meter	Medium	2.4 GHz

Table 1-1 short-Range wireless Properties [8]

In particular, UWB systems under FCC part 15 rules provide reliable communications only over small to medium distances. Typically Pulse Position Modulation (PPM), Pulse Amplitude Modulation (PAM), Binary Phase Shift Keying (BPSK) or On-Off Keying (OOK) modulations are employed for UWB system. PPM modulation uses the precise collocation of the impulses in time to convey information and BPSK uses the phase modulate them, while PAM and OOK use amplitude for this purpose.

With the application of different classical modulation techniques proposed for UWB, previously mentioned, a variety of different spreading approaches are examined for UWB communications, including time hopping (TH), direct sequence (DS). Several papers on these subjects can be found in literature [9-21] . Most of them focus on particular pulse lengths, modulation schemes, or spreading techniques to evaluate the performance of UWB systems, giving a limited overview of the possible sensitivity of the performance of UWB systems to various system and signal parameters.

The potential classes of UWB devices, as indicated by the FCC, are many [5], ranging from imaging systems (ground penetrating radar, wall-imaging systems, medical systems, and surveillance systems) to vehicular radar systems, communication and measurement systems. They all have spectrum efficiency potential in common. With the FCC acceptance for the operation of UWB, the development of UWB technology for application in communication systems has been greatly accelerated. UWB technology is likely to fill the void left by the existing standards like Bluetooth and IEEE 802.11/a/b/g standardisation.

Choice of the right modulation type is critical to develop a functional UWB system design. Rate of data transfer, transceiver complexity, BER performance and transmitted signal's spectral characteristics are some of the factors that depend on the selected modulation scheme. Therefore, not choosing the right modulation scheme for the right application can cause a lot of problems. The generic conditions are a common limitation among various UWB modulation alternatives investigated in the past. The error performance for a given energy per bit should give best results in a desired modulation technique. The desired modulation technique needs to provide the best error performance for a given energy per bit. The function of the transceiver is to extract the information bit sequence, modulated on the pulse train, from the desired and corrupted receiving waveforms with a high accuracy. Having generated a signal with minimal spectral features, it is also necessary to have an optimal receiving system. The optimal receive technique is a correlation receiver "correlator". For the extraction of the information bit sequence modulated on the monocycle train from the distorted and corrupted receiving waveforms with a high accuracy, a receiver is used. After generation of a signal with minimal spectral features, having an optimal receiving system is also essential. The optimal receive technique, and the technique used in Time Modulation- Ultra wide band TM-UWB is known as correlation receiver sometimes also referred to as, the correlator [22]. The received RF signal is multiplied with a "template" waveform and then the output of that process is integrated to yield a single DC voltage in a correlator; this integration helps the system decide whether the received bit is logic "1" or logic "0". The direct conversion (also referred to as homodyne or zero-IF) architecture is more common in UWB receivers in comparison to a heterodyne (or super-heterodyne) receiver. In the UWB direct conversion receiver the multiple RF and IF stages, local oscillators and mixers can be skipped. There is no need for the synchronisation of a carrier.

This thesis aims to study the impact of changing the system and signal parameters on the performance of PPM systems combined with time hopping, as a spreading approach, operating in asynchronous multiple access environments. The analytical method used for calculating the average probability of error shows the sensitivity of TH-PPM UWB systems to various parameters affecting the operation of the system, such as the pulse width, the time-shift parameter, and the repetition code. The exact expression of the average BER for TH-PPM system is also showed in an additive white Gaussian noise (AWGN) environment based on the characteristic function (CF) technique [15] and [19]. The AWGN channel model is important in its own right for some UWB applications in order to estimate and generalise performance on UWB channel [23], and is a necessary intermediate step for future work examining UWB on fading channel models [15] and [19].

In addition, the exact analytical results are also used to assess the Gaussian approximation (GA) model used to simulate the multiple access interference (MAI) in a multi user environment. Unfortunately, the GA is shown to significantly underestimate the BER for TH-PPM systems, rendering the results of [14] less useful. And, the analytical results and comparisons provide important and valuable criteria for choosing appropriate multiple access model, signal, and system parameters in practical applications. In addition, the exact results, based on the precise analysis, can also be used to evaluate the performances of different UWB modulation schemes in the general case for certain specific applications.

The main objective of this research:

1. To study the impact of changing the system and signal parameters like the pulse shape, the time-shift parameter associated with PPM, the pulse length, the number of pulses per bit, *Ns*, and the number of time slots per frame, N_h, on the performance of PPM systems combined with time hopping, as a spreading approach, operating in an asynchronous multiple access environments, in order to optimise system performance.

2. Extraction a new expression based on the CF to get the exact expression of the average BER for TH-PPM system.

3. Examine the Gaussian approximation (GA) model used to simulate the multiple access interference (MAI) in a multi user environment by comparing with the exact analytical.

4. Analysis and evaluation of the TH-PPM UWB system.

1.4 Contribution of Knowledge

The research presented in this Thesis has made a contribution to knowledge in the field of UWB TH-PPM by presenting an optimised analysis of system parameters that enhance the BER of the overall system.

1.5 Research Methodology

The following steps will be used to develop and implement the research program:

Stage 1 : Reviewing previous work and relevant literature.

This stage reviews existing literature and highlights any problems that can be anticipated.

Stage 2 : Identification, Studying and analysing the research problem.

The stage starts by identifying the UWB, UWB Signal Definition, UWB Modulation Technique, and the problems related to the functionality required to meet the objectives of the project.

Stage 3 : Study the structure of TH-PPM System Multiple Access Interference.

This stage consists of studying the Time Hopping-PPM system in a multiple access environment.

Stage 4 : The numerical analysis of TH-PPM.

In this stage we will extraction a new expression to get the exact expression of the average BER for TH-PPM system in the presence of multiple-access interference (MAI) on additive white Gaussian noise (AWGN) channels, based on the analytical study in [20]. It is called the characteristic function (CF) technique. This mathematical process will extract

an exact BER calculation, which is used to evaluate the TH-PPM UWB systems with multiple access interference (MAI) in AWGN environment. Furthermore, the analysis of TH-PPM system will be further extended to evaluate the influence of changing and optimising some of system or signal parameters. To know how the system will be sensitive to variations in signal parameters, such as the pulse shape, the time-shift parameter associated with PPM, and the pulse length.

Stage 5 : Software implementation / testing.

This stage will consists of simulation Analysis using Matlab to examine the performance of the TH-PPM system.

Stage 6 : Analysis and evaluation.

In this stage we will be comparing the results came from the Gaussian approximation (GA) model and exact model to get a clear view of this system. Results from the software implementation will be recorded and analysed. These will be critically evaluated to determine if further modification is necessary and if required Stage 4 will redesign it, until the results meet the objective of the research.

Stage 7 : Modification / improve performance.

This stage will be care the system by modifying it to get the best performance for this mathematical method which is mentioned in stage 4.

Stage 8 : The final step is to complete write the PhD thesis.

All steps of the research methodology are as outlined in Figure 1-1.

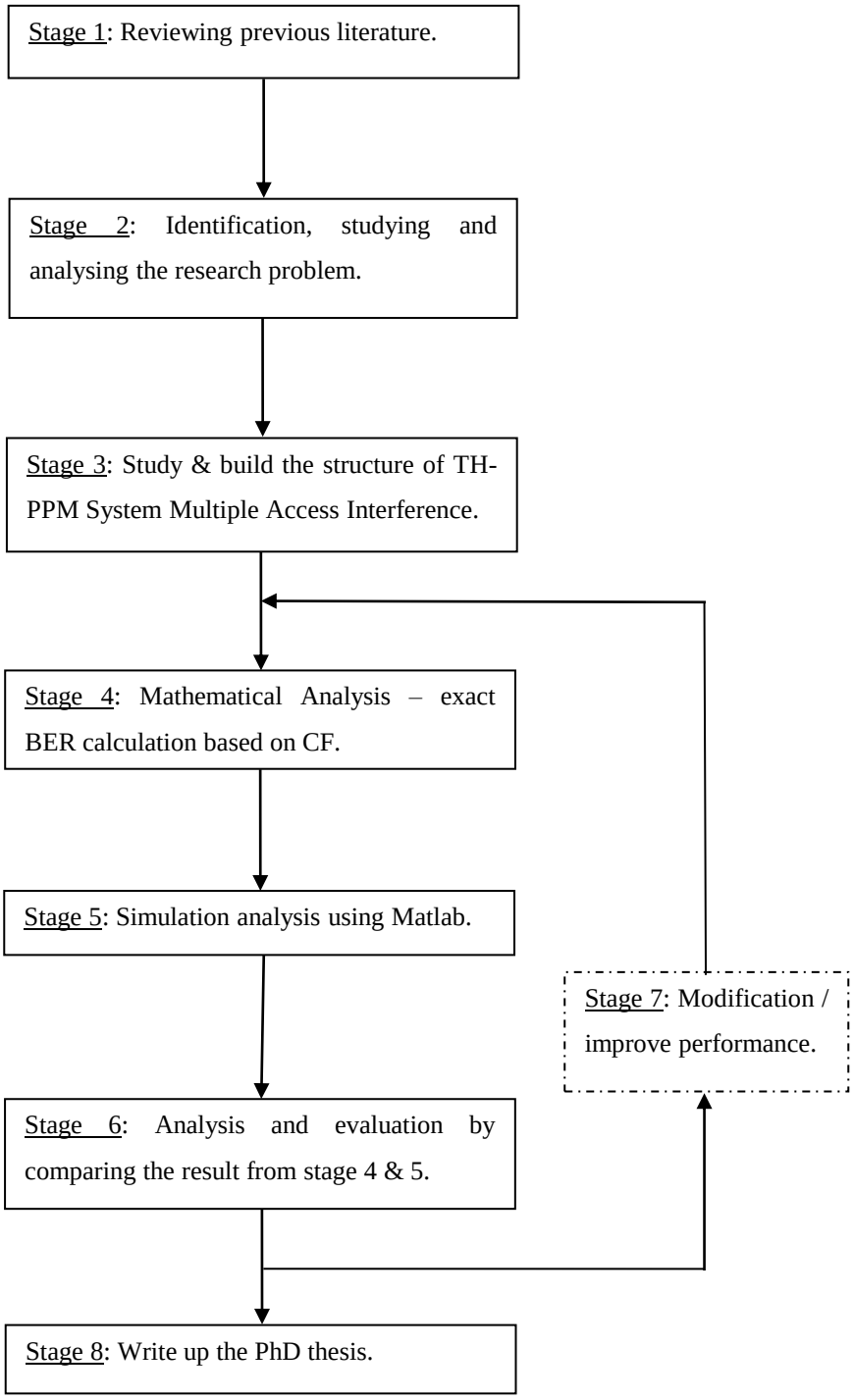

Figure 1-1 Research Methodology

1.6 Thesis Structure

This thesis is organised to cover the different aspects of an indoor localising system using Ultra Wide-Band technology.

Chapter (1): Introduction and Motivation: it reviews the necessary background on UWB systems.

Chapter (2): Background and Literature Review: this chapter reviews UWB system, specifically its definition, advantages, applications and the regulatory issues of UWB system. It also describes the pulse generation in time and frequency domains.

Chapter (3): UWB Modulation Techniques and UWB Waveform: this chapter reviews UWB modulation schemes such as PPM, PAM, BPSK and OOK will mainly discuss in Time Hopping Spread Spectrum format. It also reviews the UWB waveform symbol representation in Time Domain.

Chapter (4): The Mathematical Models for a Synchronous Multiple Access TH-PPM UWB Systems: shows the basic analytical evaluation models of BERs of TH-PPM systems operating in asynchronous free space multiple access environments.

Chapter (5): Results and Discussion: this chapter will review the obtained results and the corresponding discussions.

Chapter (6): Conclusion: Finally, the conclusion of the present work and suggestions for future work will be mention in this chapter.

At the end, a list of the "110" up-to-date references used in this thesis, are presented.

CHAPTER 2

2 Background and Literature Review

2.1 UWB System

Any wireless transmission scheme occupying a bandwidth greater than 25% of a centre frequency, or more than 1.5 GHz is known as Ultra-wideband (UWB) technology. UWB is a practical candidate for short-range communications in dense multipath environments because of its distinctive properties of high data rate, robustness to multipath fading, low power requirement, low implementation cost, and simple design, making it suitable for indoor wireless and home entertainment uses. UWB technology has been under development since the nineteen eighties, but was used in military applications for radar applications and secure communications only. The Federal Communications Commission (FCC) report for the use of UWB sped up the growth of UWB technology for application in communication systems [5]. UWB technology thought to outperform standard systems such as Bluetooth and IEEE 802.11/a/b/g standardisation. Certain limitations in making UWB technology perform to its full potential still exist and there is need to resolve them. For the analysis of the system performance and for optimisation of the physical layer design a reliable channel model must be in place. For the improvements in the robustness and long term viability of UWB technology , the modulation technique play an important role in the UWB system designs including the transceiver designs [24].

2.2 UWB Early Motivation and History

The origin of Ultra wideband emissions can be dated back to spark gap "impulse" transmissions of Marconi over a century ago. Guillermo Marconi demonstrated the first wireless system in 1897, which, according to the standards,was also an UWB radio, as it occupied a large portion of spectrum, from very low frequencies up through the High-Frequency (HF) band and beyond, using manual time domain Morse code processing. In 1901 the first of its kind over-the-horizon wireless transmission from the Isle of Wight to Cornwall was sent by Guglielmo Marconi on the British mainland [25]. With other analogue techniques such as voice broadcasting and telephony, radio technology also

advanced with time and recently transitioned to digital telephony. A few scientists have tirelessly worked for development of various techniques and uses for UWB technologies.

From 1960s, this technology has been referred to as "baseband," "impulse," "short-pulse," and "carrier-free," technology. When computer development was in its initial stages, the time domain processing techniques of the UWB led to formation of the higher speed computation in late 1960s and early 1970s. A radar system was patented by Morey in 1974, that used a very wide band of frequencies penetrate the ground to distances of tens of meters. In the late 1800s the first transceiver was developed by Heinrich Hertz and Marconi before the carrier wave was used to convey communications [26]. The modern UWB systems came into being owing to the work done at Sperry research centre by Ross, their research mainly focused on the use of UWB as an analytical tool for the exploration of the properties of microwave networks. There was still a need for a system for delivery and distribution of large amounts of digital data between the computer central processor and various inputs and output devices, which was resolved by employing the technique of multiplexing multiple signals on a single transmission line using time-domain processing methods described in a patent by Ross, et al. This patent is considered a crucial part of foundation of modern UWB communications. After this developing wireless UWB communications was no longer a complex procedure.

The decade between 1980s and 1990s was the time when the principle of time domain electromagnetic was introduced to wireless communications, especially to short-range communications in dense multipath environments. UWB technology was developed in 1980s, but was used in military applications for radar applications and secure communications only. The term “ultra wideband” was coined by the US Department of Defence in 1990s [27]. Many scientists focused their work on detailed investigations into UWB propagation with introduction of UWB as a wireless network in late 1990s and early 2000s. The advantages and disadvantages along with the detailed description of the possible applications were discussed by Scholtz [19], various examples of such systems that could operate in the same space and that such wide bandwidth signals are more immune to the deleterious effects of multipath than are narrow bandwidth signals were also shown in this research. Accommodation of many users in high-multipath environments is another possible application for UWB communications; however, the coexistence in

already highly-populated radio spectrum poses to be a limitation. The advantages and the disadvantages even out one another. There is a possibility that other approaches to wireless operation in dense, high-multipath environments may give similar results as UWB approach. The remote sensing, high-resolution radar, surface ground penetrating radar is some applications of the UWB approach.

A Notice of Inquiry was issued by the FCC in 1998 about the amendment of Part 15 rules to allow the unlicensed use of UWB devices. In June 1999, NOCs were issued for three UWB devices [28]. They are listed below:

1. Time domain for through-wall imaging device.
2. Zircon for a "stud-finder" for rebar in concrete.
3. US radar for ground-penetrating radar.

The FCC received over 1,000 documents from more than 150 different organisations in response to their Notice of Inquiry by the year 2000. These documents contained information that would help the FCC in development of an appropriate set of specifications [28]. One of the main concerns of FCC was the possible interference from UWB transmissions on global positioning system (GPS) signals and commercial/military avionics signals. UWB has been used in radar systems and in army communication for several years as discussed above, it was made available commercially in year 2002. The First Report and Order (R&O) adopted on 14 February 2002 [5], and released carried this information, which was later published with slight modifications, on 22 April 2002 with the title *"Revision of part 15 of the commission's Rules Regarding Ultra-Wideband Transmission Systems"*.

The first FCC certified commercial system was installed in 2003, and in April of the same year the Time Domain Corporation announced the first FCC-compliant commercial UWB chipsets [25]. Known today as the Ultra Wideband Radio (UWB), uses pulses instead of the commonly used carrier wave for transmittance of information. The main advantage, UWB has is the potential to send high data rates (480 Mbps) over short distances making it favourable for Wireless Personal Area Network (WPAN) systems and other similar systems [5].

2.3 UWB Standards

2.3.1 Standards Definition

A standard is defined as a commonly consented definition or format authorised by a recognised organisation or one that is accepted as a model by industry. Standards are of two types i.e. *de jure* or *de facto*. *de jure* is when these are set by official standards organisations, and *de facto* is when these unofficial standards are established on the basis of common use. Following the standards makes is important to ensure different manufacturers create products that are compatible or interchangeable with each other. It is due to established standards that the wide acceptance and dissemination of products from multiple manufacturers and vendors with an economy of scale that reduces costs to consumers. Given below is a list of some famous standards organisations :

- ANSI (American National Standards Institute)
- ETSI (European Technical Standards Institute)
- IEEE (Institute of Electrical and Electronic Engineers)
- IRCC (International Radio Consultative Committee)
- ISO (International Standards Organisation)
- ITU (International Telecommunication Union).

The *de facto* standards are formats that became established standards on the basis of their popularity among a large number of companies have agreed to use them. These cannot be considered officially approved standards; however, they are a different type of standards. An example of *de facto* standard is Adobe's PostScript printer-control language. The IEEE takes active part in defining an UWB radio physical layer standard. ETSI is responsible for UWB conformance testing standards in support of European regulatory action. The IEEE standards process play an international role, which is why they have an on impact regulations and sometimes standards on a global level [28].

2.3.2 Defining a UWB Standard

The IEEE 802 local area network (LAN)/metropolitan area network (MAN) standards Committee is working on developing a UWB radio physical layer standard. Among the Ethernet family, Token Ring, and Wireless LAN, aforementioned is the most popular standard. Figure 2-1 shows a portion of the IEEE 802 organisation [28]. IEEE 802.15 is an international standard working group that consisting of multiple major companies. A number of wireless personal area network (WPAN) standards have been developed by IEEE. Figure 2-1 shows four major groups in which IEEE is functionally divided.

The IEEE 802.15.1 task group has the responsibility to come up with new standards on the basis of on Bluetooth v1.1 [29]. Bluetooth data is transmitted using a short-range radio link (up to 10 m) between personal devices, forming an ad-hoc network in the unlicensed 2.4 GHz band. IEEE 802.15.2 is focusing on coexistence issues that come up when multiple wireless systems share an environment of operation. The IEEE 802.15.4 task group is responsible for low data rate, low power WPAN (LP-WPAN) and focuses on unlicensed and international frequency bands [29].

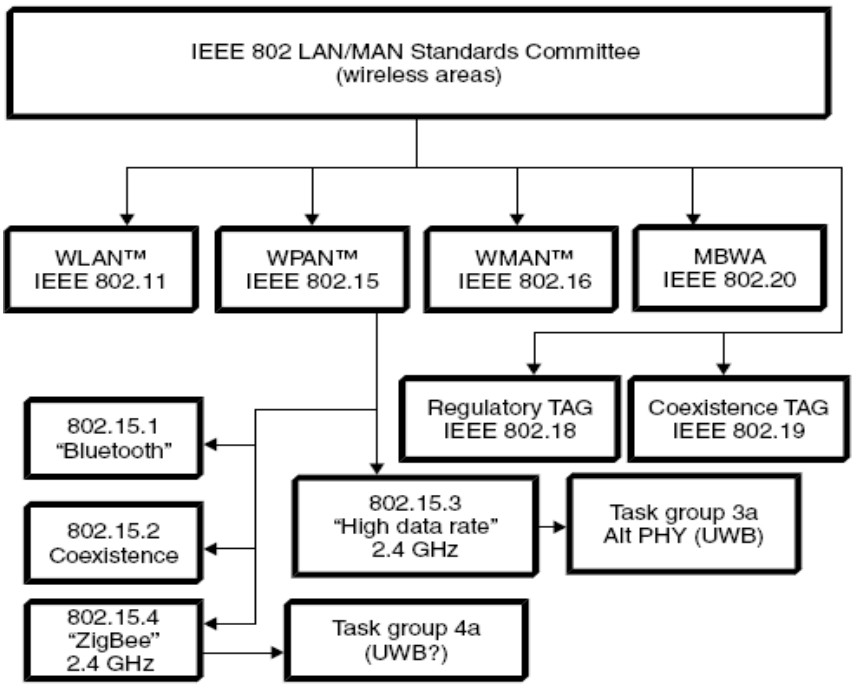

Figure 2-1 The IEEE 802 organisation, [28].

As shown in Figure 2-1, the IEEE 802.15.4 project in a new group 4a, along with the ZigBee Alliance. A new physical layer is being considered to be added to the standard for including positioning and distancing capabilities. The ZigBee Alliance is a group of companies that the work with the common objective of enabling trustworthy, cost-effective, low-power, wirelessly networked monitoring, and control products based on an open global standard [29]. UWB technology has the position for providing distance and location capabilities to wireless sensor networks. In the coming year, the popularity of wireless sensor networks is anticipated to undergo dramatic increase, as they offer practical and cost-effective machine-to-machine communication. The UWB entails some unique characters that fulfil the need for positioning, low data rates at longer distances, and high system capacities, UWB proposals are inevitable.

2.3.3 UWB IEEE 802.15.3a Standard

WPANs up to 55Mbps are being developed by the IEEE 802.15.3 task group [29]. Five 15 MHz channels in the 2.4 GHz ISM band are being used for the operation of the draft standard two of which interfere with IEEE 802.11b traffic. IEEE 802.15.3a standardisation activities pertain to very high data rate WPAN, where UWB is being used. IEEE 802.15 WPAN task group 3a (also called “TG3a”) was formed in late 2001 for the identification of a higher speed physical layer alternative to 802.15.3. Development of physical layer standards is done with the goal to support data rates between 110 Mbps and 480 Mbps over short ranges of less than 10 meters [29], [30]. Only physical layer alternatives are considered and the same media access control (MAC) layer is used for operations as defined by IEEE 802.15.3. Multimedia requiring more than 100 Mbps, like for wireless video conferencing is some of its many applications.

A more recent approach to UWB is a multiband system where the total UWB spectrum from 3.1 GHz to 10.6 GHz total 7.5 GHz divided into several smaller bands. Each of these bands has a bandwidth greater than 500MHz, to comply with the FCC definition of UWB [31]. In 2004, Batra et al. from Texas Instrument proposed the MB-OFDM scheme for IEEE802.15.3a [32], [33]. The proposed scheme divides the available UWB spectrum into 14 nonoverlapping subbands of 528 MHz bandwidth for each channel. Here the first four band groups have three subbands each, and the last band group has two subbands as shown in Figure 2-2. The advantage of the grouping is that the transmitter and receiver can

process a smaller bandwidth signal while taking advantages from frequency hopping. Here the combination of three subbands 8, 9 and 10 make additional band group 6. So for IEEE 802.15.3a (WPAN) with MBOFDM ultra wide band communication system required designed antenna having bandwidth more than 1.5 GHz.

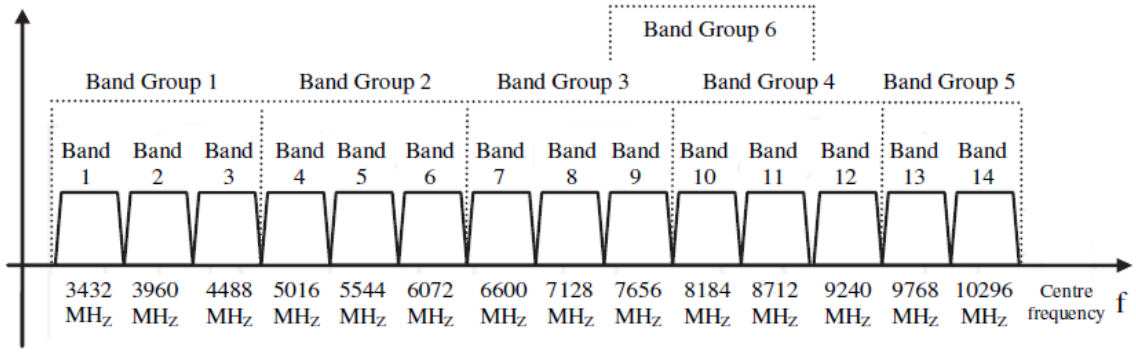

Figure 2-2 Division of the UWB spectrum from 3.1 to 10.6 GHz into band groups containing subbands of 528 MHz in MB-OFDM systems [34].

2.4 Why Ultra-Wideband Impulse Radio?

With the increase in the number of users of digital communications, equipment there is also an increased need to support more users per unit area. A developing network performance metric for personal area, local area, and wide area networks is the spatial information capacity measured in bits per second per unit area, which show that there is no need to support a large number of users within a confined space each requiring a high data rate [35]. It must be noted that long range transmission is not the goal here as usually seen in communications systems. For having great spatial capacity, the signal strength must decline rapidly to allow frequency reuse in nearby areas. UWB impulse radio has great potential when this application is considered. Any radio system that has a bandwidth greater than 25 present of its centre frequency or greater than 500 MHz is known as UWB system. The signal in the frequency domain from baseband to the actual carrier frequency where the system is allowed to operate move with the help of Radio Frequency (RF) carriers in conventional "narrowband" and "wideband" systems. UWB implementations have the potential to directly control "impulse" having a very sharp rise and fall time, thus the waveform obtained occupies several GHz of bandwidth. Under ideal conditions UWB could send a large amount of data, very far, very fast, for many users simultaneously.

However, under realistic conditions to achieve best results with one aspect compromise must be made with one or multiple aspects. UWB systems are not suitable for long-range communication use as they have very low radiated power, however, they are very useful for short-range, very fast wireless use, particularly for Personal Area Networks (PANs), which have a range of around 10 meters.

For understanding the feasibility of UWB within the current trends in wireless communications, the general problem must be considered and their solutions through communications systems must be found. If wireless is considered an ideal medium, it could be used to send:

1. a lot of data,
2. very far,
3. very fast,
4. for many users, and
5. all at once.

Practically all the five attributes cannot be achieved at once for the systems to support unique, private, and two-way communication streams. We must compromise on one or more so that others do well. Originally, wireless systems came into being to bridge the large gaps for linking two parties together [36]. However, recent studies on radio shows that all the other four attributes can be achieved if compromises are made on the part of distance. Given below is a list of trends that govern the short-range wireless generally and ultra-wideband particularly [36]:

1. The increased demand for wireless data capability in portable devices at higher bandwidth that is cost-effective and reduces power consumption in comparison to currently available options.
2. The crowding in the spectrum authorised and licensed by regulatory authorities in traditional ways.

3. The growth of high-speed wired access to the Internet in enterprises, homes, and public spaces.

4. The decreasing semiconductor cost and power consumption for signal processing.

There is a direct relation between the number of users of digital communications equipment and the need to support more users per unit area. A developing network performance metric for personal area, local area, and wide area networks is the spatial information capacity, defined by the Shannon-Hartley theorem in equation (2.1), and unit to measure it is bits per second per unit area. There is no need to support a large number of users within a conned space each requiring a high data rate [36].

$$C = B\log_2\left(1+ S\big/N_0\right) \tag{2.1}$$

Where

C: Maximum channel capacity (bps) for AWGN,

B: Channel bandwidth (Hz),

S: Signal power (watts), and

N_0: Noise Power (watts).

It must be noted that long range transmission is not the goal here as is typically the case with communication systems. In order to have a large spatial capacity, it is desirable for the signal strength to decay quickly enough to allow frequency reuse in nearby areas. UWB impulse radio may offer a good performance for this application. With all wireless standards there is a limit on its spatial capacity. Where impulse radio communicates with baseband pulses of very short duration, typically on the order of a nanosecond, thereby spreading the energy of the radio signal very thinly from near dc to a few gigahertz. When this pulse is applied to an appropriately designed antenna, the pulse propagates with distortion. The antennas behave as filters, and even in free space, a differentiation of the pulse occurs as the wave radiates.

Impulse radios, operating in the highly populated frequency range below a few gigahertz, must contend with a variety of interfering signals, and also must insure that they do not interfere with narrow-band radio systems operating in dedicated bands. These requirements necessitate the use of spread-spectrum techniques. A simple means for spreading the spectrum of these ultra-wide bandwidth (UWB) low-duty-cycle pulse trains is time hopping, with data modulation accomplished by additional pulse position modulation at the rate of many pulses per data symbol.

From figure 2-3, it can be seen that Ultra-wideband out performs the best of the current technologies in terms of spatial capacity by almost 20 times. This can be attributed to the Hartley-Shannon Law equation (2.1), because the upper bound of a channel's capacity grows linearly with the total bandwidth, UWB systems, which occupy a bandwidth of 500 MHz or more, have a much greater amount of space for expansion than the narrower band systems [37].

Spatial capacity can be defined as the amount of data transmitted per unit area per unit time. Spatial capacity is a major concern associated with all other wireless systems; A pictorial comparison between several wireless technologies is shown in Figure 2-3 [38].

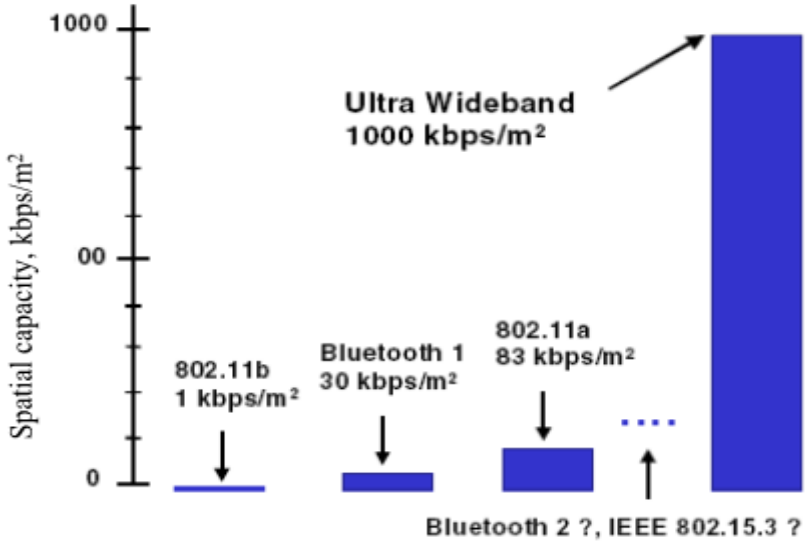

Figure 2-3 Comparison of Short-Range Wireless Spatial Capacities

According to the Shannon-Hartley theorem the channel capacity undergoes linear growth with bandwidth and has an exponentially direct relation with the signal to noise ratio (SNR). Conclusively, more rapid increase in radio capacity can be brought about with increase in the occupied bandwidth and the SNR wouldn't influence the values in a similar way [29]. In WPANs that work within small distances, and signal propagation loss is small and less variable; it is more likely to achieve increased capacity by occupying greater bandwidth. Therefore, it can be deduced that there is linear growth in capacity of a channel with the total bandwidth. UWB systems, which occupy a bandwidth of 500 MHz or more, thus, have a much greater amount of space for expansion in comparison to the narrower band systems.

A detailed comparison between UWB and 802.11a on the basis of distance coverage and the performance of each system is shown in Figure 2-4. The better performance of UWB in comparison to IEEE 802.11a for only small distance coverage is quite evident making it a better choice for indoor applications.

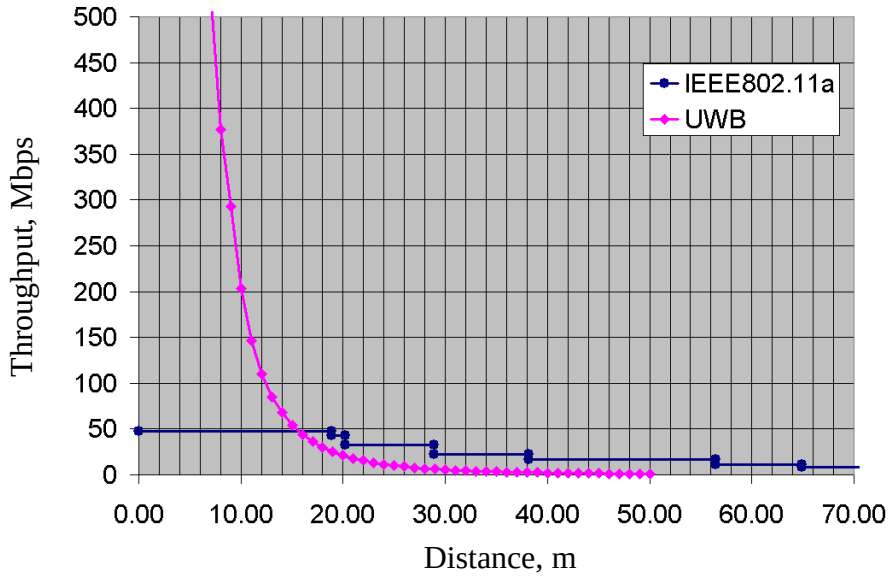

Figure 2-4 Comparison between UWB and IEEE 802.11a in terms of throughput and the distance covered.

The intentional radiation between 3.1-10.6 GHz for UWB products under a strict power level mask has been sanctioned by the Federal Communications Commission (FCC) [5], [39].

The abovementioned levels were already within acceptable limits under FCC Part 15 guidelines for unintentional radiators. It is important to note that the FCC already allowed unintentional interference to existing narrowband users in the band, which shows that the permissible power level 9 is among very low values. The permissible power levels over the band for indoor and outdoor devices are shown in Figure 2-5 [30], [25]. Figure 2-5a focuses on the permissible power level over the band for indoor devices whereas in Figure 2-5b, the maximum levels for hand-held outdoor devices are indicated. The low permissible power levels lead to designing systems that give better outputs with a flat transmit spectrum [40].

The regulations in Europe and Asia are very strict but that hasn't stopped researchers from studying and evaluating the less-utilised parts of the spectrum for the implementation of UWB techniques without the harsh restrictions imposed on the 3.1-10.6GHz band [2]. The spectrum around the unlicensed 60 GHz band (e.g. 57-64GHz in United States) is the strongest among all candidates for a revival of the UWB technology [41-43]. The 60 GHz band has several benefits such as the 7 GHz band is approved by the US FCC and high frequency reuse and high data rates can be achieved with it [43]. Also it can be exploited with antennas with lower relative bandwidth (approx. 10%) which are easier to design compared to UWB antennas with relative bandwidth of 110% (3.1- 10.6 GHz). However, these systems will face other challenges, such as very high sampling rates required which would increase the cost and complexity of the receivers. 'Appendix-A'.

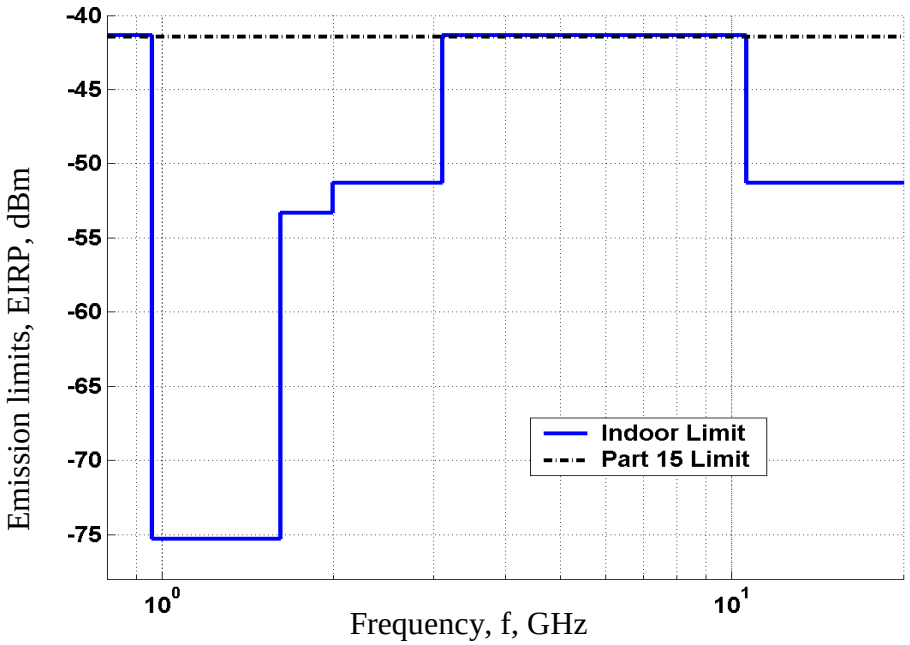

(a) Indoor UWB emission limits.

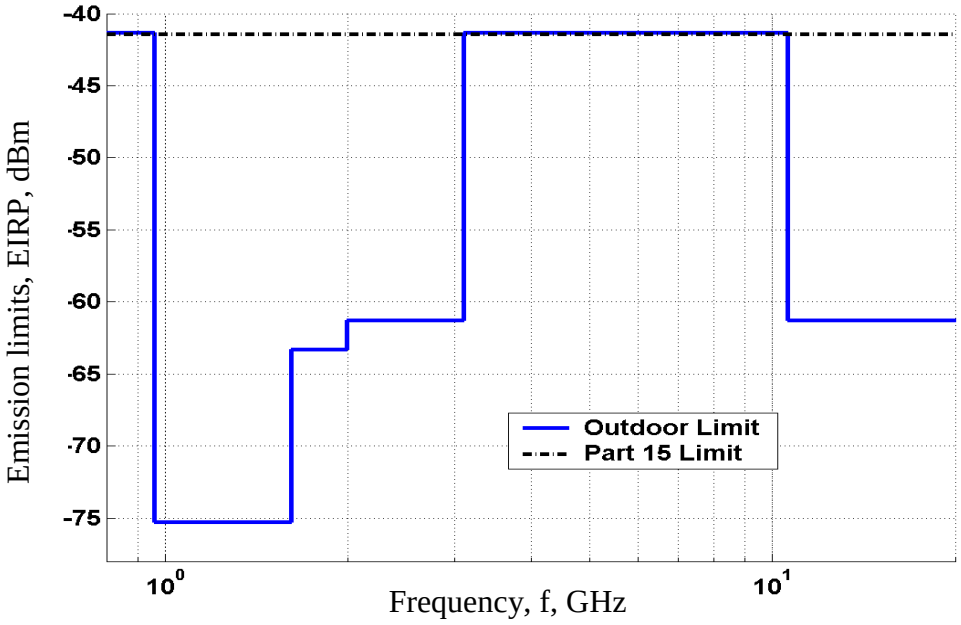

(b) Outdoor UWB emission limits.

Figure 2-5 UWB Emission Limit for Indoor and Outdoor Systems [44].

The potential interference of UWB emission to other devices sharing the same frequency band such as Bluetooth devices which operate in the 2.4 GHz Industrial, Scientific and Medical (ISM) band and IEEE 802.11a standardisation wireless LANs which operate in the 5 GHz ISM band are the main limitations of this system. For ensuring the proper protection of existing and planned radio services the operation of UWB devices appropriate technical standards presented in Part 15 of FCC rules is crucial. Low power radio frequency devices are allowed to operate without license in Part 15. The technical standard of Part 15 ensures that these unlicensed devices will not likely cause harmful interference to other users of the radio spectrum. According to the Part 15 rules the UWB transmission is undetectable or has minimal impact to narrowband receiver, which means that power spectral density is lower than the thermal noise floor levels (see Figure 2-6).

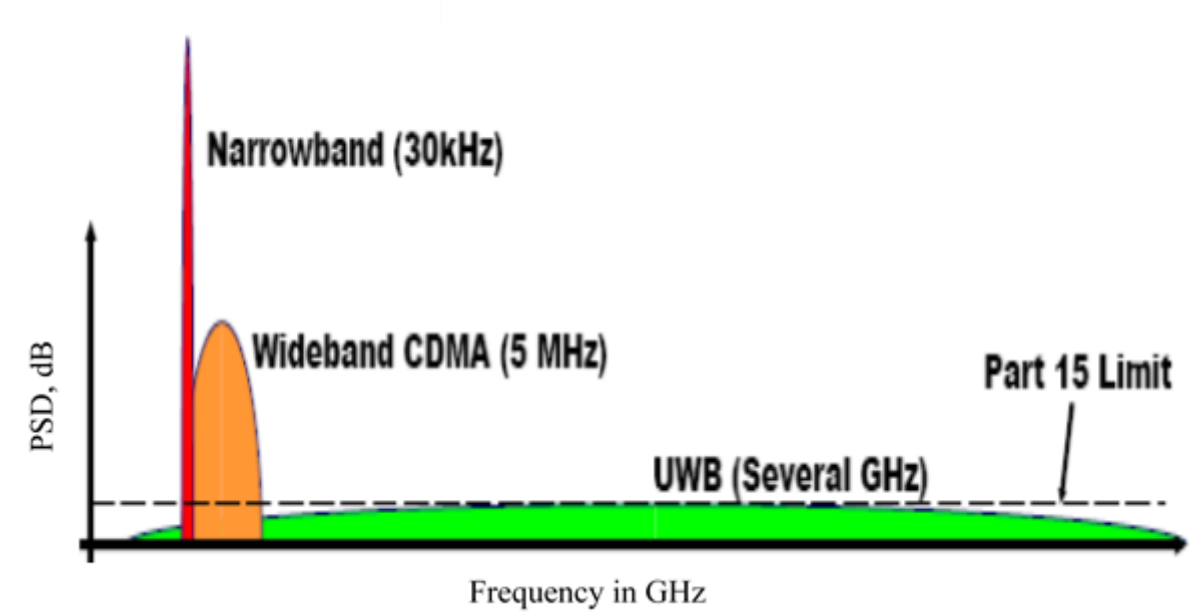

Figure 2-6 Power Spectral Density of an UWB Signal Compared to Noise Floor

The comparison of UWB and different modern wireless technologies according to the emitted signal power and the occupied bandwidth is given in Figure 2-7. The huge spectrum occupancy of UWB in comparison to other systems is quite evident, which indicates large spatial capacity, as discussed before. In addition, the very small emitted power of UWB systems (-41.3 dBm/MHz) compared to other systems is also very

prominent, this indicates that UWB systems can safely coexist with other systems without any potential interference [45].

In contrast to Carrier-Wave (CW) technologies employing sine waves for transmittance of data, large amounts of information over short distances are encoded by UWB technologies employing rather minimal power bursts of radio energy, which are spread across a wide range of frequencies. High capacity, multipath robustness, position location capability, low transmission power, low implementation cost and multi-access capability are some of the salient features of the UWB systems. Power limitation, synchronisation, coexisting, channel characterisation and system design are some of the disadvantages associated with these systems.

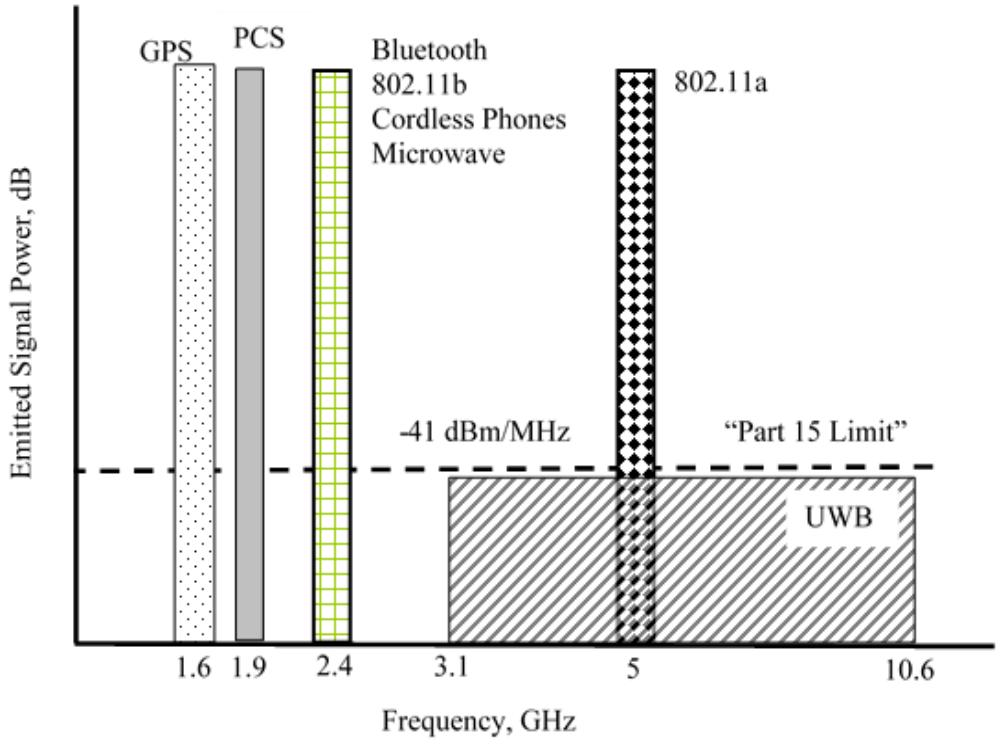

Figure 2-7 Frequency Occupation of UWB and Other Current Radio System

The low radiated power of UWB renders these systems unsuitable for long range communication use, however, they are perfect for indoor, short range, very fast wireless use, particularly in terms of PANs, which are spread over areas no more than 10 meters [46]. Ground Penetration Radar (GPR), imaging systems, vehicular radars (collision

avoidance/detection, road conditions sensing), wireless offices and homes (indoor-video/data/voice distribution), security systems for alarming arid tracking movement and Wireless personal area networks (PANs)/ local area networks (LANs) are some of the possible practical applications of the UWB systems. Conclusively, UWB is a great technology for consumer communications applications, which is also very cost effective [5].

The pulses themselves appear as more of a “shaped noise” to a UWB receiver as they are in form of curves over the spectrum. Conversely, noise appears somewhat similar over a range of frequencies and would appear flat on a spectrum. Therefore, sometimes noise having same intensity as the pulse, causes no interference to the pulse. For an interference to faint out the pulse would have to spread uniformly across the entire spectrum [47]. Only a part of the spectrum would be occupied and the amount of the overall signal collected by the would be reduced, however, it has the potential to recover part of the pulse to restore or rebuild the signal. One bit of information is spread over multiple pulses (usually called monocycles) for providing the receiver sufficient information for extraction of the averaged signal from the noise.

The pulse rate can be used to derive the bit rate. The receiver sums (or correlates) the required number of pulses for recovering the transmitted data from beneath the noise floor. The potential of the UWB impulse radio for narrowband jamming immunity is rather good owing to the spreading of the signal over an ultra-wide bandwidth. A small portion of the UWB users' spectrum is occupied by the spectrum of the narrowband jammer and large portion of the spectrum left un-jammed. The specific receiver design is crucial to tolerate the narrowband jammer. A narrowband jammer (The universal mobile telecommunication system (UMTS) spectrum of the frequency division duplex (FDD) uplink band 1.92-1.98 GHz) interfering with the UWB spectrum in a very narrow band leaving the rest of the spectrum unjammed is shown in Figure 2-8 [48].

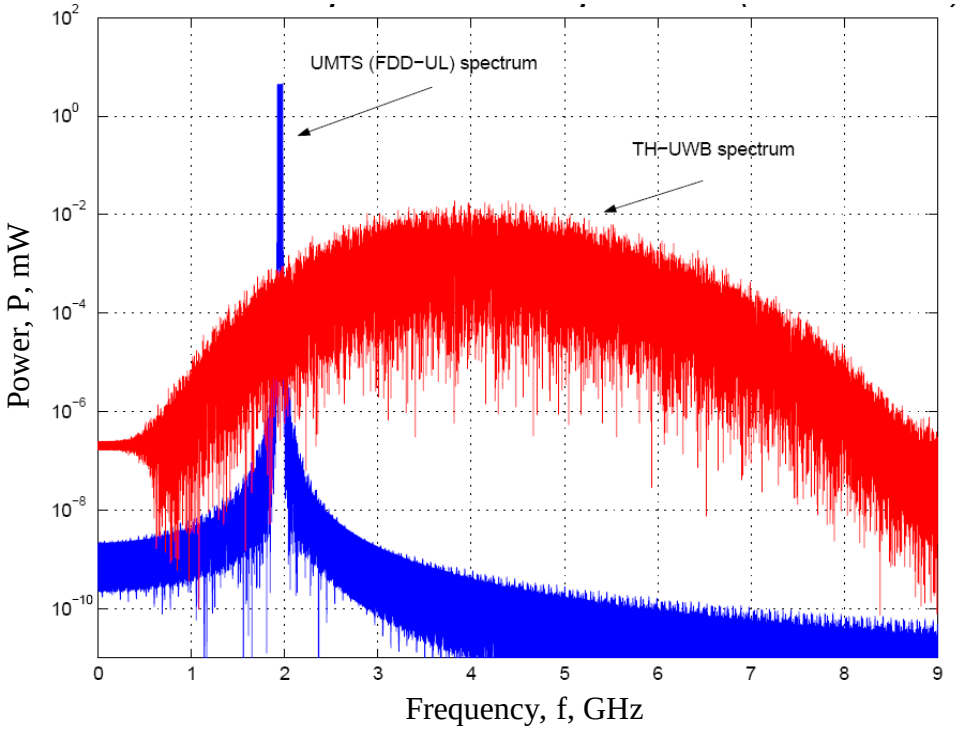

Figure 2-8 Spectra of fully loaded UMTS FDD uplink band and UWB signal using a Gaussian pulse waveform, [48]

With low power spectral density of UWB signals, the chances of its detection and interception also become low when traditional narrowband detection equipment is used. With the passage of time better detection equipment will be selected for operations.

2.5 UWB Technology

In this section, the high-level perspective on the potential of UWB technology in indoor wireless communications is presented. According to the FCC definition [5], Any wireless transmission scheme occupying a fractional bandwidth, η, greater than 25% of a centre frequency, or more than 500 MHz, which of the two is lower, is known as Ultra-wideband (UWB) technology. The frequency limits of the emission bandwidth using the formula influences the value of the fractional bandwidth η [49] [50] [51]:

$$\eta = \frac{2(f_H - f_L)}{(f_H + f_L)} \tag{2.2}$$

Where f_H and f_L are the upper and lower frequency of the -10 dB emission point, the centre frequency is defined as the average of f_H and f_L, i.e.

$$f_C = \frac{(f_H + f_L)}{2} \tag{2.3}$$

The narrowband (NB) and UWB spectrums with the defined f_C, f_H and f_L are shown in Figure 2-9.

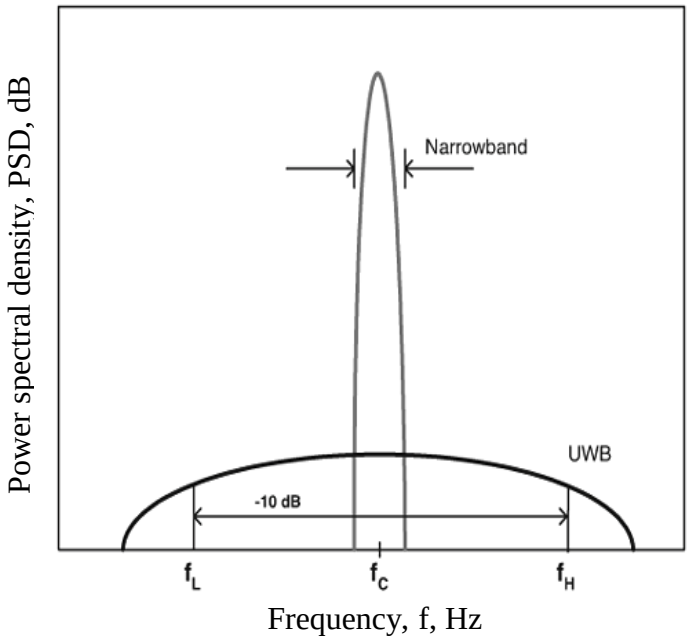

Figure 2-9 Comparison of the Fractional Bandwidth η of a Narrowband (NB) and Ultra-Wideband (UWB) Spectrums

The examples of two different common forms of UWB radio systems are provided by IEEE 802.15.3a task group i.e. (i) very short duration pulses are transmitted for conveying information, known as impulse-UWB (I-UWB), (ii) multiple simultaneous carriers are transmitted for conveying information, known as multi-carrier UWB (MC-UWB). One of these two approaches has not been standardised, leaving it on the disposal of physical descriptions of a radio to pick the more suitable approach. The same radio regulatory definitions of the FCC are employed again, a flexibility advantage of UWB standard implementation. Both approaches have their pros and cons. The basic differences between the two approaches on the basis of spectrum management are shown in Figure 2-10 [25]. The orthogonal frequency division multiplexing (OFDM) is the most popular form of multi-carrier modulation, which has become the leading modulation technique for high data rate systems.

Contrary to classic communications pure impulse radio does not use a modulated sinusoidal carrier for transmittance of information. The baseband pulses are used for this purpose. The pulses are extremely short and last for nanoseconds or less, consequently, the transmit signal bandwidth is on the order of Giga Hertz [25].

The use of multi-carrier communications started between the 1950s and 1960s to achieve higher data rate transmittance in military communications. The densely spaced sub-carriers and overlapping spectra are used by the OFDM, which is special case of multi-carrier modulations. OFDM was patented in the US in 1970 [25]. And is in application in Asymmetric Digital Subscriber Line (ADSL) services, Digital Audio Broadcast (DAB), Integrated Services Digital Broadcasting (ISDB) in Japan, IEEE 802.11a/g, 802.16a, and Power Line Networking (HomePlug) today. OFDM also being considered for the fourth generation (4G) wireless services, as it is suitable for high data rate systems IEEE 802.11n (high speed 802.11) and IEEE 802.20 (MAN) [25].

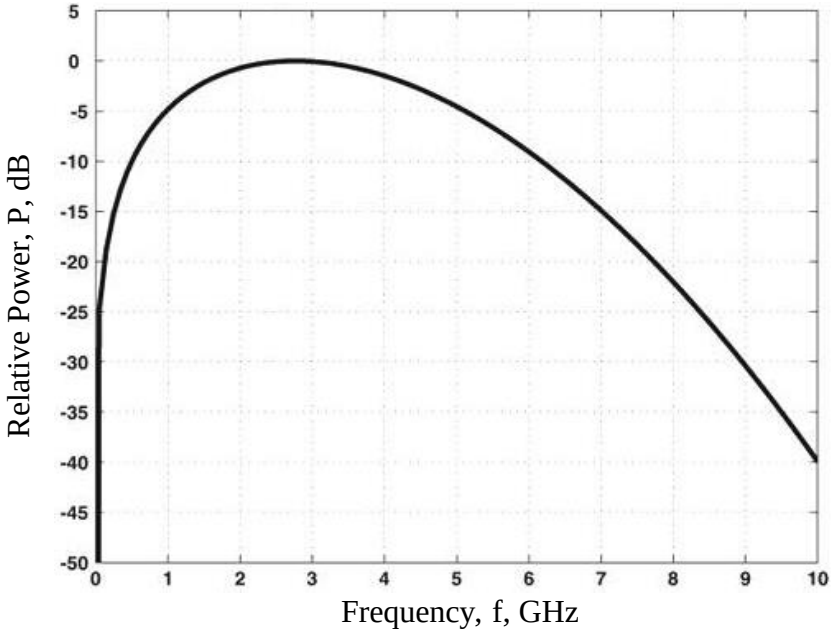

(a) Spectrum of a Gaussian monocycle-based I-UWB

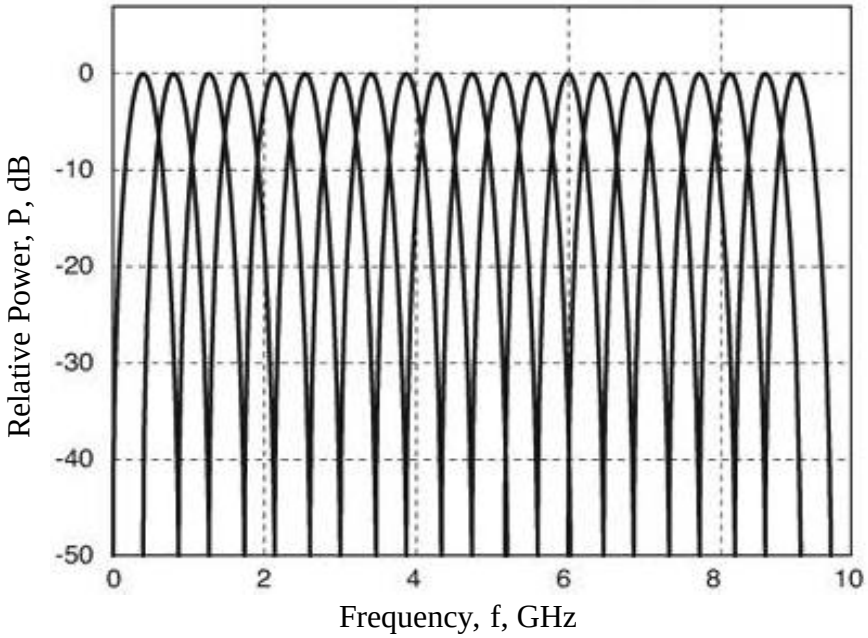

(b) Spectrum of an OFDM-based MC-UWB signal.

Figure 2-10 Comparison of impulse and multi-carrier UWB spectrums, [25]

The balance between advantages and disadvantages of I-UWB and MC-UWB is complicated to find and the standards bodies have debated over them for a long time. In a UWB system, it is most important to minimise interference in transmitted and received signals. MC-UWB is takes care of this issue by avoiding interference with its precisely

selected carrier frequencies to dodge the narrowband interference to or from narrowband systems. Moreover, the flexibility and scalability provided by MC-UWB is also relatively better; however, an additional layer of control in the physical layer is required. The impact of interference on the UWB system can be reduced by application of spread spectrum techniques in both forms of UWB [25].

Fast switching times for the transmitter and receiver are required by I-UWB. While designing the radio and antenna the transient properties must be considered. The interference to UWB systems can be resolved with the help of high instantaneous power during the brief interval of the pulse; however, doing so increases the probability of interference from UWB to narrowband systems. The RF front-end of an I-UWB system appears like a digital circuit, therefore, most problems associated with mixed-signal integrated circuits can be avoided [25]. Simple I-UWB systems are rather cost effective. In contrast, implementation of a MC-UWB front-end is complex because of the continuous variations in power over a very wide bandwidth. The job of the power amplifier becomes difficult because of this. High-speed Fast Fourier Transform (FFT) processing having significant processing power is required for OFDM.

The general detection theory assumption that the system operates in an additive white Gaussian noise (AWGN) environment poses as an additional limitation in the implementation of a UWB system. Even though under real circumstances this does not always apply to communication system and particularly to UWB systems [25]. Other signals may also exist within the UWB pass band having Gaussian noise statistics. The operation of the system is performed at higher transmit power due to these narrowband signals or the in-band interference needs to be removed.

I-UWB is the main focus of this thesis, which is more popular but is a poorly understood form of UWB. We will explore different types of modulation techniques operating on this system. Mainly focusing on pulse position modulation systems (PPM) operating with time hopping spread spectrum (THSS) as a spreading approach and a multiple access technique.

2.6 UWB Signal Definition

Generation of a suitable signal is the first step in a radio communication link, these signals are later modulated with desired information. The factors that influence the appearance of UWB signal are listed as under:

1. What is permissible under the rules and regulations?
2. What level of coexistence with other services in the band is desirable?
3. The application within which the UWB signal is intended to operate.
4. What technological constraints there are from the feasibility, cost, and marketability points of view?

The UWB is not defined by the Rules and regulations of authorities such as FCC. The broad rules are defined by the regulations and the conditions for UWB communication systems to access and share a 7,500 MHz swath of spectrum extending from 3.1 to 10.6 GHz are also set by these regulations. The UWB radios need to coexist with, share, and interoperate with existing radio services to gain a place in market. It is also very important for UWB technology to be physically implemented in cost-effective integrated circuits, which will pose a challenge in performance across the frequency band [28].

The universal characteristics of UWB signals and signalling systems are based on the regulations. UWB communications and measurement systems are focus of concern particularly in high-speed home and business networking devices. The -20 dB bandwidth of the emission contained within the UWB frequency band must be ensured while designing intentional UWB radiators. 500 MHz is the minimum bandwidth measured at points 10 dB below the peak emission level is. −41.3 dBm/MHz is set as the permissible emission levels for UWB signals in the UWB band. We will be focusing on -10 dB bandwidth in UWB signal design for ensuring compliance with minimum bandwidth requirements. The -20 dB bandwidth ensures that the signal remains below the -20 dB band edge corners on the UWB communications power spectral density (PSD) mask. The frequency of highest radiated emission must be maintained below the maximum allowed PSD. The above mentioned limits are shown in Figure 2-11 [28].

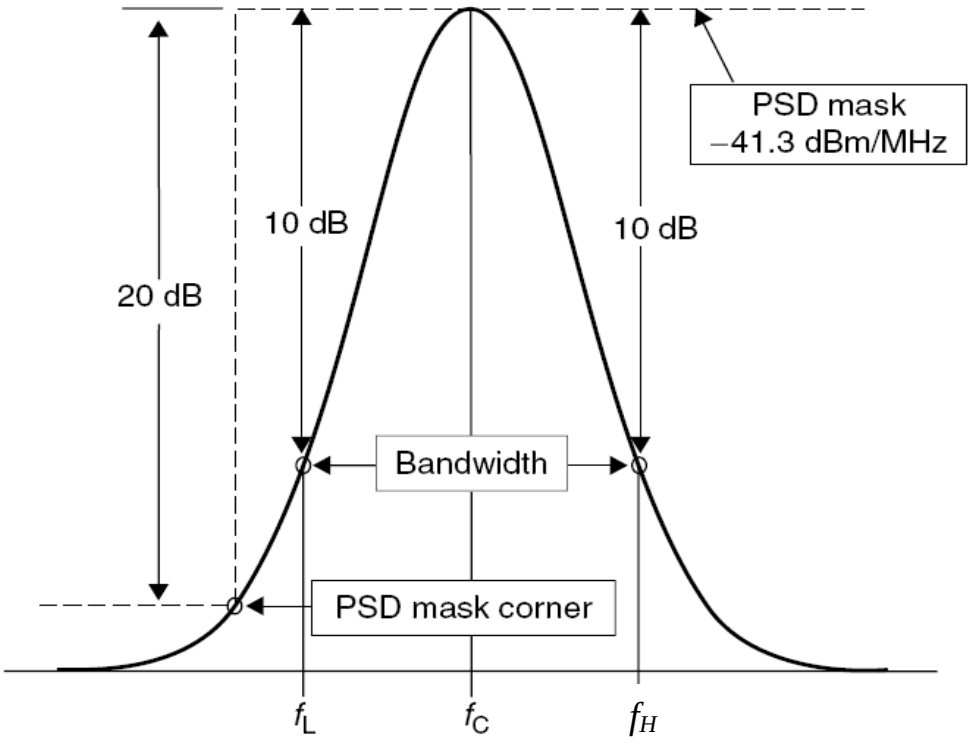

Figure 2-11 UWB Signal Design Points, [28]

Signals are designed by shaping their properties as a function of time. There is a one-to-one mapping between what a signal looks like in time and its frequency spectrum. This relationship is mathematically expressed by the Fourier transform. The key point here is that once the signal is fully specified or described in one domain (time or frequency), its properties in the other domain are given by the Fourier transform. This property is used to define the signal in one domain and to extract the desired properties in the other domain. However, it must be noted that an important concept of UWB is that the signal is a function of time, not frequency. Frequency in UWB primarily determines propagation characteristics, such as the distance the signal can be sent, because higher frequencies are more susceptible to fading, absorption, and other effects.

2.7 UWB Waveform Generation (A Train of Gaussian Monocycles)

Pulsed emissions are used to produce UWB signals. A relation between very wide RF bandwidth and a narrow pulse width has been established in UWB. Traditional radio transmitters use a modulated signal which is unconverted and amplified to transmit the data; the Ultra Wideband Radio (UWB), uses pulses instead of the commonly used carrier wave for transmittance of information. Accurate pulse shaping is required by transmitters for production of the required spectrum and maximising the antenna's emission. Very precise pulse designs are required for production of emissions with flat and wide PSDs. Due to regulations and approval most of UWB developments are still in the laboratory; however, some companies have started pioneering this technology into their equipment such as avalanche transistors, tunnel diodes, and other exotic devices.

The Time Modulated UWB (TM-UWB) technology is developed by Time Domain Corporation. Ultra-short "Gaussian" monocycles with tightly controlled pulse-to-pulse intervals, commonly known as Pulse Repetition Interval (PRI) are emitted by the TM-UWB. The pulse widths usually range between 0.2 and 1.5 nanoseconds and the range for PRI is 25-1000 nanoseconds. PRI is different for each pulse and depends on two factors: an information signal and a channel code that is a Pseudo-Random Noise (PN) sequence.

Different pulse shapes were proposed for UWB, ranging from the rectangular pulse, to the bell shaped Gaussian pulse [52]. The Gaussian pulses and their derivatives are mostly used pulses in UWB systems today, particularly in communication and measurement systems because they have effective simultaneous high time and frequency resolution, and often referred as monocycles [13]. Gaussian monocycles are obtained when successive derivatives of the basic Gaussian waveform are taken. A typical definition of a Gaussian function is out line in [25] [53] and shown in equation (2.4)

$$p_G(t) = \frac{1}{\sqrt{2\pi}\sigma} e^{-\frac{(t-\mu)^2}{2\sigma^2}} \tag{2.4}$$

Where μ, is the mean and σ is the variance of the statistical distribution characterised by the function. Considering $\mu = 0$, we have the definition of the so-called "zero-order Gaussian pulse"

$$p_{G_0}(t) = \frac{1}{\sqrt{2\pi}\sigma} e^{-\frac{t^2}{2\sigma^2}} \tag{2.5}$$

The other UWB waveforms can be obtained by differentiating $p_{G_0}(t)$ w.r.t "*t*", i.e.

$$p_{G_n}(t) = \frac{d^n}{dt^n} p_{G_0}(t) \tag{2.6}$$

Where *n* is the order of the derivatives.

The following formulae show the first five derivatives of the Gaussian pulse [54]

$$p_{G_1}(t) = -\frac{t}{\sqrt{2\pi}\sigma^3} e^{-\frac{t^2}{2\sigma^2}}, \tag{2.7}$$

$$p_{G_2}(t) = -\frac{1-\frac{t^2}{\sigma^2}}{\sqrt{2\pi}\sigma^3} e^{-\frac{t^2}{2\sigma^2}}, \tag{2.8}$$

$$p_{G_3}(t) = \frac{3t-\frac{t^3}{\sigma^2}}{\sqrt{2\pi}\sigma^5} e^{-\frac{t^2}{2\sigma^2}}, \tag{2.9}$$

$$p_{G_4}(t) = \frac{3-\frac{3t^2}{\sigma^2}+\frac{t^4}{\sigma^4}}{\sqrt{2\pi}\sigma^5} e^{-\frac{t^2}{2\sigma^2}}, \tag{2.10}$$

$$p_{G_5}(t) = -\frac{15t-\frac{10t^3}{\sigma^2}+\frac{t^5}{\sigma^4}}{\sqrt{2\pi}\sigma^7} e^{-\frac{t^2}{2\sigma^2}}. \tag{2.11}$$

The pulse length T_p is related to the variance σ through the linear transformation outline in [25] as

$$T_p = 2\pi\sigma \tag{2.12}$$

The value of practical pulse is almost negligible outside the interval {-$T_p/2$, $T_p/2$}, and most of the pulse's energy, is within this range. For the analysis of the spectral behaviour of these waveforms, following equation is used to calculate the Fourier transform as described in [54]

$$F\left[e^{-\pi\left(\frac{t}{T}\right)^2} \right] = Te^{-\pi(fT)^2} \tag{2.13}$$

Then, considering $T = \sqrt{2\pi}\sigma$ one can get

$$P_{G_0}(f) = \frac{1}{\sqrt{2\pi}\sigma} \sqrt{2\pi}\sigma \times e^{-2\pi^2\sigma^2 f^2} = e^{-2(\pi\sigma f)^2} \tag{2.14}$$

The property given below can be used to calculate the Fourier transform of the first five derivatives of the Gaussian pulse as described in [54]

$$F\left[\frac{d^n}{dt^n} p_{G_n}(t) \right] = (j2\pi f)^n P_{G_0}(f) \tag{2.15}$$

Thus giving

$$P_{G_1}(f) = j2\pi f \; e^{-2(\pi\sigma f)^2}, \tag{2.16}$$

$$P_{G_2}(f) = -4(\pi f)^2 e^{-2(\pi\sigma f)^2}, \tag{2.17}$$

$$P_{G_3}(f) = -8j(\pi f)^3 e^{-2(\pi\sigma f)^2}, \tag{2.18}$$

$$P_{G_4}(f) = 16(\pi f)^4 e^{-2(\pi\sigma f)^2}, \text{ and} \tag{2.19}$$

$$P_{G_5}(f) = 32\, j(\pi f)^5 e^{-2(\pi\sigma f)^2}. \tag{2.20}$$

The centre frequency $f_c^{(n)}$ of the spectra of the *n*-th derivative of the Gaussian pulse can be defined as the point where the spectrum reaches its maximum, satisfying the equality

$$\int_{-\infty}^{f_c^{(n)}} \left|P_{G_n}(f)\right|^2 df = \int_{f_c^{(n)}}^{+\infty} \left|P_{G_n}(f)\right|^2 \tag{2.21}$$

According to this relationship, it can be noticed that $f_c^{(n)}$ increases proportionally with the square root of the derivative order, as described in [54] i.e.,

$$f_c^{(n)} = \frac{\sqrt{n}}{T_p} \tag{2.22}$$

Hence, the centre frequency of the first five derivatives of the Gaussian pulse can be summarised in Table 2-1 as

Waveform name	Centre frequency
Gaussian 1st derivative	$f_c^{(1)} = 1/T_p$
Gaussian 2nd derivative	$f_c^{(2)} = \sqrt{2}/T_p$
Gaussian 3rd derivative	$f_c^{(3)} = \sqrt{3}/T_p$
Gaussian 4th derivative	$f_c^{(4)} = 2/T_p$
Gaussian 5th derivative	$f_c^{(5)} = \sqrt{5}/T_p$

Table 2-1 Summary of the centre frequencies of the first five derivatives of the Gaussian pulse.

In Figure 2-12 the time behaviour of $p_{G_0}(t)$ and its first five derivatives are represented for $T_p = 0.5ns$, as an example. For the analysis of the time properties of each order, Figure 2-12a represents the zero, first, and second order Gaussian pulses, the third, fourth, and fifth order Gaussian pulses are shown in Figure 2-12b. The corresponding spectral behaviour of all the five order Gaussian pulses in the frequency domain for normalised amplitude represented in volts is represented in Figure 2-13a and their spectral behaviour for normalised amplitude represented in dB are shown in Figure 2-13b.

Figure 2-12 shows that even though the pulses are very narrow, their amplitudes show variations across time, the side's lobes become negligible in the frequency domain. Alternatively, Figure 2-13 shows that the extra shift in the nominal centre frequency of each pulse in the frequency domain to the higher frequencies is in accordance with the formula in equation (2.22) for a specified pulse length T_p.

Additionally, the -10 dB fractional bandwidth for all monocycles is more than 20%, so it is a UWB system according to the definition discussed before. The PSD of each monocycle is the representation of envelope around which the spectrum of the modulated pulse train will be drawn.

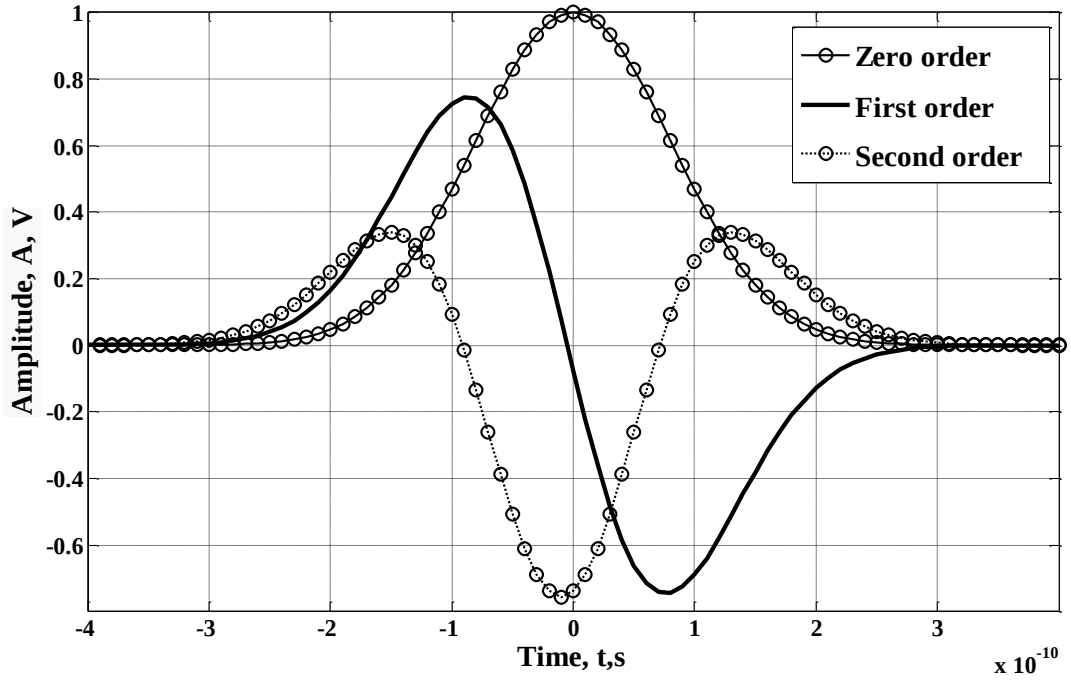

(a) Zero, first, and second order Gaussian pulses in t-domain.

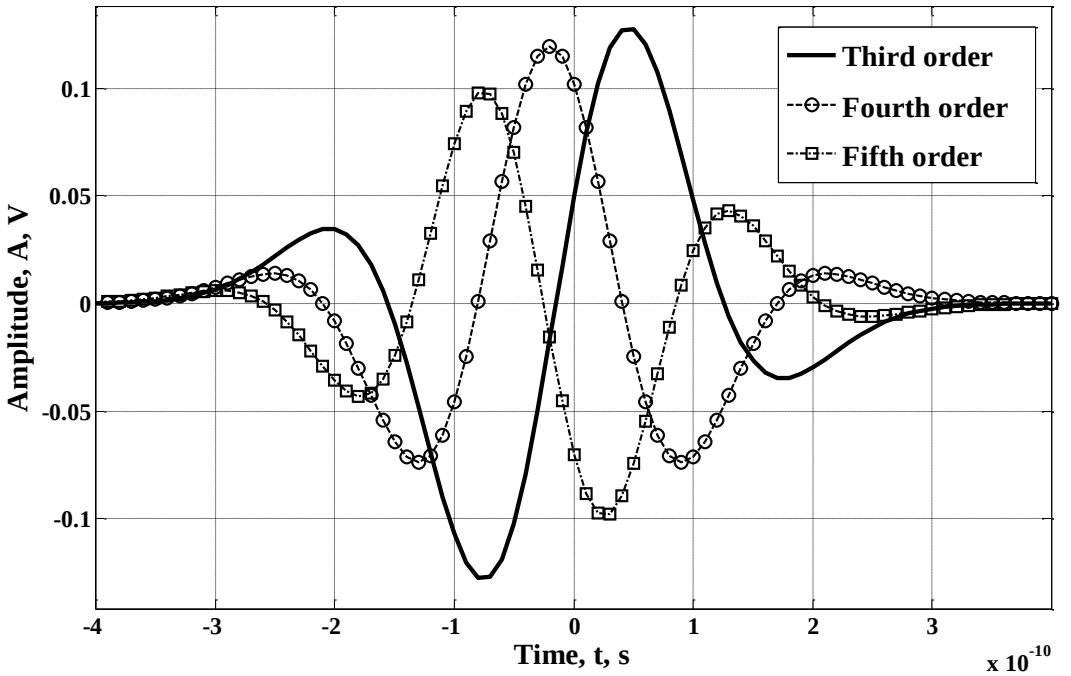

(b) Third, fourth, and fifth order Gaussian pulses in t-domain.

Figure 2-12 Different order Gaussian pulses in t-domain.

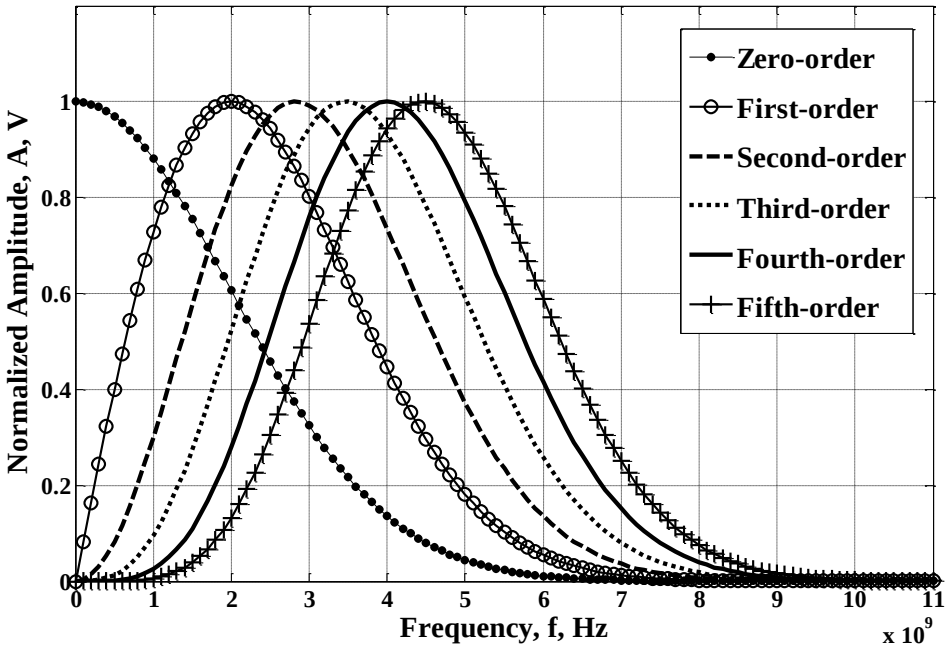

(a) For normalised amplitude represented in volt.

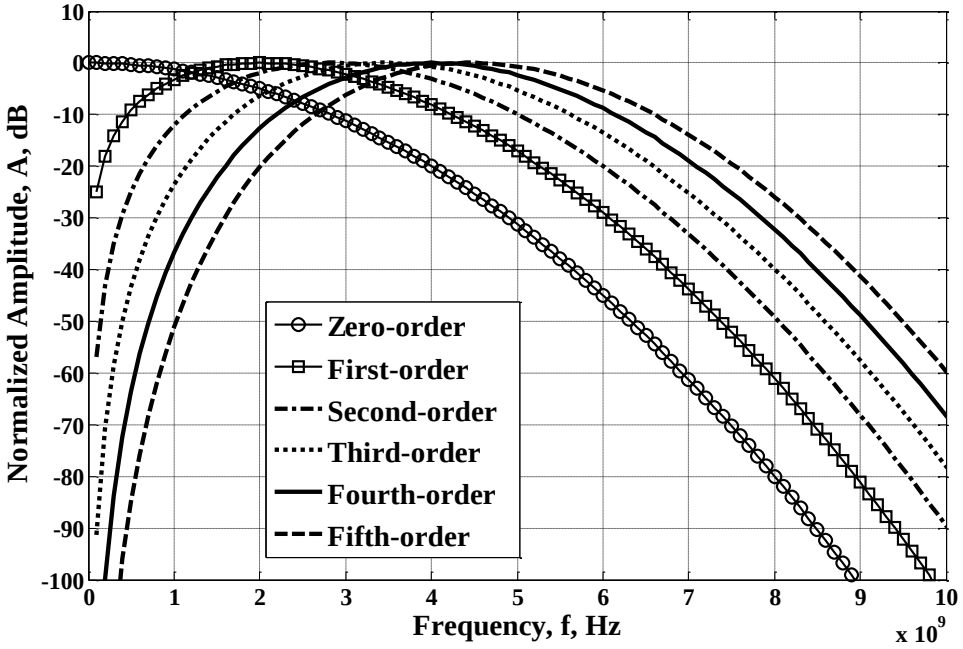

(b) For normalised amplitude represented in dB.

Figure 2-13 Different order Gaussian pulses in f-domain.

Following the FCC regulations, regarding the fractional bandwidth, f_L and f_H are the corresponding lower and higher -10 dB points in frequency which solve the equation

$$P_{G_n}(f) = \frac{1}{10} P_{G_n}(f_c), \tag{2.23}$$

And $B_{\text{-10dB}}$ is the bandwidth of the pulse simply defined as

$$B_{-10dB} = f_H - f_L \,. \tag{2.24}$$

All the properties for two different examples of pulse widths (T_p = 0.5 ns, and 1 ns) are briefly described in Table 2-2. The increase in the pulse length results in a proportional decrease in the -10dB bandwidth following equations (2.22) and (2.24) as per the prediction.

Waveform name	T_p **[ns]**	f_c **[GHz]**	f_L **[GHz]**	f_H **[GHz]**	B_{-10dB} **[GHz]**
Gaussian 1st derivative	0.500	2.00	0.39	4.42	4.03
	1.00	1.00	0.19	2.21	2.02
Gaussian 2nd derivative	0.500	2.83	1.03	5.19	4.16
	1.00	1.41	0.51	2.60	2.08
Gaussian 3rd derivative	0.500	3.47	1.59	5.79	4.20
	1.00	1.73	0.80	2.90	2.10
Gaussian 4th derivative	0.500	4.00	2.08	6.31	4.23
	1.00	2.00	1.04	3.16	2.12
Gaussian 5th derivative	0.500	4.50	2.52	6.79	4.27
	1.00	2.25	1.26	3.39	2.14

Table 2-2 Typical parameters of Gaussian waveforms for defined pulse lengths.

Figure 2-14 sheds more light on this property where the first-order Gaussian monocycle is used to demonstrate the effect of changing the pulse width on the corresponding spectral characteristics of the pulse.

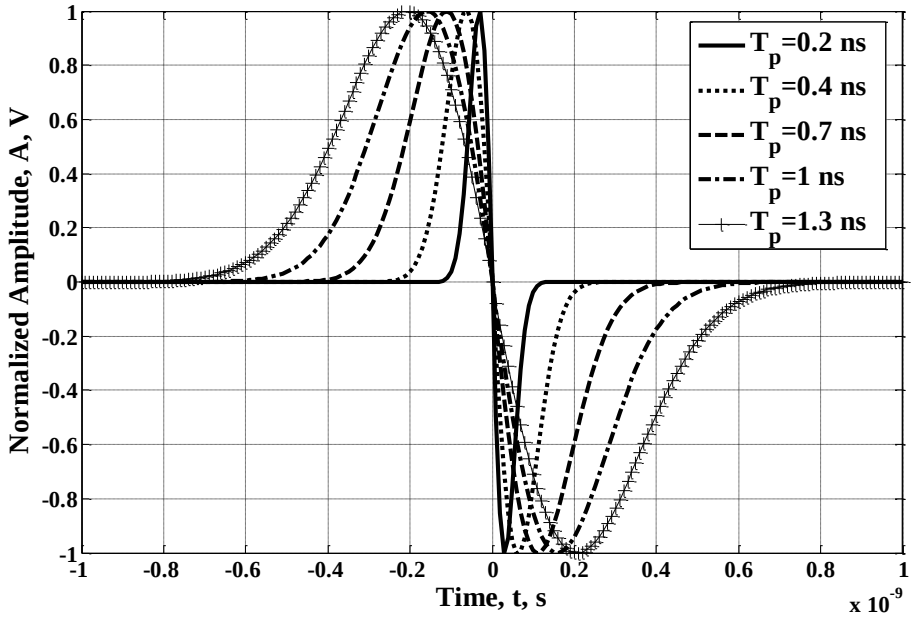

(a) First order Gaussian pulse in t-domain with different pulse widths.

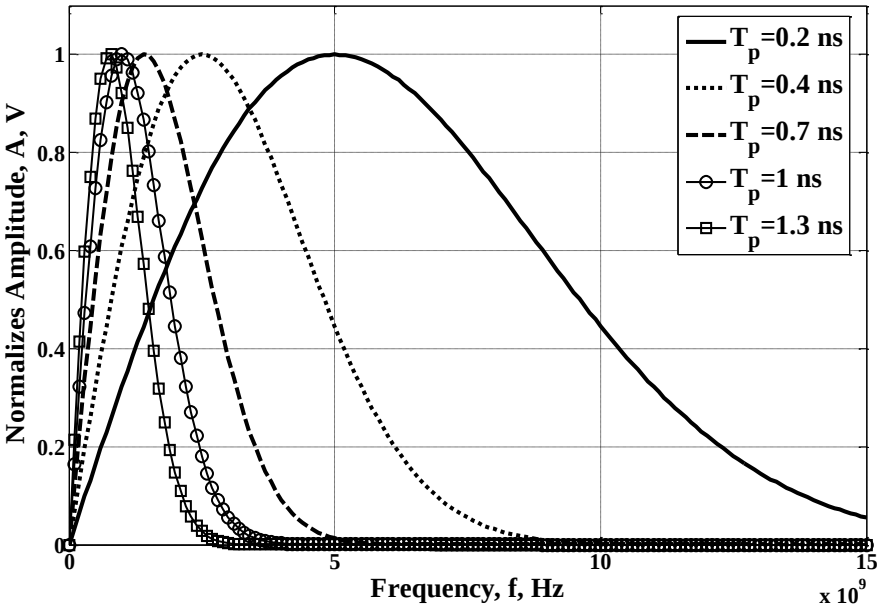

(c) First order Gaussian pulse in f-domain with different pulse widths.

Figure 2-14 First order Gaussian pulse in t- and f-domains with different pulse widths.

Different values of T_p are used in the first order Gaussian pulse as shown in Figure 2-14a. The Fourier transformation is validated in Figure 2-14b with the help of all the corresponding curves. Figure 2-14b and equation (2.22) can be used to establish that the centre frequency can be changed either by changing the order of the pulse, when the pulse width is constant, or by changing the pulse width, for the same order.

2.8 UWB Multipath Channel Model

Indoor radio communication covers a wide variety of situations ranging from communication with individuals walking in residential or office buildings, supermarkets, or shopping malls, etc to fixed stations sending voice messages to robots in motion on assembly lines in factory environments of future. If indoor radios propagation channels are modeled as linear filters, they can be characterized by reporting the parameters of their equivalent impulse response functions [55]. Wireless channel model is described in the IEEE 802.15.3a standardization group has developed for the evaluations of ultra-wideband communications systems and discuss the measurements that form the basis of this model. These measurements establish important differences between UWB channels and narrowband wireless channels, especially with respect to fading statistics and time-of-arrival of multipath components (MPCs) [56]. Most contributors distinguished between Line-Of-Sight (LOS) channels, in which there is an unobstructed path from transmitter to receiver, from Non-Line-Of-Sight (NLOS) channels. The path loss for LOS and NLOS conditions by the commonly used distance power law and the shadowing by lognormal distributions. The average Power-Delay Profiles (PDP) exhibit a clustered structure, which means that rays arrive at the receiver in groups, each having a given decay constant [57]. All the measurement environments were an indoor as this is the target application for IEEE 802.15.3a standardization devices. Different types of indoor environments were analyzed, including residential (homes, apartments) and office environments. The building materials and geometrical layouts are quite different in those cases, and result in distinct channel characteristics. This is due mostly to the higher proportion of metal construction materials found in office buildings as compared to residential buildings. In addition to these environment types, most contributors distinguished between line-of-sight channels, in which there is an unobstructed path from transmitter to receiver, from non-line-of-sight channels [58]. Also, the choice of measurement points were different: some campaigns

used regular grids in order to isolate small-scale from large-scale fading effects, while other campaigns used only random placement of measurement points on a large scale [56].

2.8.1 Multi-path Fading

Multipath fading is the major decline of a great impact on system performance in wireless channel, and the causes are complex [59]. Video steaming requires steady flow of information and delivery of data packets. Wireless mobile communication systems face challenges to meet these requirements due to random nature of mobile radio channels characterized by multipath fading and shadowing that cause variability in link capacity and

transmission error rates [60] .The AWGN channel has been considered for UWB communications, but unfortunately this not realistic in many cases and therefore a more realistic channels model must be constructed [61]. This is due to the fact that not only one path exists between transmitter and receiver in a typical environment as illustrated in Figure 2-15. In this propagation example pulses transmitted from the transmitter on the left to the receiver on the right. Due to reflection, diffraction and scattering, all the electromagnetic pulses will add up creating the electromagnetic field imposed on the receiving antenna. An environment such as this that gives rise to more than one path from transmitter to receiver is known as multipath propagation environment, this phenomenon leads to multipath fading effects.

The three radio propagation mechanisms impact the strength of the received signal in different ways. If there is a strong LOS between the transmitter and receiver, diffraction and scattering are not the dominant factors in the propagation of the radio waves. However, in the absence of a LOS between the transmitter and receiver, diffraction and scattering become the dominant factors in the propagation. Typically, the received signal is a sum of the components arising from the above three phenomena. The strength of the received signal fluctuates rapidly with respect to time and the displacement of the transmitter and receiver [62].

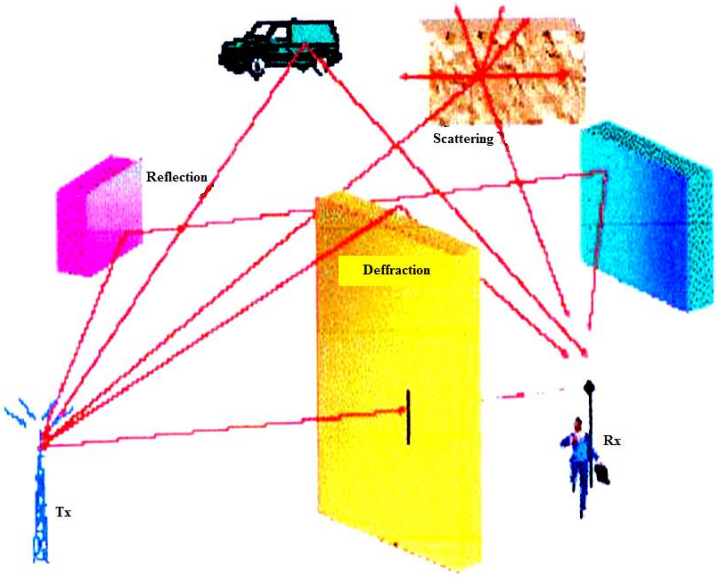

Figure 2-15 Illustration of Multipath Propagation Environment.

2.8.2 Types of Fading Effects

Radio propagation is studied in terms of large-scale and small-scale effects. Figure 2-16, shows that large-scale effects involve the variation of the mean received signal strength over large distances or long time intervals, whereas small-scale effects involve the fluctuations of the received signal strength about a local mean, where these fluctuations occur over small distances or short time intervals [63].

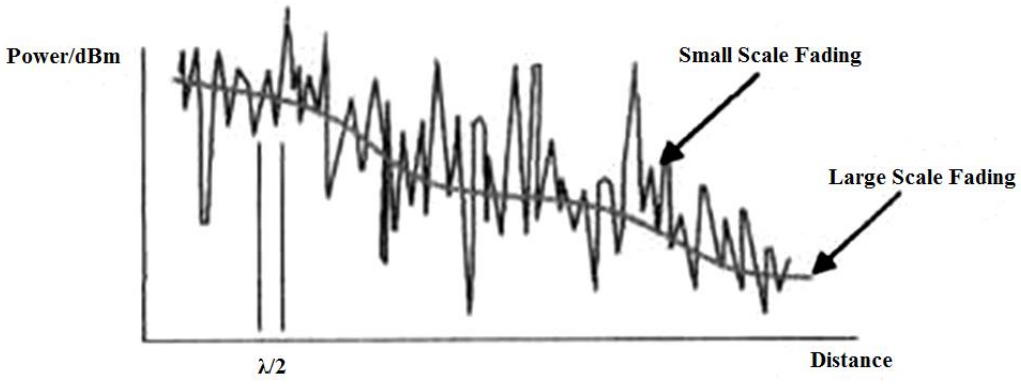

Figure 2-16 Small-Scale vs. Large-Scale Fading.

2.8.2.1 Small-scale Fading

Small-scale fading can be classified into different types depending on multipath delay spread and Doppler spread as shown in Figure 2-17 [63]. In the following, we describe these categories. Rapid motions and high velocities typical of the mobile users are absent in the indoor environment. The indoor channel's Doppler shift is therefore negligible.

Small-scale fading describes the rapid fluctuations of the channel envelop due to multipath (interferences between different components of the transmitted signal) and Doppler spectrum [64].

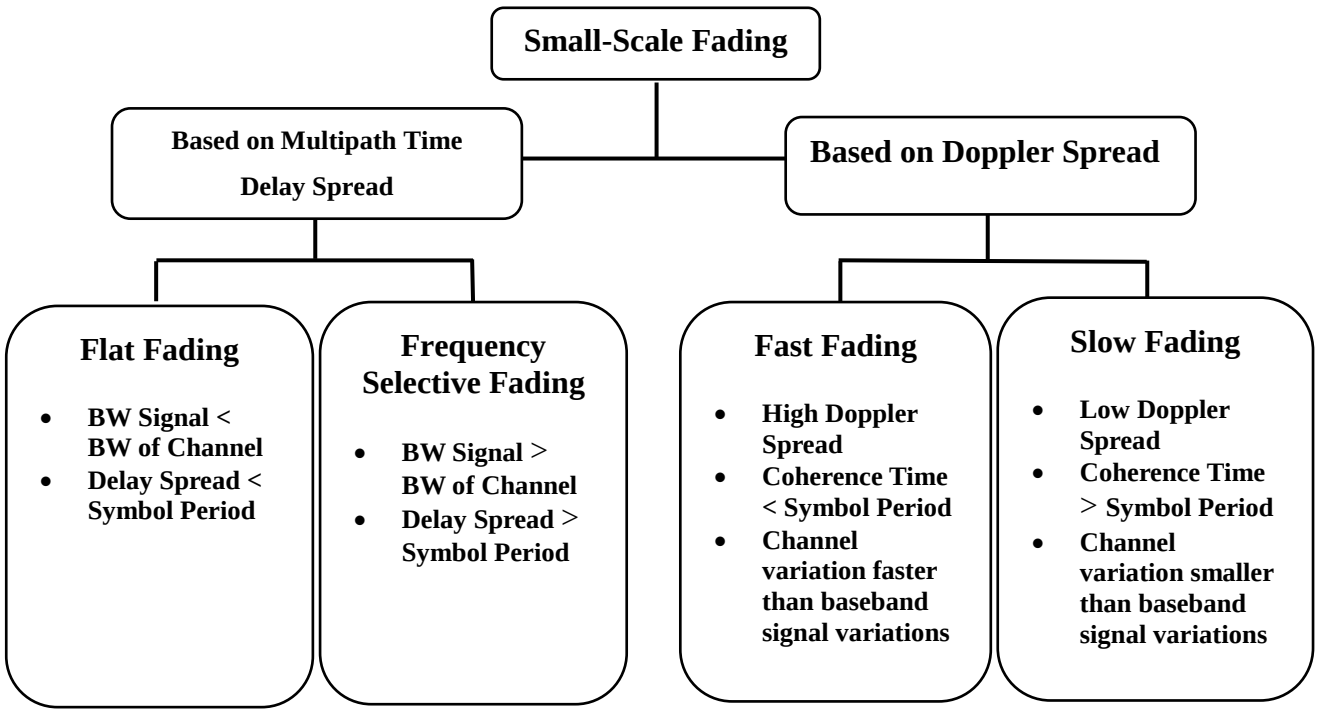

Figure 2-17 Types of Small-Scale Fading.

More details on these types in [63], [65],

2.8.2.2 Large-scale Fading

Large-scale fading analysis is concerned with predicting the mean signal strength as a function of transmitter-receiver T_x-R_x separation distance *d* over T_x-R_x separations of hundreds, thousands, or millions of meters. For the applications discussed in this waiver application, the T_x-R_x separations will be less than one kilometer for part 15 power levels. In order to quantify the path loss over this separation, *d* the d^n path loss model will be utilized. This model has proven to be a good first order of approximation (representation of the large-scale effects) for predicting the distance dependant received power in a wireless system [66].

A. **Outdoor Environment**

The path loss exponent *n* is an empirical constant that is often measured, but can also be derived theoretically in some environments. The rate at which the signal falls off, or the path loss exponent is dependent on the environment where the wireless system is located. The environment can be as different as a multi-story office building to propagation over a wide open field or desert on outdoor environments.

Rappaport [66] provides typical path loss exponents, *n*, for outdoor environments listed in Table 2-3.

Environment	Path loss Exponents n
Free Space	2
Urban area cellular / PCS	2.7 to 4.0
Shadowed urban cellular / PCS	3 to 5

Table 2-3 Typical Path Loss Exponents for Outdoors Environments.

The path loss exponent *n*, is approximately 3.2 for 1920 MHz (close to the center frequency of Time Domain's UWB system) for separation distances of 0.5 – 10 km. Experiments performed on a much smaller scale by Time Domain also reflect a path loss exponent of about 3. The Longley-Rice [67] model is another industry standard for propagation models. This model also confirms the values in Rappaport's table above. The

Longley-Rice model also lends credence to the d^n method used in this overview as a good first approximation because there are several effects that are negligible for the frequency range, separation distances, and antenna heights specific to the applications brought forth in this waiver application. For instance, since the separation distances will be at most 1 km and the frequency range approximately 1-3 GHz, the atmosphere will have little effect, as well as atmospheric absorption (Particularly water vapor) and rainfall attenuations are negligible. Since these models show that *n* is generally greater than 2 and since the greater the value of *n*, the more quickly the field strength of the signal decays, then it is conservative to use a value of $n = 2$ for predicting the interference potential of UWB emission in an out-of-doors environment.

B. **Indoor Environments**

For indoor environments, the propagation mechanisms can be substantially different that in outdoor environments. There can also be a wide range of variability ever amongst indoor environments, for instance, large open factories and warehouses compared to skyscraper office buildings with many offices on a single floor. The building materials used in walls, both internal and external, as well as ceilings and floors can also vary the results. Furthermore, there will be more attenuation of the higher frequencies in building penetration. Rappaport provides path loss exponents for indoor environments [66], as shown in the Table 2-4.

Environment	Freq. (MHz)	n
Hard partition office	1500	3.0
Soft Partition Office	1900	2.6
Factory (LOS)	1300	1.6 – 2.0
Factory (LOS)	4000	2.1
Factory (Obstructed)	1300	3.3
Factory (Obstructed)	4000	2.1

Table 2-4 Typical Path Loss Exponents for Indoor Environments [67].

Owen and Pudney [67] in "In-Building Propagation at 900 MHz and 1650 MHz for Digital Cordless Telephones", offer experimental results in support of the model proposed by Motley and Keenan [68] .

2.8.2.3 Lognormal Shadowing

In wireless communication, lognormal shadowing is the dominant contributor to interferences. Outage probability computation based on the sum of interferes requires providing the sum of lognormal Random Variables (RVs) distribution. However, there is no closed form expression for this distribution yet [69].

As the receiver moves in an indoor environment, it often travels into a propagation shadow behind obstacles much larger than the wavelength of the transmitted signal and therefore, experiences a severe attenuation of the received signal power. This phenomenon is called shadowing. A lognormal distribution is often used to characterize the shadowing process in narrowband systems and is assumed for UWB transmission [70].

2.8.3 Statistical Representation of fading Channels

Fading in a multipath environment may follow different distribution depending on the area covered by measurements, presence or absence of a dominating strong component, and some other condition. Most common distributions are described below [71]. The probability density function pdf is an important statistic that is used to represent a channel model. Major common distributions are Rayleigh, Rician, Nakagami and Lognormal Distribution.

2.8.3.1 Rayleigh Distribution

The Rayleigh distribution is the most widely used distribution to describe the received envelope value [72], [73]. The Rayleigh flat fading channel model assumes that all the components that make up the resultant received signal are reflected or scattered and there is no direct path from the transmitter to the receiver.

2.8.3.2 Rician Distribution

The Rician shadowed (RS) fading channel was originally proposed by Loo to describe land mobile satellite (LMS) links with completely or partly blocked line of sight (LOS) component [74] .

The Rice distribution is also a two-parameter distribution that may be used to characterize the signal in a Graussian fading channel in which the impulse response has a nonzero mean component, usually called a specular component. When the received signal is made up of multiple reflective signals plus a significant Line-Of-Sight (LOS) component, the statistical distribution of envelop amplitude has best fit to Rician distribution due to nature of simulated LOS propagation indoor channel [75].

2.8.3.3 Nakagami m-Distribution

Two distributions thathave been used in the non-Rayleigh regime are the K and the Nakagami distributions [76], [77], [78] . In creating a Nakagami m-distribution, Nakagami was able to span with one distribution the entire range from one-sided Gaussian fading to non-fading [72]. The real importance of the Nakagami-m fading model lies in the fact that it can often be used to fit experimental data, the measurements on a variety of propagation paths spanning nearly all frequency bands. Estimating the probability density function (pdf) of observed signal is imperative in many engineering applications. There are two ways to estimate a given pdf, viz. parametrically or non-parametrically. Both have their own merits and demerits [79] .

2.8.3.4 Lognormal Distribution

Lognormal distribution is quite effective in analysing positively skewed lifetime data, and has found wide applications in reliability engineering, life testing, and industrial experiments. Almost a book length treatment on this distribution can be found in Johnson et al. [80], [81].

The fading over large distances causes random fluctuations in the mean signal power. Evidence suggests that these fluctuations are lognormally distributed. The distribution has

often been used to explain large scale variations of the signal amplitudes in a multipath fading environment [72].

2.8.4 Multipath Delay Spread

Time dispersion varies widely in a mobile radio channel due to the fact that reflections and scattering occur at seemingly random locations, and the resulting multipath channel response appears random, as well. Because time dispersion is dependent upon the geometric relationships between transmitter, receiver and the surrounding physical environment, communications engineers often are concerned with statistical models of time dispersion parameters such as the average RMS or worst-case values. Some important time statistics may be derived from Power Delay Profiles (PDPs), and can be used to quantify time dispersion in mobile channels. Power delay profiles can be measured in many ways [82]. Typically, a channel sounder is used to transmit a wideband signal, which is received at many locations within a desired coverage area. This channel sounder may operate in time or frequency domain, and, of course, the two measurement techniques are equivalent and related by the Fourier transform. A swept in the frequency response will reveal that the channel is frequency-selective, causing some portions of the spectrum to have much greater signal levels than others within the measurement band [83], [84].

2.8.5 UWB Channel Models

UWB communication systems maybe achieved in the form of single band impulse radio (Time Hopping (TH) or Direct Sequence (DS)) and multi-band orthogonal frequency division multiplexing (OFDM) communication systems [85].

The goal of UWB channel modeling is to understand the characteristics of the propagation channel where UWB devices are operating in order to help implement an efficient high data rate communications system. The model chosen by IEEE 802.15,Task Group 3a (TG3a) should be relatively simple so that physical layer proposes can easily use the model to test and evaluate the performance of their proposal in typical environments. In order to optimize the utility of this channel model, TG3a must balance the trade-off between the need for a simple model and the accuracy of the model. The IEEE 802.15.3a standards task group has established a standard channel model to be used for the evaluation of PAN physical layer proposals [86]. This section discusses models for indoor fading channels

that are being considered by IEEE 802.15.3a standardization (since these are the channels of interest for most UWB devices) [62].The basic parameters to consider in a channel model are path loss and the behavior of multipath in the relevant environments (such as office or home, Line Of Sight (LOS) or Non-Line Of Sight (NLOS), etc.). For a path loss model of a UWB channel, the narrowband model (known as Friis free space model) based on the assumptions of a flat frequency response and isotropic antennas can be used to give a good approximation of the UWB channel. Since it may be difficult to consider all the characteristics of a multipath channel in a single simple model, TG3a has chosen to focus only on the following primary characteristics of the indoor multipath channel: RMS delay spread, the power decay profile and the number of multipath components. Different of measurements and proposed models are discussed below [87], [88], [89], [90], [91], [92], [93], and [94].

- J. Foerster and Q. Li Model

- M. Pendergrass Model

- J. Kunisch and J. Pamp model

- A. Molisch, M. Win, and D. Cassioli Model

- UWB (S-V) Channel Model.

CHAPTER 3

3 UWB MODULATION TECHNIQUES AND UWB WAVEFORM

3.1 UWB Waveform - Symbol Representation in Time Domain

In UWB systems, information is encoded in a series of baseband pulses and transmitted without a carrier. Hence, the transmitters require precise pulse shaping to produce the required spectrum and maximise the antenna emission. Producing emissions with flat and wide power spectral densities (PSDs) requires extremely accurate pulse designs [25].

As previously mentioned, ultra wideband (UWB) signals are produced by pulsed emissions, where a very wide RF bandwidth is related to a narrow pulse width. Unlike many conventional radio transmitters, (in which a modulated signal is up-converted and amplified), in UWB systems, information is encoded in a series of baseband pulses and transmitted without a carrier [25]. Hence, the transmitters require precise pulse shaping to produce the required spectrum and maximise the antenna emission.

Common approaches include using avalanche transistors, tunnel diodes, and other exotic devices [95]. The technology developed by Time Domain Corporation is called Time Modulated UWB (TM-UWB). The TM-UWB transmitters emit ultra-short "Gaussian" monocycles with tightly controlled pulse-to-pulse intervals, commonly known as Pulse Repetition Interval (PRI). When using time hopping (TH) as a multiple access technique, the PRI is varied on a pulse by pulse basis in accordance with a channel code that is a pseudo-random noise (PN) sequence.

Generally, UWB systems use long sequences of monocycles for communications, not single monocycles. Each information bit is represented by a group of pulses. Hence, each duration bit, T_b, is divided into a group of time frames, referred to as T_f, where the pulses are to be located somewhere, as shown in Figure 3-1. The number of pulses used to convey data bit, referred to here as N_s, introduces a processing gain to the system due to the pulse repetition. This processing gain is also increased by the low transmission duty cycle.

Therefore $N_s = T_b / T_f$ and the bit rate is defined as $R_b = 1 / N_s T_f$ [15], [96]. Note that this redundancy is very useful for receiver confirmation, so as to be able to overcome channel noise or distortion. This means that, if one pulse is distorted during transmission, the receiver can still recover the information bit from the rest of the pulses. Since UWB operates under the noise floor, therefore, there is a minimum limit to the number of pulses used to represent a single bit. If the number of pulses decreases than this minimum limit, bit recovery may be very difficult [47].

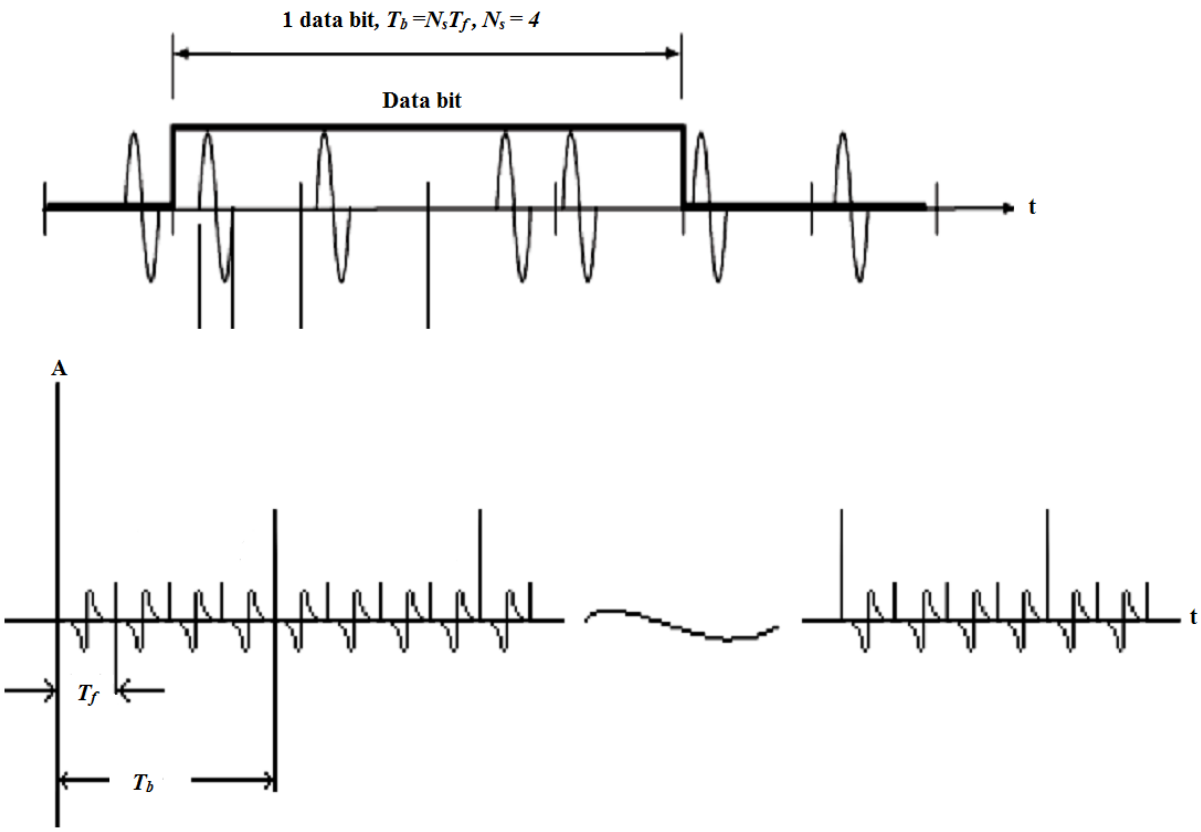

Figure 3-1 Symbol Representation of A Single Bit for UWB Waveform in Time Domain.

Since UWB operates under the noise floor, therefore, there is a minimum limit to the number of pulses used to represent a single bit. If the number of pulses decreases than this minimum limit, bit recovery may be very difficult. In Chapter 5, it will be shown that this parameter (N_s) strongly affects the performance of the system considering the bit error rate

(BER) for the modulation technique used. It will be clearly shown that as N_s increases, the performance of the system greatly improves and the BER decreases.

3.2 Time Hopping Spread Spectrum (THSS)

Spread spectrum communications systems are often used when there is a need for message security and confidentially or where there is requirement that the message be received error free [97]. A spread spectrum system is able to offer a very high degree of message security in a number of ways, depending on the system implementation. Such a system may spread the data over a very wide bandwidth, making it almost impossible for a narrowband receiver to decipher any useful information. A long a similar vein, the same system may be able to over a very high degree of interference rejection, both from international and unintentional sources. A spread spectrum transmission technique in which a Pseudo Noise (PN) code, independent of the information data, is employed as a modulation waveform to "spread" the signal energy over a bandwidth much greater than the signal information bandwidth [98]. At the receiver the signal is "dispread" using a synchronised replica of the PN code as shown in Figure 3-2.

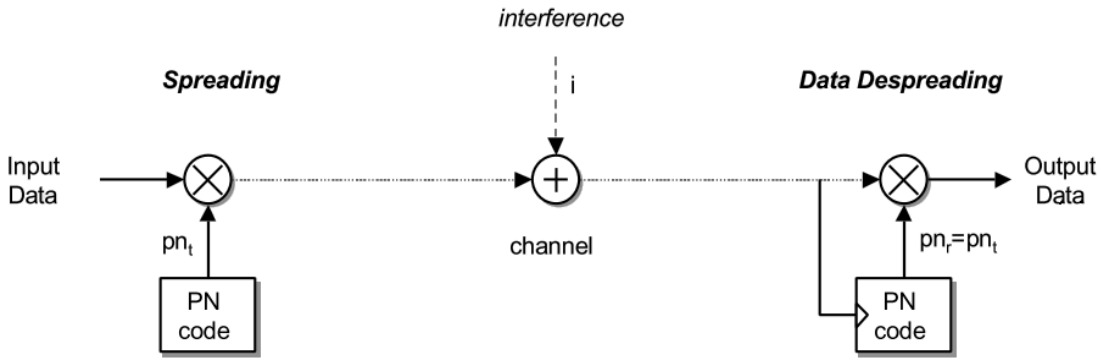

Figure 3-2 Block Diagram of the Spread Spectrum System.

Several known techniques can be used to achieve spread spectrum such as Direct Sequence Spread Spectrum (DS/SS), Frequency-Hopping (FH/SS), and Time-Hopping Spread Spectrum (TH/SS) however, Time-Hopping (TH) is currently the most popular approach for UWB. In a time-hopping system the transmission time is divided into intervals known as frames. Each frame is divided into N_h time slots with duration T_c. During each frame

one and only one time slot will be modulated with a message. All of the message bits accumulated in the previous frame are transmitted in a burst during the selected time slot [99]. Without time-hopping (or some other multiple access scheme), catastrophic collisions could occur if the frames from different transmitters aligned at the receiver.

Although a large number of pulses make the reception process more confirm to the receiver, however, their periodicity in time introduces some problems. Firstly, the highly regular pulse train produces energy spikes as “comb lines” in the frequency domain at regular intervals, as shown in Figure 3-3, which might interfere with other existing conventional radio systems [100].

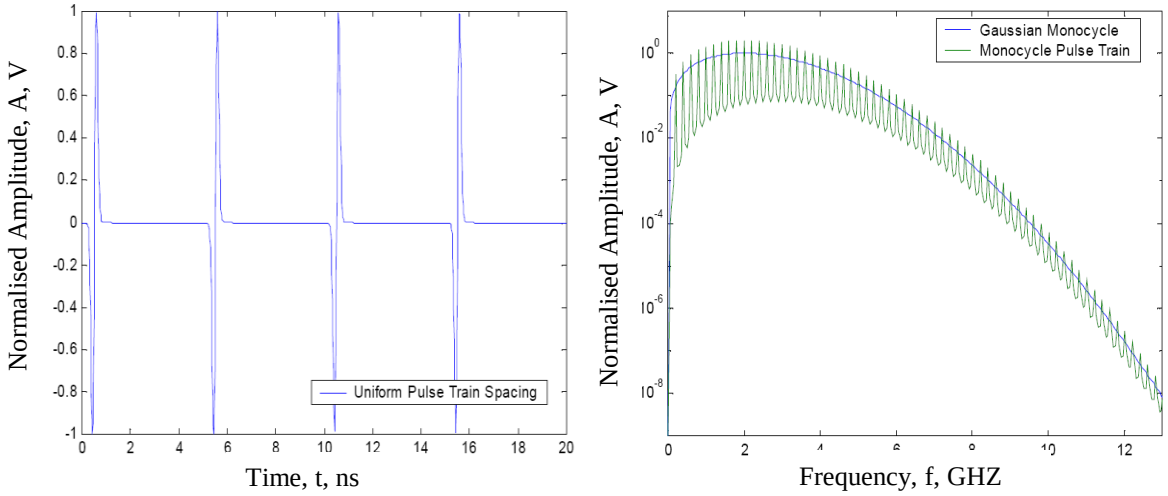

Figure 3-3 Uniform pulse train in time and frequency domains.

It has been proven that, varying the pulse-to-pulse time interval (PRI) can reduce or perhaps eliminate the comb lines, as shown in Figure 3-4 [27], [47], [100].

Secondly, if other users are simultaneously using the system, catastrophic collisions between their pulses can occur resulting in an irreversible corruption of the transmitted message which makes the system inappropriate for multiple access environments.

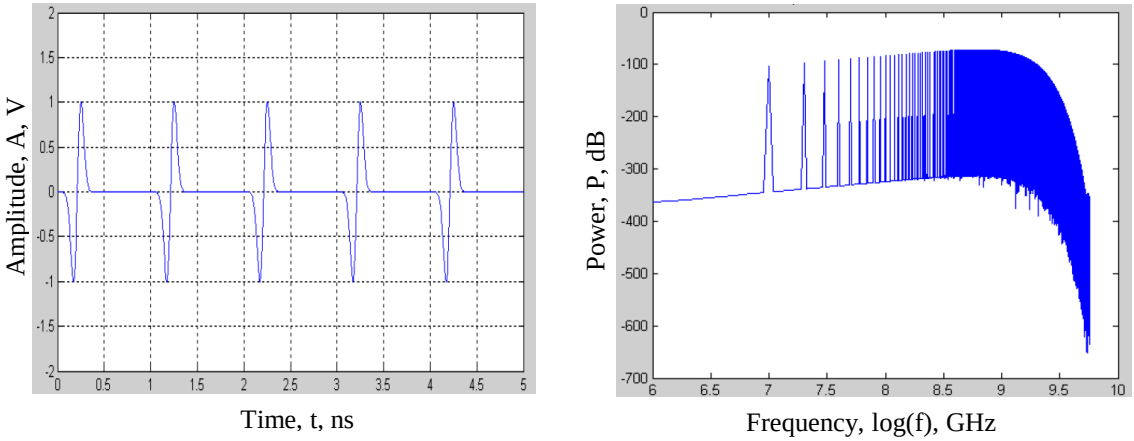

(a) Periodic pulse train and its spectrum

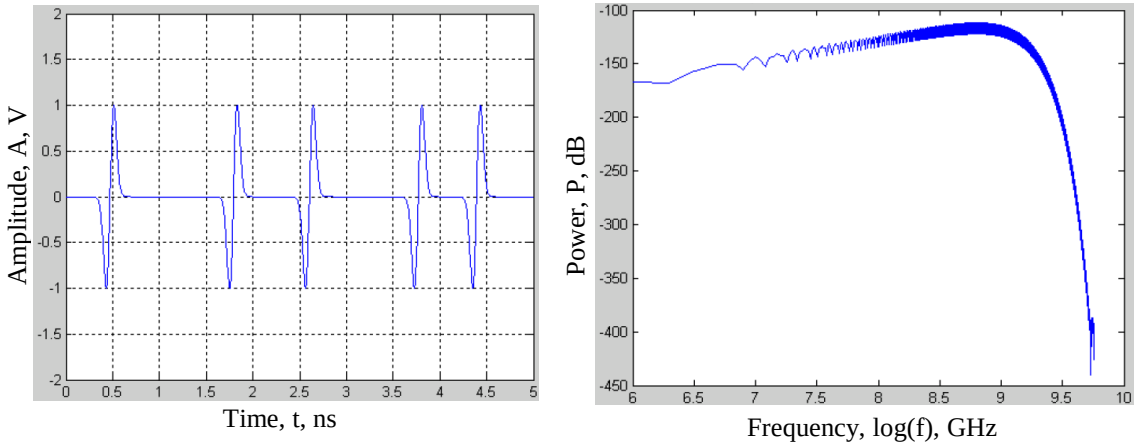

(b) Random positioned pulse train and its spectrum

Figure 3-4 Periodic and un-periodic pulse trains and their spectra.

Therefore, some form of spreading technique must be introduced to eliminate these problems. There is a lot of spreading techniques that can be applied to UWB. However, a very useful candidate to overcome these problems, is the time hopping spread spectrum (THSS) multiple access technique which we will focus on in this research [18], [19], [101], [102].

Thus, In THSS, each monocycle's transmission time is determined by a PN noise code which is used as a channel code to add a time off set to each impulse. Therefore, each time frame is further divided into smaller compartments, called time slots, of duration T_c where the pulses are to hop in between, as shown in Figure 3-5. The number of time slots per frame will be referred to as N_h (Therefore $T_f = N_h T_c$), where each user is supposed to transmit his/her pulse in only one of them. Hence, an extra time shift is added to the pulse, namely $c_j^{(k)} T_c$, where $c_j^{(k)}$ is a decimal PN code assigned for the j^{th} monocycle for the k^{th} user and takes an integer value in the range $\{0,1,\ldots, N_h\text{-}1\}$ [103].

Figure 3-5a shows a typical example of a TH-UWB system where $N_s = 4$ and $N_h = 5$. The value of the PN code is $c_j = 0, 3, 1, 3$, with a maximum possible value of 4. Figure 3-5b further amplifies a single time frame of another system which is divided into 8 possible hop positions (i.e., $N_h = 8$) and a single pulse is depicted at the 4th position. It can also be shown in Figure 3-5 that the pulse width T_p should be less than or equal the chip length T_c to avoid overlapping of the pulses from different users.

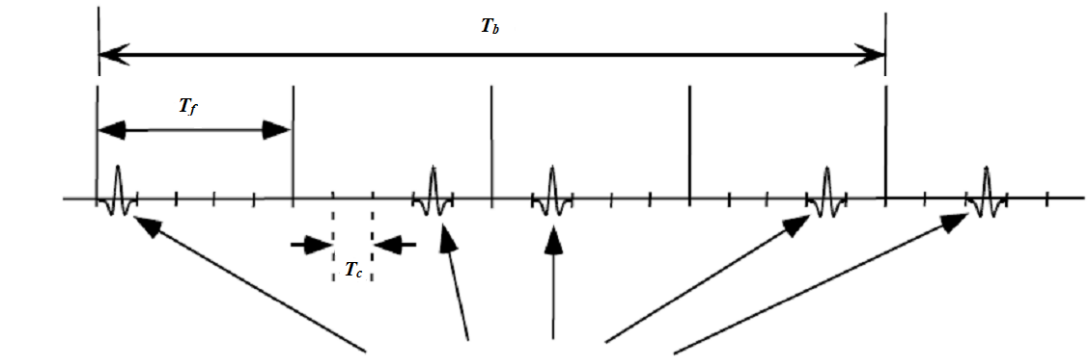

(a) TH-UWB system with $N_s = 4$ and $N_h = 5$.

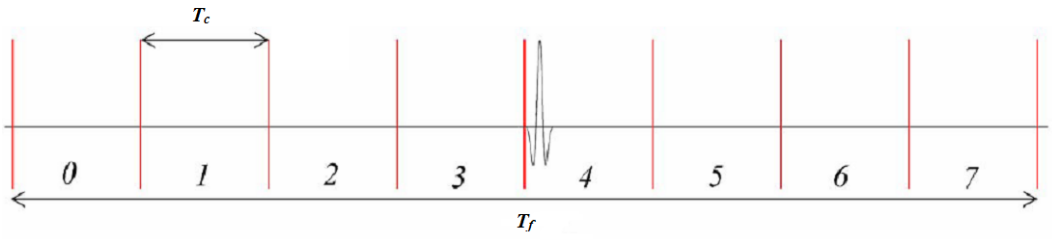

(b) Example of a pulse shifted to the 4^{th} position in a frame with $N_h = 8$.

Figure 3-5 Typical Behaviour of a Time Hopping UWB Signal.

Since each user k has their own unique PN code, therefore as the number of users increases, each time frame T_f begins to carry more than one pulse; each is located in a specific time slot T_c owned by a specific user according to their specific PN code The advantages of using PN codes in TH-UWB systems are many as suggested by [103] [101].

1- By shifting each monocycle's actual transmission time over a large time frame in accordance with a pulse code, a pulse train can be channelized permitting a multiple access environment to take place where each user would have a unique PN code sequence.

2- If multiple access signals would have been composed of uniformly spaced pulses only, then collisions from the train of pulses coming from the signals of the other users simultaneously using the system can corrupt irreversibly the message. Therefore, a channel code is needed to protect from collisions in multiple accessing.

3- This channel code also allows the data to be detected by the intended receiver, i.e., only a receiver operating with the same PN code sequence can decode the transmission. Therefore, data transmitted is more secure in hostile environments and also with less interference with multiple users.

4- Shifting each monocycle at a pseudorandom time interval, the pulses appear to be a white background noise to users with different PN codes in the time domain.

5- The periodic monocycles in time domain are transformed to energy spikes "comb lines" at regular intervals in the frequency domain that can interfere with existing radio systems. Varying the pulse-to-pulse time interval reduces these comb lines. By eliminating the energy spikes in the frequency domain, no interference will happen with conventional RF systems than if the pulses were placed uniformly in the time domain since in this case the UWB signal appears indistinguishable from white noise.

6- The use of PN sequence in TH may theoretically imply that the system could have an infinite number of users all on a different PN channels.

Although, theoretically, the use of PN codes in TH may imply that the system could have an infinite number of users, however, practically this does not guarantee that collisions cannot happen, whatever the randomness of the PN codes are, specially when the number of users increases. A possible solution, proposed by work later, as it will be show in Chapter 5, to overcome this problem, is by simply increasing the number of time slots per frame (i.e., increase N_h) for a given number of users. However, this approach is limited by the pulse width and the modulation scheme applied. Increasing N_h will further decrease the chip width T_c which is limited to the pulse width T_p to avoid overlapping of pulses. In Chapter 5, it will be shown that the performance of the system greatly improves when N_h is increased for a given number of users. The probability of a single user's pulse occupying a particular time slot decreases. Hence, collisions from pulses of different users decrease, leading to a decrease in the BER.

3.2.1 The Modulation Schemes in Time-Hopping Format

After discussing the modulation type and introducing the time-hopping technique we can now formulate the transmitted signal for all previous modulation schemes using time-hopping technique. Thus the transmitted signal in (TH-SS) using PPM is given by the equation (3.1), and will be explained in more detail in Chapter 4.

$$s(t) = \sum_{j=-\infty}^{\infty} p(t - jT_f - c_j T_c - \delta d_j) \tag{3.1}$$

With the energy of the pulse p(t) being unity. On a large scale, the time is partitioned to frames with duration T_f. Within each frame, there are N_s (number of monocycles, modulated by each information bit) monocycles. Each monocycle experiences a distinct extra delay $c_j T_c$ different from the rest of the monocycles within the frame in order to avoid catastrophic collisions in multiple-access. Depending on the information bit, all the monocycles in the form experience an extra common delay δ (> 0) for information symbol '0'. Similarly, the transmitted signal in (TH-SS) using PAM, BPSK and OOK with respect to b_j is different for each one can be written as follows

$$s(t) = \sum_{j=-\infty}^{\infty} b_j \; p(t - jT_f - c_j T_c) \tag{3.2}$$

3.3 UWB Modulation Schemes

Of course, a simple monocycle pulse train does not carry information. In order to convey information, some form of modulation is required for communication. Modulation also helps to further “smooth” the spectral spikes associated with the unmodulated pulse train.

The program information, can vary between a movie, song, or text message, this data is impressed onto the pulse train having a specific amplitude, spacing, phase, shape, or duration of the individual pulses in the train [46]. In the conventional modulation techniques, which are still used in most digital wireless systems, data is transmitted through carrier wave; whereas in UWB changes in the phase of the radio wave are used to transmit information. However, the basic concept remains the same: the transmission information is carried through changes in some parameters of the signal, be it a pulse position or a sinusoid phase [46].

From this point, a set of many different modulation techniques have been originally proposed for UWB signals. Additional processing is needed to modulate the monocycle pulse train, so the system can actually transmit information. Although numerous modulation techniques are used with impulse-radio UWB, the common schemes are often found in research papers and journals. Pulses can encode information in the amplitude (PAM), polarity (BPSK), position (PPM), or in the existence of a pulse (OOK) and popular UWB modulation techniques due to their simplicity and flexibility towards low duty cycle pulsed communication systems and all the pulses have the same shape [104]. Moreover, modulation techniques vary from simple binary pulse position, to the more efficient M-ary (multilevel or multi state) modulations. The choice of an appropriate modulation scheme is a major challenge in the design of a UWB system. Data rate, transceiver complexity, and the BER performance of the transmitted signal are all related to the implied modulation scheme.

In the following section, we will briefly illustrate the operation of the commonly used UWB modulation schemes, namely, PPM, PAM, BPSK, and OOK, all combined with the TH multiple access technique under research, except OOK. This is because OOK cannot take advantage of TH spreading because of the blank transmission of the bit "0", and because it would create further problems for synchronisation [52].

It must be noted that, in this research, we only focus on the TH-PPM technique to investigate how the choice and optimisation of some system or signal parameters can greatly enhance and improve its performance. Therefore, there is no need to additionally increase the transceiver complexity, either by working with higher multi levels or even thinking of making hybrid modulation techniques, which is a combination of different modulation methods.

3.3.1 Pulse Position Modulation (PPM)

Pulse Position Modulation (PPM) is one of the most popular modulation techniques in UWB literature. In N-ary PPM shifting a pulse to N different pulse positions so that they will overlap [105]. The simplest form of PPM is binary PPM, where a pulse in a uniformly speed pulse train represents a "0" and a pulse offset in time from the pulse train represents a "1". The most advantageous feature of PPM is orthogonal signalling present in its data. Each of the pulses in time is independent of one another, meaning the time during the symbol period can be broken up to look for each pulse within a specified time slot.

The main demerit of PPM is its performance, where the distance between symbols is the same as in OOK. This lack of signal energy causes binary PPM to have the same probability of bit error as OOK, or 3 dB worse than Biphase Modulation [105]. Additionally, PPM is vulnerable to Inter Symbol Interference (ISI), because multiple positions are required to transmit at a higher data rate. The transmitted pulse rate must be lowered to resolve this issue. Conclusively, there is a data rate limitation when using N-ary PPM in impulse-radio UWB applications. Even after the reduction of ISI at the transmitter through decreasing the pulse rate, multipath have the potential to cause an overlap with the next data pulse, causes bit errors at the receiver if the reflections are strong.

TH combined with PPM was originally proposed for UWB systems by [20]. With PPM, the information is carried in the fine-time shift of the pulse by an amount of time, referred to as $'\delta'$. This small time shift, determines the position of the pulse in accordance to an information bit (i.e. PPM is used to adjust the timing of a series of monocycles).

Figure 3-6 illustrates this property by showing how two 1st order Gaussian monocycles, separated by $'\delta'$, can be used to represent two different bits '0' and '1' [52].

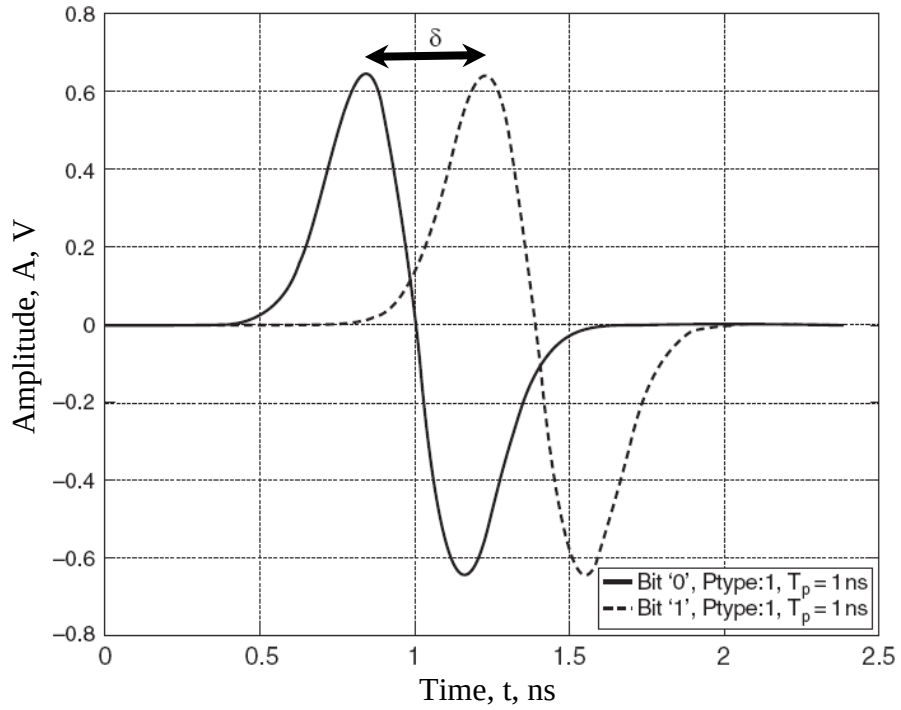

Figure 3-6 PPM Pulse Shapes for '1' and '0' Bits.

The original proposal for UWB PPM systems in [96] considers information bits {0, 1}. In this modulation scheme, no additional time shift modulates the pulse when the data bit is '0', and a time shift of *'δ'* is added to the pulse when the data bit is '1'. This scheme is called a type-A TH-PPM UWB system in this thesis. Another approach uses antipodal data bits. In this case, the pulse train is modulated by delaying or advancing individual pulses in time, according to a given reference. The pulse is delayed by '*δ*' when the data bit is '0', and is advanced by '*δ*' when the data bit is '1'. This scheme, here called a type-B TH-PPM system, is also shown to make the review of TH-PPM complete. However, the model used to evaluate the performance of the system will be based on type-A TH-PPM systems.

3.3.1.1 Type-A TH-PPM UWB System

Type-A PPM is a commonly used implementation in which a small time shift *"δ*" is added to the monocycle if the data symbol is logic "1", with no time shift applied to a data symbol of logic "0" [20]. This is an implementation decision, and no restriction can be imposed to either approaches.

Figure 3-7 shows a uniformly distributed pulse train with an extra time shift only added to pulses representing a logical '1'. In this example, the repetition code is set equal to 4 (i.e., each bit is represented by 4 pulses). Note that no TH is applied (the case of a single user where $T_f = T_c$) to clearly show the operation of type-A PPM.

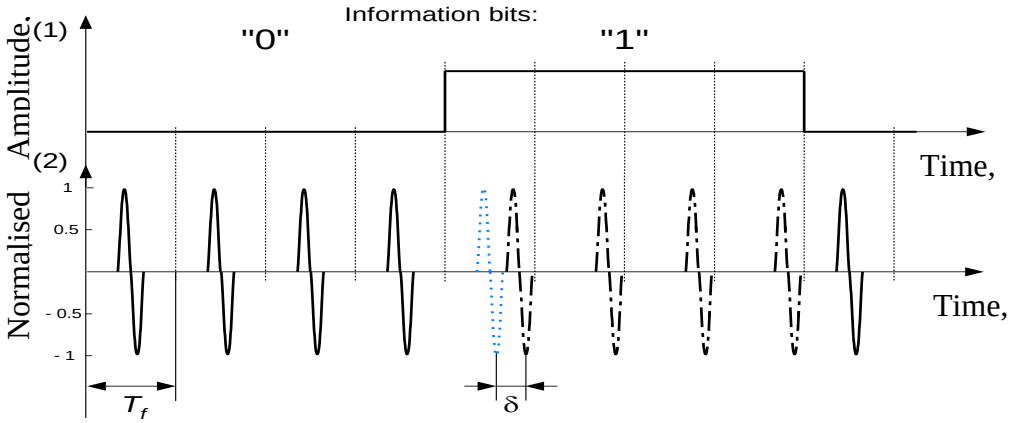

Figure 3-7 Uniformly Spaced Pulse Train with PPM dithering.

Figure 3-8, shows a brief example of a TH-PPM asynchronous UWB system operating in a multiple access environment of three users. Only two frames are depicted for each user, each is subdivided into six time slots {0, 1,…,5} (i.e. $N_h = 6$) where the pulse of each user is to hop in between according to his/her unique PN separate code. For simplicity in the example, one assumes that each bit is represented by a single pulse (i.e. $N_s = 1$ and $T_b = T_f$). The TH pattern and the information bit sequence of each user used in this example are as follows:

Users	TH pattern	Bit sequence
User 1	1 , 3	1 , 0
User 2	0 , 4	0 , 1
User 3	5 , 3	1 , 0

Table 3-1 TH Pattern and Bit Sequences used in the example of Figure 3-8.

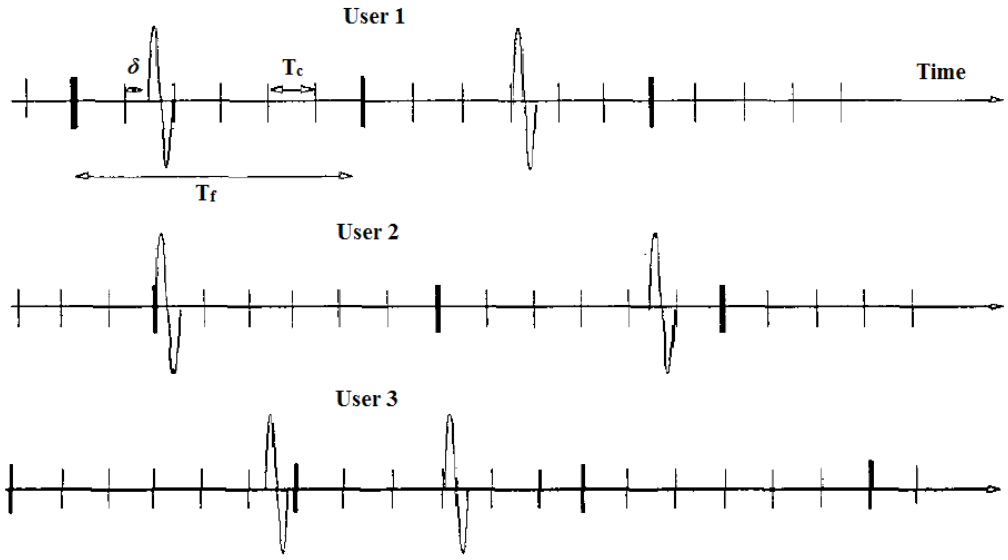

Figure 3-8 Example of Type-A TH-PPM Asynchronous Multiple Access Format.

It can be clearly seen in this example that a time shift of "δ'' is added to pulses representing a logical "1", with no time shift added to pulses representing logical "0". On the other hand, to exactly (or optimally) determine how much time shift must be applied to the pulse in order to represent an information bit, one must refer back to the autocorrelation properties of the pulse in use. As will be seen in Chapter 5 the performance evaluation of the TH-PPM is highly dependent on the choice of an appropriate "δ'' which in turn depends on the shape and time properties of the pulse. It will be shown that best BER performance is obtained when the autocorrelation of a pulse has a minimum value at which the value of "δ'' is that of an optimum one.

3.3.1.2 Type-B TH-PPM UWB System

Figure 3-9 illustrates a very simple example of type-B PPM showing how the transmission time of a single pulse can be adjusted by delaying or advancing the pulse according to a given reference point.

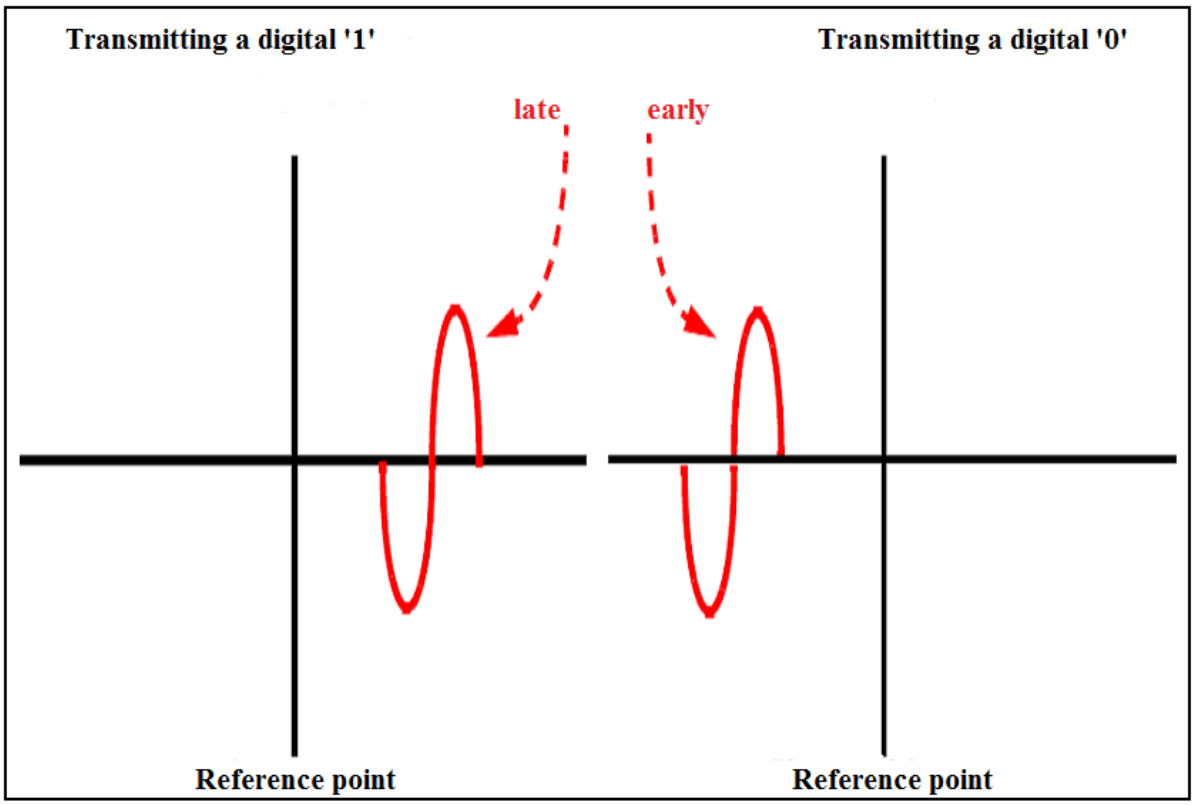

Figure 3-9 Type-B PPM Transmission of Bit '0' and '1'.

Figure 3-10 shows the pulse train used by Time Domain Corporation (TDC) is a developer of Ultra Wideband products in time and frequency domains [103]. Figure 3-10a illustrates a uniformly distributed Gaussian monocycle pulse train. In the frequency domain, this highly regular monocycle pulse train produces energy spikes ("comb lines") at regular intervals; thus, the already low power is spread among the comb-lines. This monocycle pulse train carries no information and, because of the regularity of the energy spikes, might interfere with conventional radio systems at very short ranges. TDC's systems use type-B pulse position modulation as illustrated in Figure 3-10b, which varies the precise timing of transmission of a monocycle about the nominal position. In such a system a "0" digital bit might be represented by transmitting the pulse early and a "1" digital bit by transmitting

the pulse late. As shown in Figure 3-10b, PPM distributes the RF energy more uniformly across the band (it "smoothes" the spectrum of the signal), thus making the system less detectable.

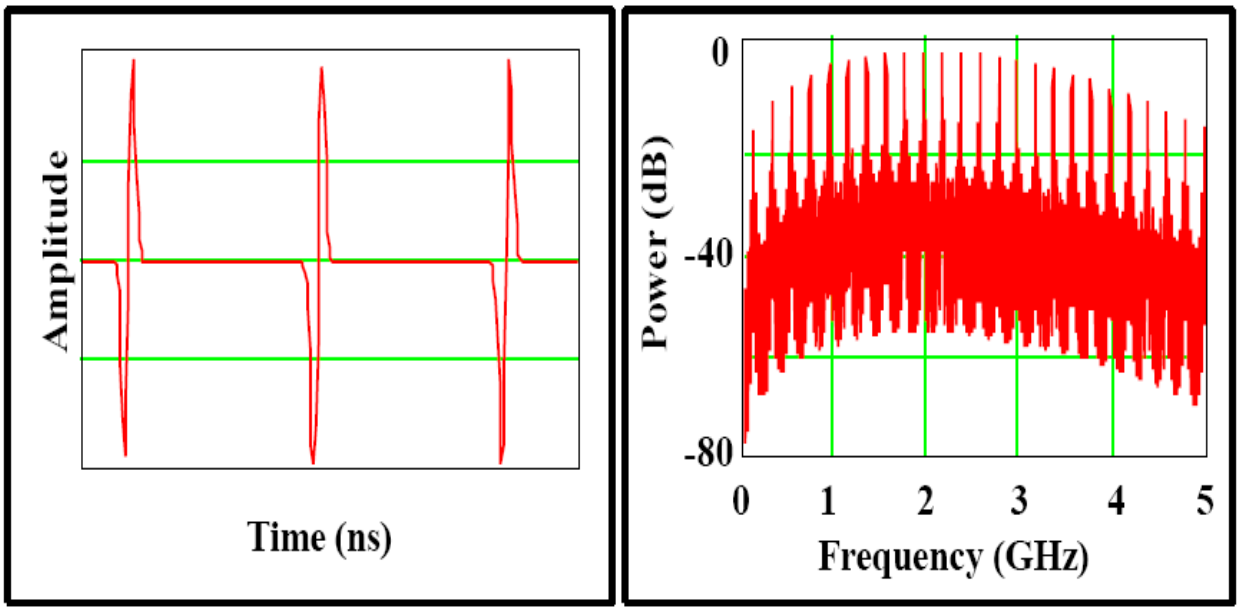

(a) A uniformly spaced pulse train in time and frequency domains

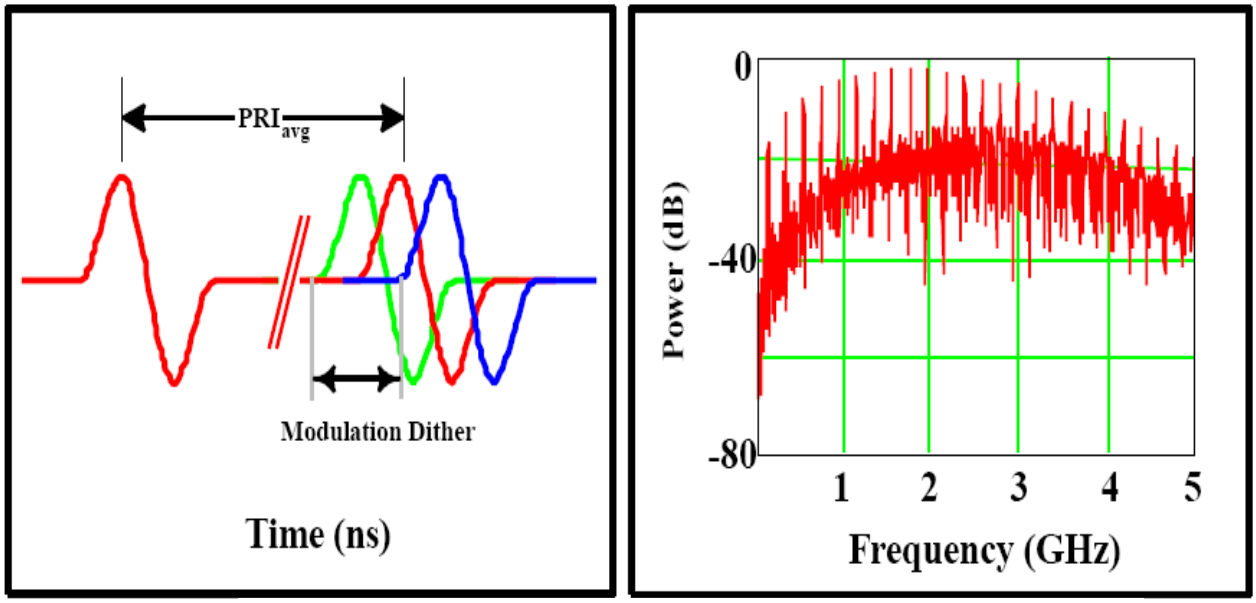

(b) TDC's PPM technique in time and frequency domains

Figure 3-10 TDC's Illustration of PPM Modulation Technique.

However, because information modulation moves the pulses only a fractional part of a pulse width, this spectral smoothing impact is small. Extra spectral smoothing is introduced by the application of THSS technique.

From a multiple access point of view, Figure 3-11 shows the TH-PPM system of two users operating simultaneously. In this example, the repetition code is assumed to be absent (N_s = 1), for simplicity. Also, each time frame is subdivided four time slots (N_h = 4) where the pulses of each user are to hop in between according to each user's unique PN code shown in figure. It can be also shown the extra fine time shift associated with each pulse within each time slot depending on each user's transmitted data shown in figure.

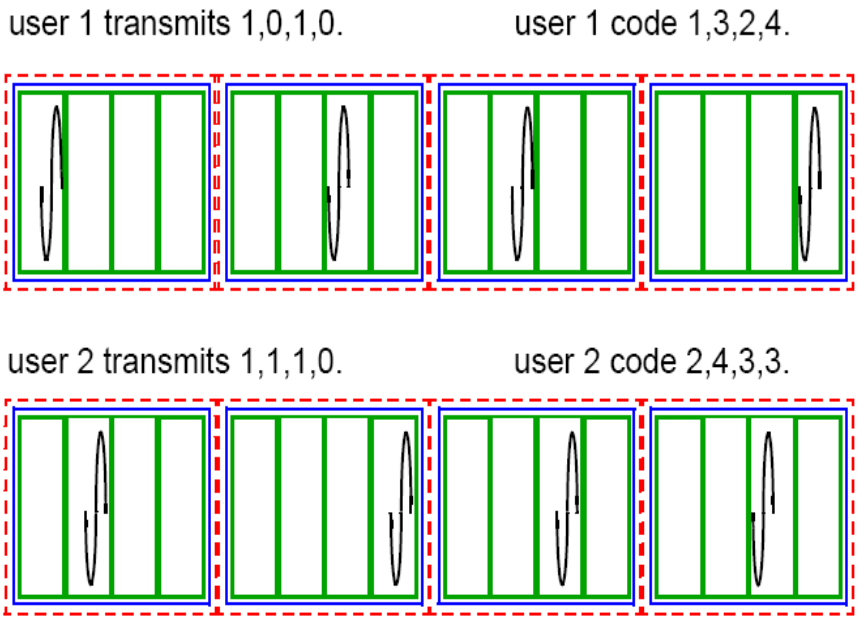

Figure 3-11 Multiple Access with TH-PPM.

The introduction of a repetition code is further illustrated in Figure 3-12 where the pulse of a single user is to hop between 4 different time slots contained in each time frame (N_h = 4). In this example a single time frame is further amplified to clearly show the operation of type-B TH-PPM in a multi user environment, where:

• c_j represents the TH code. It is pseudorandom with each element taking an integer in the range $0 \le c_j < N_h$, where N_h is the number of hops.

• d_i represents the i^{th} binary data bit transmitted by the k^{th} source.

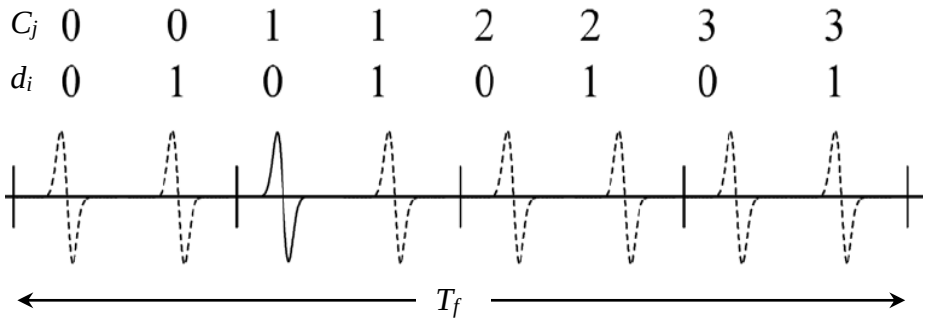

Figure 3-12 Type-B TH-PPM UWB System.

3.3.2 Pulse Amplitude Modulation (PAM)

Binary-PAM works by separating large and small amplitude pulses. By varying the amplitude the receiver can tell the difference between "1" and "0" and thereby decode the data from received signal [106] as illustrated in Figure 3-13 . PAM is based on the principle of encoding information in the amplitude of the impulse where the bits "0" and "1" are specified by a certain levels of amplitudes [52].

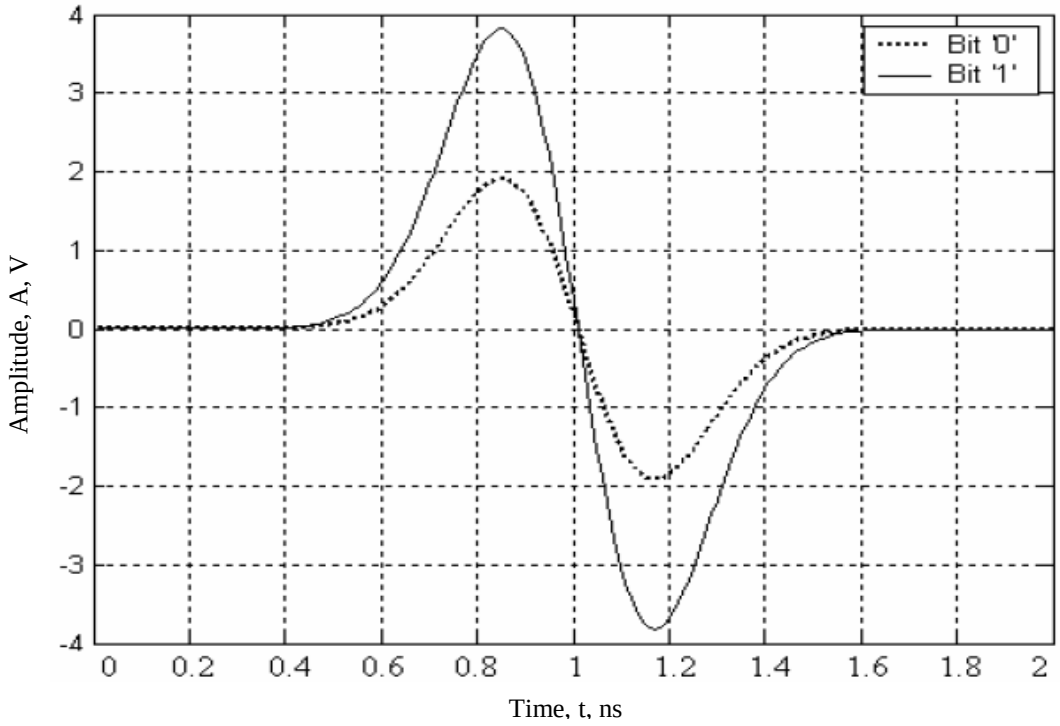

Figure 3-13 PAM with Two Different Levels for Logical Bits '0' and '1', [52].

With PAM, the amplitude of the pulse is varied depending on the data bits. For example, with a pulse that has sixteen amplitude levels, we can encode 4 bits. This scheme is simple because it eliminates the need for a coherent review. However, this scheme is not power efficient. Also in the wireless channel, attenuation is a significant problem. Due to that, the receiver will need the attenuation gain control. Therefore, this modulation is not very popular for implementation as suggested in [107].

One approach usually used to increase the bit rate is to use multilevel M-ary PAM methods to represent a symbol containing more than just two bits. However this technique, although increases the bit rate, it increases the probability of error, as shown in Figure 3-14, and also increases the transceiver complexity as suggested in [28].

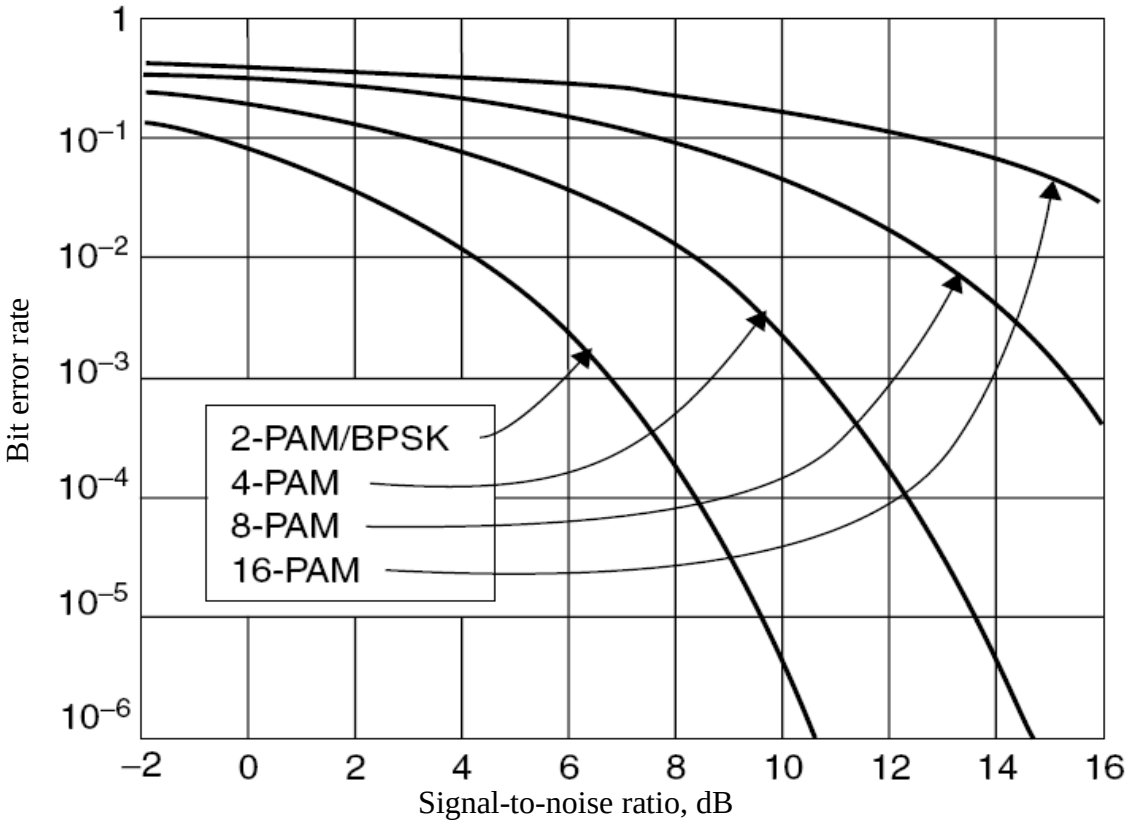

Figure 3-14 Probability of error for M-ary PAM modulation, [28].

3.3.3 Binary Phase Shift Keying (BPSK) or Biphase Modulation

BPSK (sometimes called bi-phase modulation), in which the phase or polarity of the signal (0 or 180^0) determines bit value ("0" or "1") rather than position [47]. In this case, only one bit per impulse can be encoded, because there are only two polarities available. The ability to eliminate spectral lines is a key feature of BPSK. It is crucial for UWB to minimise the presence of those spectral lines since they might interfere with conventional radio systems.

In BPSK or Biphase Modulation, the polarity of a pulse modulated. In the situation, a positive pulse is transmitted for a "1" and a negative pulse is transmitted for a "0". The signalling waveform for the classical BPSK presented using e.g. two antipodal Gaussian pulses is shown in Figure 3-15 [52].

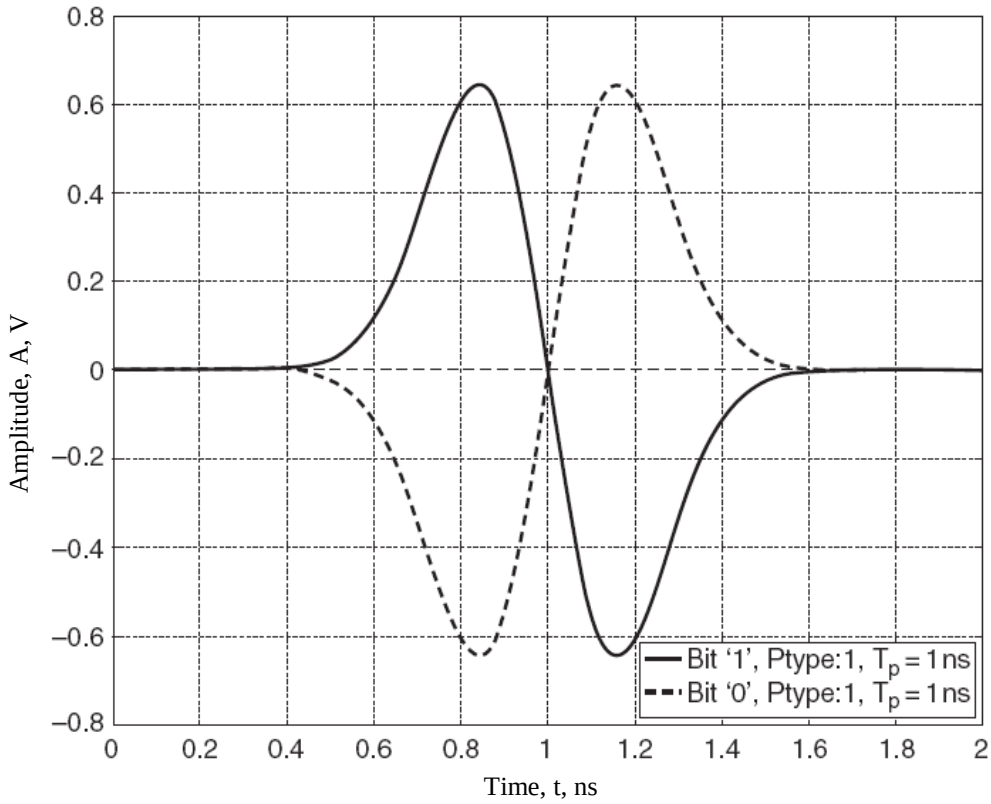

Figure 3-15 BPSK Pulse Shapes for '1' and '0' Bits, [52].

Figure 3-16 illustrates a very simple example of an UWB system where six pulses are shown each representing a single bit (i.e. $N_s = 1$). The information bit sequence is {110101} modulated using BPSK where there is a phase shift of 180^0 between logical bits "1" and "0". Each time frame (or each T_b, since in this case $T_b = T_f$) is subdivided into four time slots (T_c's) where the pulses are to hop in between according to the predetermined PN code hopping pattern. Hence, $N_h = 4$ and $c_j = 0,\ldots, 3$. The TH sequence shown is {2, 1, 2, 3, 1, 0}.

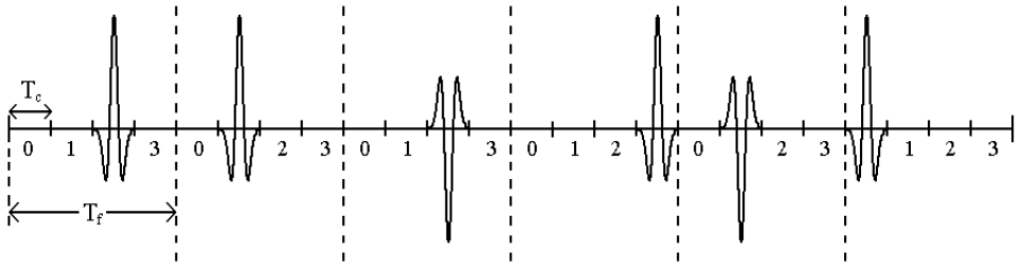

Figure 3-16 TH-BPSK in Time-Domain Using 2nd Order Gaussian Monocycles.

The enhancement of BPSK modulators is one of its benefits over OOK in BER performance. The capability to eradicate spectral lines because of the alteration in pulse polarity is another advantage of Biphase modulation. This feature decreases the extent of interference with conventional radio systems. A reduction in the total transmitted power could also be achieved, creating BPSK modulation a widespread method in UWB systems when energy competence is the main concern. A drawback of Biphase modulation is the physical application is more complicated, as two pulse generators, one being the opposite polarity, are important instead of one, as is the case with OOK. This presents a difficulty when trying to transmit a stream of pulses, as the time between pulses can become non-periodic if the pulse generators are not stimulated in a timely manner. Regardless of the problems, Biphase modulation is a very proficient method to convey UWB pulses.

3.3.4 On-Off Keying (OOK)

OOK is known as unipolar signalling in the analogy baseband world, is a simple pulse modulation technique where a pulse is transmitted to represent a binary "1", while no pulse is transmitted for a binary "0". In other words, OOK is a special case of PAM, the major difference between OOK and PAM is that nothing is transmitted in OOK when bit '0' is chosen. Figure 3-17 illustrates the operation of OOK using the 1st order Gaussian monocycle.

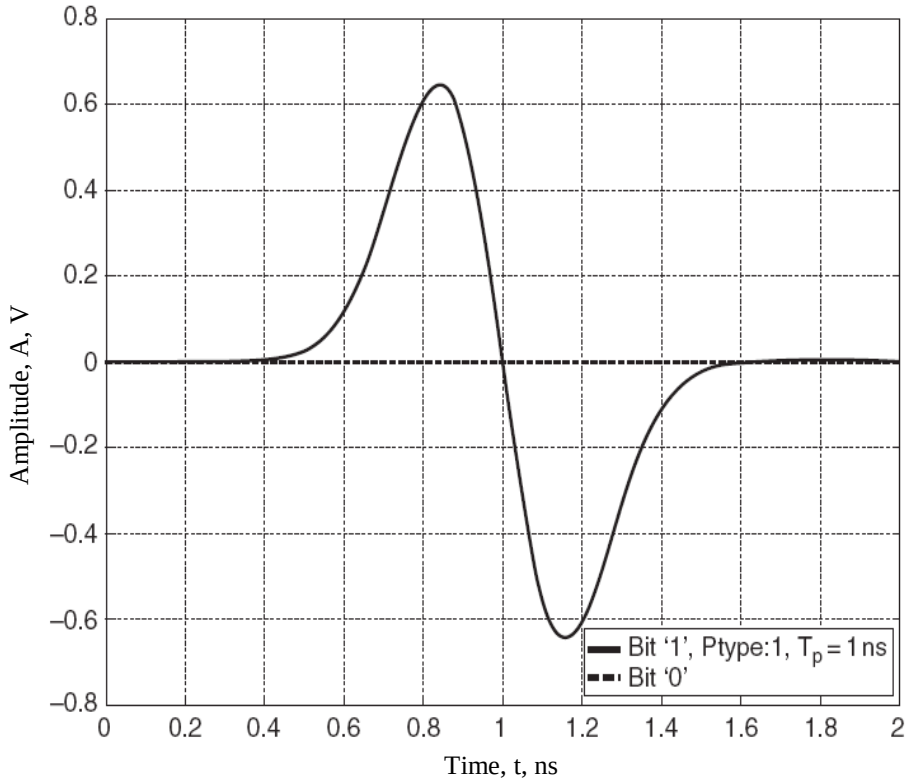

Figure 3-17 OOK Pulses Used for '1' and '0' Bits, [52].

One obvious advantage to using OOK is the simplicity of the physical implementation, as one pulse generator is necessary, as opposed to two, as is the case with BPSK modulation. A single Radio Frequency (RF) switch can control the transmitted pulses by switching on for a "1" data bit and off for a "0" data bit. This effortless transmitter configuration makes OOK popular for less complex UWB systems. Although OOK has a very straightforward implementation, there are numerous system drawbacks. In either a hardware or software based receiver design, synchronisation can be easily lost if the data contains a steady

stream of "0's." also, the performance of OOK is worse than BPSK modulation due to the smaller symbol separation for equal symbol energy. The difference in pulse amplitude is A, whereas in BPSK modulation the difference is twice the pulse amplitude, or 2A. Bit errors occur less often when the amplitude difference is greater because more distortion is necessary in the channel to affect a bit decision [108].

CHAPTER 4

4 THE MATHEMATICAL MODELS FOR A SYNCHRONOUS MULTIPLE ACCESS TH-PPM UWB SYSTEMS

4.1 Introduction

Ultra Wide band (UWB) technology has been accepted to be the solution for high speed transmission over short distances. Time hopping pulse position modulated UWB (TH-PPM UWB) is one of the well-known multiple access methods which utilise pulse position modulation (PPM) system with time hopping utilised for entertaining multiple users. Impulse radio (IR) UWB is the carrier less communication system in which narrow pulses are utilised for transmission [9].

Time hopping, combined with pulse position modulation (TH-PPM), was proposed originally for ultra-wideband (UWB) multiple-access systems.

In this chapter, a new method for calculating the BER of TH-PPM in the presence of multiple-access interference (MAI) on additive white Gaussian noise (AWGN) channels, based on the analytical study in [20] and is further extended to evaluate the effect of other system and signal parameters which strongly affects performance of the system. It is called the characteristic function (CF) technique.

This technique can be used in the performance evaluation of UWB systems without introducing any unrealistic assumptions. It gives the precise BER in the general case with very limited computational complexity.

Most researchers claim that the background noise and the multi user interference can both have the combined effect of a Gaussian random process. The derived analytical expression, used for precisely calculating the bit-error probability of the TH-PPM, is used to assess the accuracy of this Gaussian approximation (GA). The analytical results show that the GA is

inaccurate for predicting bit-error rate (BERs) for medium and large signal-to-noise ratio (SNR) values.

Furthermore, it will be assumed that, the receiver is characterised by a single user detection in an asynchronous multiple access environment to simulate the real world situation, in contrast to other research like [16] which assumes chip-synchronous systems which is not realistic in practical UWB applications.

The analytical expressions used to evaluate the performance of TH-PPM systems will be divided into two parts. First, an analytical expression for bit error rate (BER) is obtained in terms of SNR (E_b / N_0), number of users, and bit rate, where the multiple access interference is modelled as Gaussian random process. Second, an analytical expression is obtained using the characteristic function (CF) method for precisely calculating the BER of TH-PPM UWB systems. The results are then used to assess the accuracy and the validity of the GA model.

4.2 The TH-PPM UWB System Model

A typical format of the k^{th} user's transmitted signal conveying the i^{th} data bit $s^{(k)}(t,i)$ is given by [20] and shown in equation (4.1):

$$s^{(k)}(t,i) = \sqrt{\frac{E_b}{N_s}} \sum_{j=iN_s}^{(i+1)N_s-1} p(t^{(k)} - jT_f - c_j^{(k)}T_c - d_i^{(k)}\delta) \tag{4.1}$$

Where $t^{(k)}$ is the k^{th} transmitter clock time, $s^{(k)}(t,i)$ is the k^{th} user's signal conveying the i^{th} data bit, and $p(t)$ is the signal pulse with pulse width T_p, normalised so that $\int_{-\infty}^{+\infty} p^2(t)dt = 1$.

• E_b is the bit energy common to all signals.

• N_s is the number of pulses required to transmit a single data bit, called the length of the repetition code in [15].

• T_f is the time duration of a frame, and thus, the bit duration $T_b = N_s T_f$.

• $\{c_j^{(k)}\}$ represents the TH code for the k^{th} source. It is pseudorandom with each element taking an integer in the range $0 \le c_j^{(k)} < N_h$, where N_h is the number of hops.

• T_c is the TH chip width and satisfies $N_h T_c \le T_f$.

• $d_i^{(k)}$ represents the i^{th} binary data bit transmitted by the k^{th} source, and different bits are assumed to be equiprobable. In Type-A TH-PPM UWB systems, the data bits can conveniently be {0, 1}, as explained in the following.

• δ is the time shift associated with binary PPM.

The repetition code, N_s, introduces a processing gain to the system and is used to help the system combat, the background noise and interference. In next chapter it will be shown that, N_s is one of the system parameters that have a noticeable impact on the system BER performance.

The structure of each time shift component of equation (4.1) is illustrated in Figure 4-1, and is described as follows:

4.2.1 Pulse Train

Multiple access signals composed of uniformly spaced pulses are vulnerable to occasional catastrophic collisions in which a large number of pulses from two signals are received simultaneously.

The uniform pulse train of the form $\sum_{j=iN_s}^{(i+1)N_s-1} p(t^{(k)} - jT_f)$ consists of monocycle pulses spaced T_f seconds apart in time. The pulse repetition interval (PRI) or frame time may be a hundred to a thousand times the monocycle width, resulting in a signal with very low duty cycle.

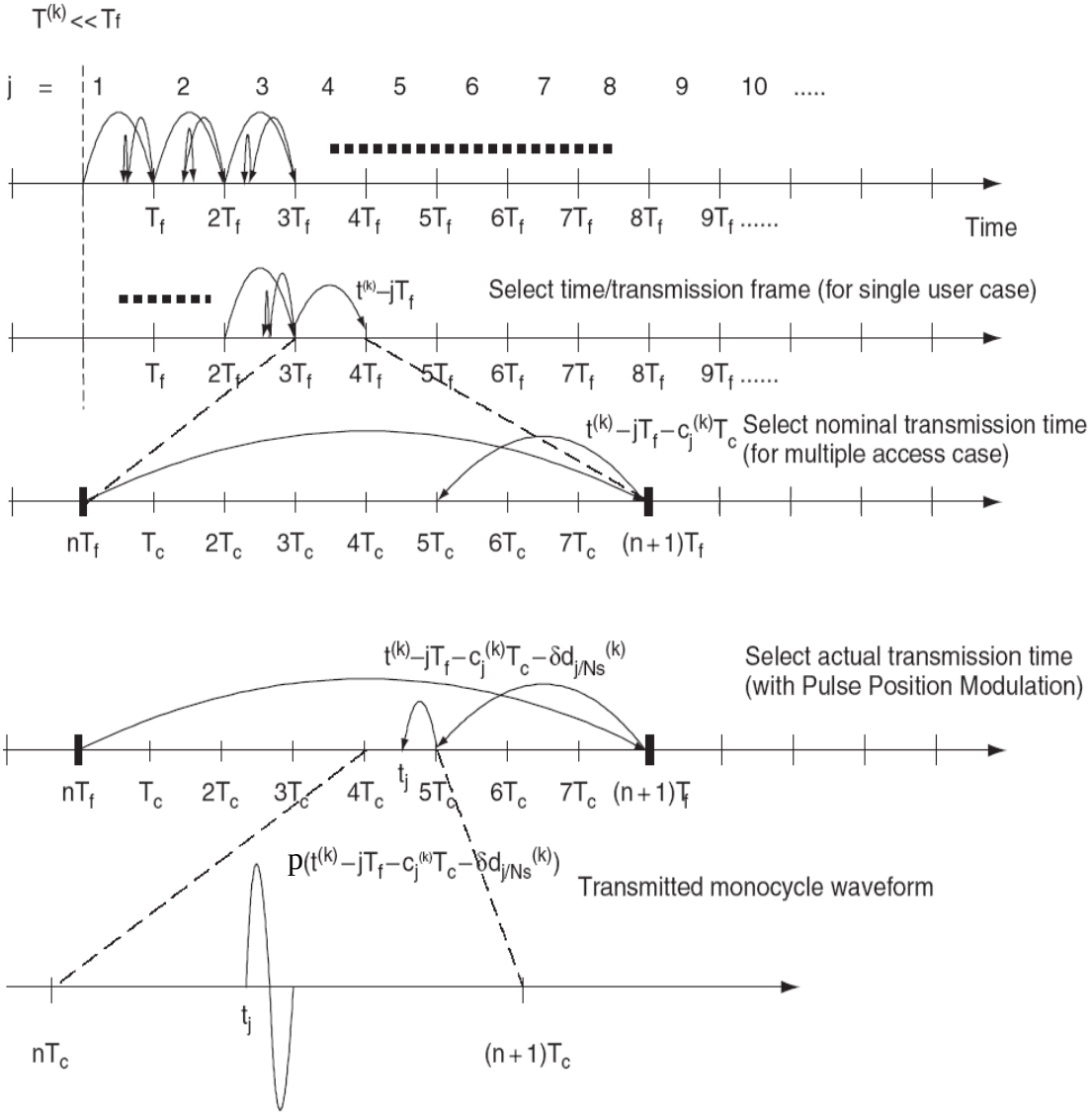

Meaning of each parameters in the formula.

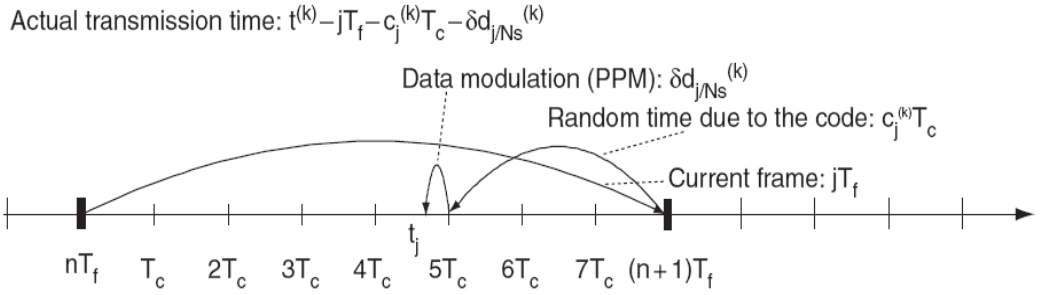

Figure 4-1 TH-PPM UWB System in Time Domain.

4.2.2 Time Hopping Process

The TH sequence, provides an additional time shift to each pulse in the pulse train, with the j^{th} monocycle undergoing an added shift of $c_j^{(k)}T_c$ seconds, where T_c is the TH chip width, with discrete values between 0 and N_hT_c s. each link (indexed by k) uses a distinct pulse-shift pattern $\{c_j^{(k)}\}$ called a TH sequence, to eliminate catastrophic collisions during multiple access. These hopping sequences are pseudorandom with a period T_p, with each element an integer value in the range $0 \le c_j^{(k)} < N_h$ {0, 1, ..., N_h-1}, where N_h is the number of hops.

Since a short time interval may be required to read the output of a monocycle correlator and to reset the correlator, N_hT_c / T_f may be strictly less than one. The ratio N_hT_c / T_f indicates the fraction of the frame time T_f over which TH is allowed. Hence, T_c must be chosen to satisfy $N_hT_c \le T_f$ to avoid intersymbol interference of pulses of different symbols. If N_hT_c / T_f is too small, then catastrophic collisions remain a significant possibility. Conversely, with a large enough value of N_hT_c / T_f and well-designed TH sequences, the multiple-access interference in many situations can be modelled as a Gaussian random process. It can be shown in the analytical results that N_h has a significant impact on improving the performance of the system. As N_h increases, the BER decreases as long as $N_hT_c \le T_f$ and $T_p+\delta \le T_c$ are satisfied, respectively as described in [19].

4.2.3 Modulation Process

In PPM modulation, no additional time shift modulates the pulse *p(t)* when the data bit is "0", and a time shift of δ is added to *p(t)* when the data bit is "1". The parameter δ is a modulation factor which can be chosen to optimise performance. If $\delta > T_p$ then, the transmitted signals representing 0 and 1 are orthogonal. The original proposal for UWB PPM systems in [18] considers information bits $d_i^{(k)} \in \{0,1\}$. After source and channel coding the information bit $d_i^{(k)}$ represents the i^{th} binary data bit transmitted by the k^{th} source. For performance prediction purposes, the data sequence is modelled as a wide-sense stationary random process composed of equally likely binary symbols. The advantage of using Gaussian pulses and their derivatives is that their autocorrelation properties show negative values, thus, offering the possibility of performing non-

orthogonal PPM which has a better performance compared to orthogonal PPM as described in [52].

4.3 Gaussian Pulse Model

In an UWB system, the choice of the pulse shape will strongly affect the choice of receiver bandwidth, the BER performance, and the performance in multipath propagation environments. A variety of pulse shapes has been proposed for UWB impulse radio systems, including the Gaussian pulse, Gaussian monocycles, and the Manchester monocycle [109]. The Gaussian pulse given by [20] and shown in equation (4.2):

$$p_0(t) = \exp\left[-2\pi\left(\frac{t}{\tau_p}\right)^2\right] \tag{4.2}$$

And its n^{th} derivative, named the n^{th}-order Gaussian monocycle is [13]

$$p_n(t) = \varepsilon_n \frac{d^n}{dt^n}\exp\left[-2\pi\left(\frac{t}{\tau_p}\right)^2\right] \tag{4.3}$$

where τ_p represents a time normalisation or (impulse width parameter) factor to make $p_n(t)$ independent of a specific impulse duration, and ε_n is introduced to normalise the energy of the pulses $p_n(t)$. The most widely reported pulses in UWB systems is the second-order Gaussian monocycle [19], shown in Figure 4-2 which is the second derivative of the Gaussian pulse given by

$$p(t) = \left[1-4\pi\left(\frac{t}{\tau_p}\right)^2\right]\exp\left[-2\pi\left(\frac{t}{\tau_p}\right)^2\right] \tag{4.4}$$

The parameter τ_p has effect on spectral and temporal characteristics of the signal. Note that, $\int_{-\infty}^{+\infty} p(t)\,dt = 0$, which implies the absence of a DC component in the received signal.

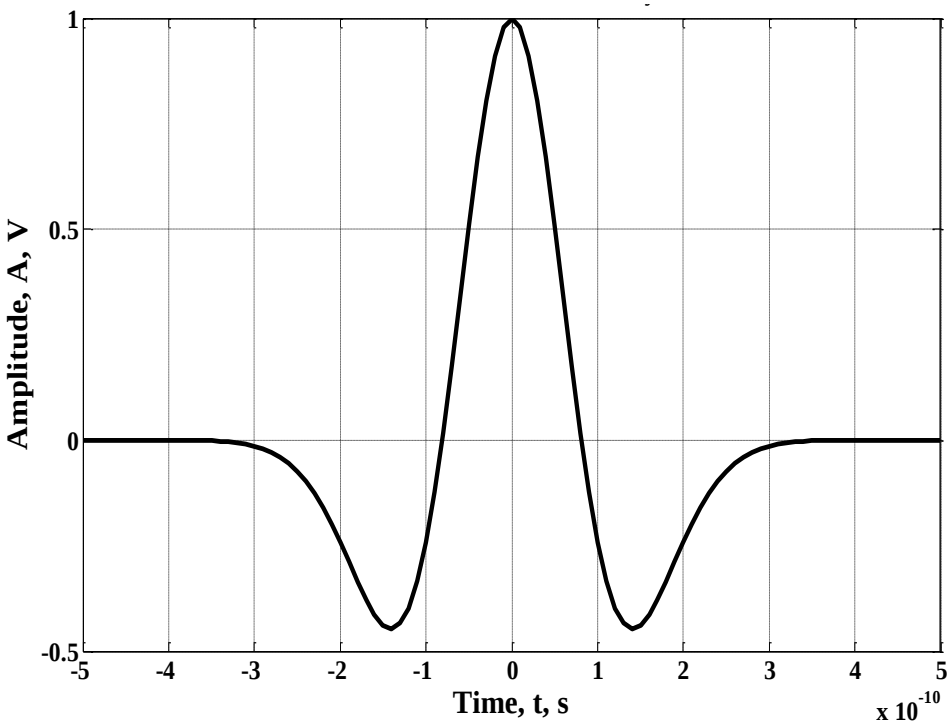

Figure 4-2 Second Order Gaussian Monocycle.

The autocorrelation of the Gaussian monocycle *p(t)* in equation (4.4) is shown in Figure 4-3, together with the other four derivatives, and is given by

$$R(x) = \left[1 - 4\pi\left(\frac{x}{\tau_p}\right)^2 + \frac{4\pi^2}{3}\left(\frac{x}{\tau_p}\right)^4\right]\exp\left[-\pi\left(\frac{x}{\tau_p}\right)^2\right] \tag{4.5}$$

And the autocorrelation of second order Gaussian monocycle is shown in Figure 4-4.

The value of δ is chosen according to the autocorrelation characteristics of the pulse In PPM UWB systems, the optimum choice of the time shift parameter, δ, strongly affects the performance of the system, as has been previously mentioned. And it is dependent on the specific shape of the pulse and the pulse width employed.

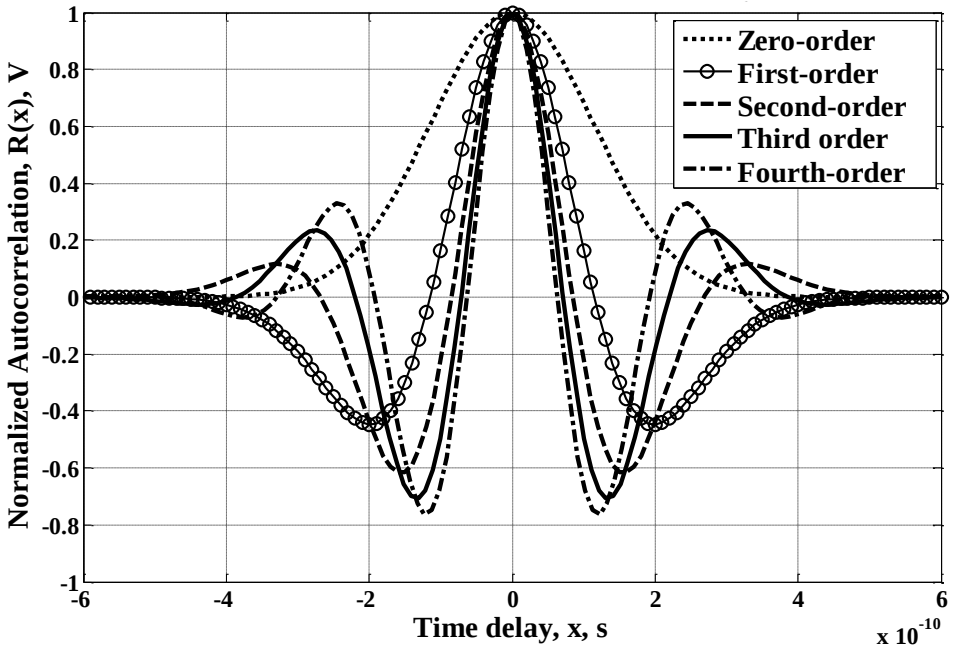

Figure 4-3 Autocorrelation of different order Gaussian monocycles.

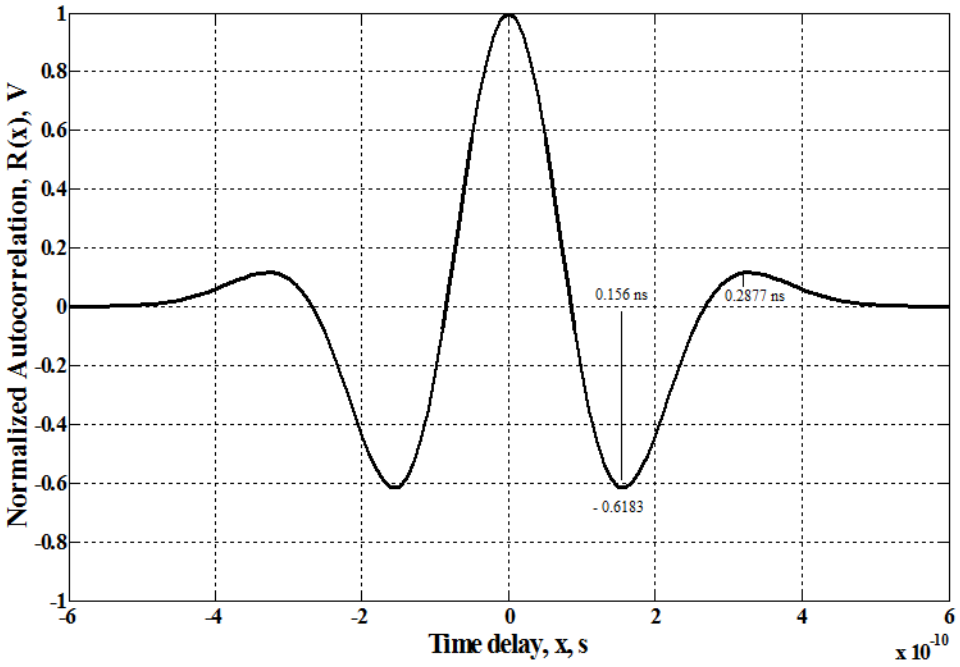

Figure 4-4 Autocorrelation of Second Order Gaussian Monocycle.

In the analytical results, it will be shown that the BER performance is highly sensitive to the appropriate choice of δ and it is greatly improved when this choice is optimum in accordance to the observation of the autocorrelation properties of the employed pulse.

The autocorrelation functions of the Gaussian waveforms as shown on Figure 4-3. It can be seen that, they have both positive and negative values. This explains why the Gaussian pulse and its derivatives can offer the possibility of performing non-orthogonal PPM (using $\delta < T_p$) with better BER performance than time orthogonal pulses (using $\delta > T_p$). Moreover, it has been previously mentioned that different pulses have different autocorrelation properties. As the order of the derivative increases, the minimum BER is reached for a lower value of δ and better BER performance is achieved. It is clear in Figure 4-4 that, the minimum value of the autocorrelation of the second order Gaussian pulse chosen occurs when δ = 0.156 ns and has a negative autocorrelation value of $R(x)$ = - 0.6183 that will correspond to the best BER performance as will be explained in the analytical results.

4.4 The Receiving Process

In type-A TH-PPM, the template wave form *v(t)* has the form [19]

$$v(t) = p(t) - p(t - \delta) \tag{4.6}$$

By the choice of the second order Gaussian pulse with τ_p = 0.2877 ns shown in Figure 4-4, then δ_{opt} = 0.156 ns and $R(\delta_{opt})$ = - 0.6183. A graph of the template signal is displayed in Figure 4-5 using the typical received waveform given in equation (4.4). The non-zero extent of the template signal is approximately δ plus the monocycle's width, i.e., about 0.86 ns. Since *p(t)* is non-zero only in the time interval $[0,T_p]$, the support of *v(t)* is $[0, T_p+ \delta]$.

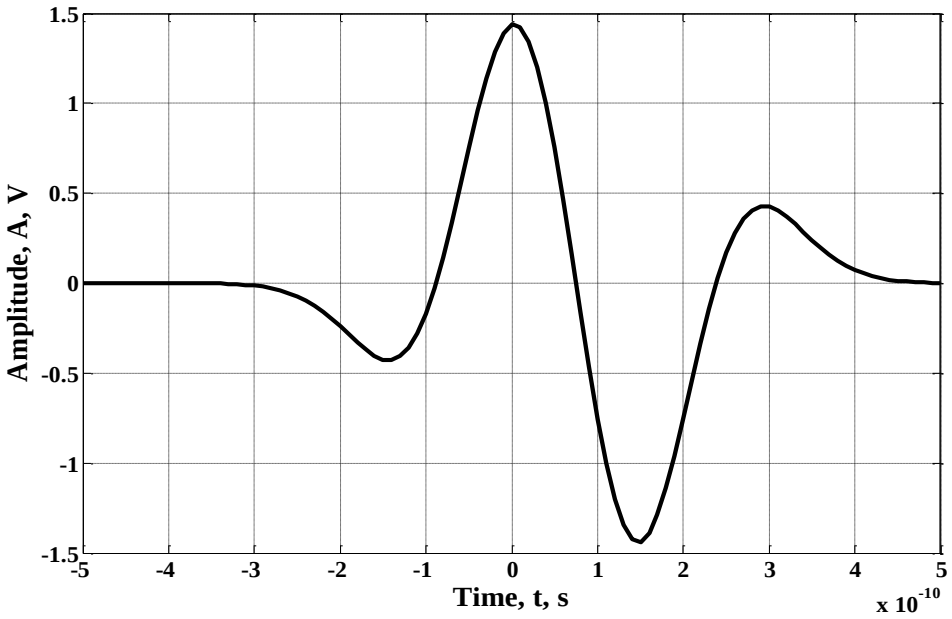

Figure 4-5 TH-PPM Template Wave Form v(t).

It must be noted that the correlation template waveform takes different forms according to the modulation scheme applied.

The optimum receiver in case one user only is present on air, is a correlation receiver, shown in Figure 4-6, that uses a template signal *v(t)* for the correlation procedure [18].

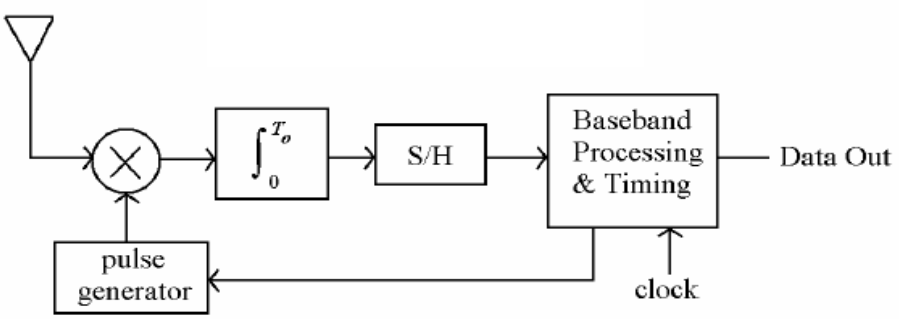

Figure 4-6 The Simple Design of a UWB Correlation Receiver.

As has been previously mentioned, the optimal choice of δ is related to the autocorrelation properties of *p(t)*, and the effect of different pulses is discussed in detail in [13].

The single user received signal can be modelled as follows

$$r(t) = s(t-\tau) + n(t) = \sqrt{\frac{E_b}{N_s}} \sum_{j=iN_s}^{(i+1)N_s-1} p(t - jT_f - c_j T_c - d_i \delta - \tau) + n(t) \tag{4.7}$$

Assuming users are transmitting asynchronously on an AWGN channel, the composite received signal *r(t)* at the output of the receiver's antenna is modelled as

$$r(t) = \sum_{k=1}^{N_u} A_k s^{(k)}(t - \tau_k) + n(t) \tag{4.8}$$

Where *n(t)* is the additive noise with two-sided PSD $N_0/2$, $\{A_k\}_{k=1}^{N_u}$ represent the channel attenuation for all transmitted signals, and $\{\tau_k\}_{k=1}^{N_u}$ represent time shifts which account for user synchronism for the N_u signals, they use the system in the same time. Equation (4.8) can be subdivided into

$$r(t) = A_1 S^{(1)}(t - \tau_1) + \underbrace{\sum_{k=2}^{N_u} A_k S^{(k)}(t - \tau_k)}_{\text{MAI}} + \underbrace{n(t)}_{\text{AWGN}} \tag{4.9}$$

let $n_{tot}(t)$ be the sum of MAI with AWGN, ergo

$$n_{tot}(t) = \sum_{k=2}^{N_u} A_k s^{(k)}(t - \tau_k) + n(t) \tag{4.10}$$

In the case of a multiple access environment of N_u users transmitting simultaneously at the same time and one is interested in receiving user 1's bits, to decide whether they are logical 1s or 0s. Hence, $s^{(k)}(t) = s^{(1)}(t)$, $\tau_k = \tau_1$, $d_i^{(k)} = d_i^{(1)}$, all belong to the reference signal of the 1st user. In this case, the optimum receiver for a single bit of a binary modulated impulse radio signal in AWGN is a correlation receiver which takes its decision, whether the data bit is logic 0 or 1, according to the following decision statistic (γ) as outlined in [19].

$$\gamma = \sqrt{\frac{N_s}{E_b}} \sum_{j=0}^{N_s-1} \underbrace{\int_{\tau_1 + jT_f}^{\tau_1 + (j+1)T_f} r(t) v(t - jT_f - c_j T_c - \tau_1) dt}_{\alpha_j} \tag{4.11}$$

The signal processing corresponding to this decision rule in equation (4.11) is shown in Figure 4-7 where $\delta_D(.)$ is the Dirac delta function which decides the clock timing of the pulses [18].

The decision statistic γ consists of summing the N_s correlations α_j of the correlator's template signal $v(t)$ at various time shifts with the received signal $r(t)$. Since the integration process calculates the area under the curve of the cross correlation between $r(t)$ and $v(t)$, therefore, the decision statistic γ increases gradually during the pulse-by-pulse integration and then all the results of the integration processes of all the pulses in all the N_s time frames representing a single bit are added by the summation process [19].

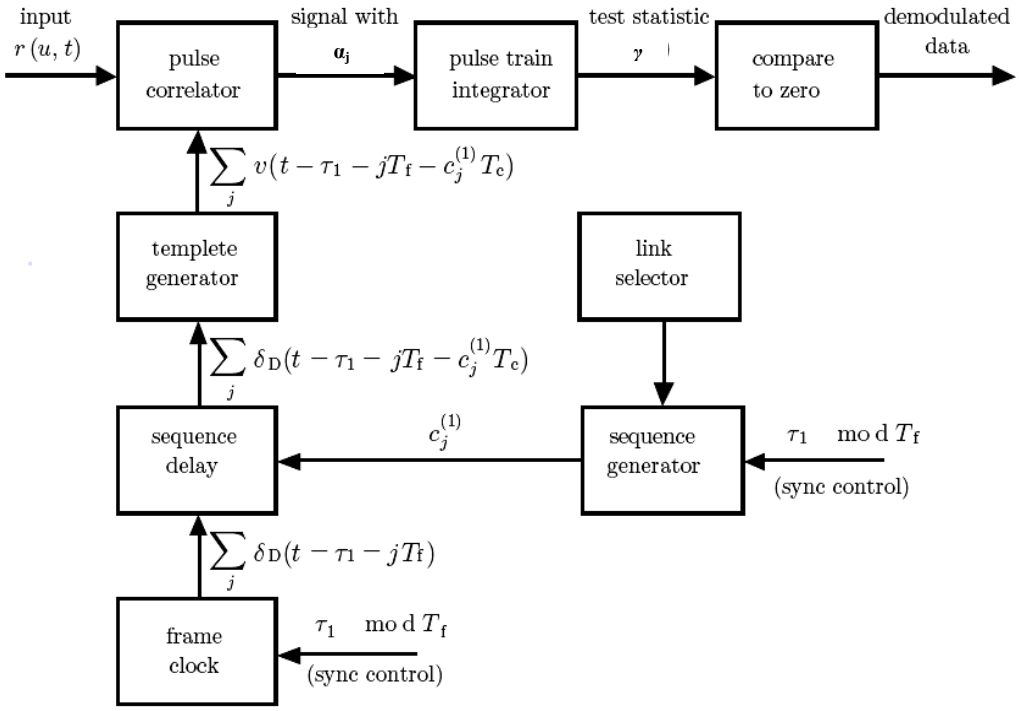

Figure 4-7 Receiver Block Diagram for the Reception of the First User's Signal, [19].

According to the chosen shape of *v(t)*, and if no errors occurred during the transmission and reception processes, then, the correct decision is taken according to:

If the received data bit is logic 0, then the decision statistic γ will be increasing gradually to reach a positive constant value, and hence, γ is positive.

On the other hand, if γ decreases gradually to reach a constant negative value, therefore the received data bit must be logic 1.

Then,

$$\text{If } \gamma > 0 \rightarrow \text{decide } d_i^{(1)} = 0$$

$$\text{If } \gamma \leq 0 \rightarrow \text{decide } d_i^{(1)} = 1$$

4.5 The Gaussian Approximation (GA) Model

The probability of error of TH-PPM can be evaluated, in the presence of AWGN channel using the standard techniques, given by [110]

$$P_e = \frac{1}{2} erfc\left[\sqrt{\frac{E_b}{2N_0}}\sqrt{1-R(\delta)}\right] \tag{4.12}$$

The probability of bit error depends only on the SNR, (SNR = E_b / N_0), and the value of autocorrelation of the chosen pulse at a particular value of the modulation shift parameter δ. In the analytical results in Chapter 5 will be investigated that the effect of choosing different Gaussian monocycles with different orders, as well as the effect of choosing different values of δ on the BER for the same pulse shape.

The optimal detection in multi user environments leads to much more complex receiver designs, because when N_u transmitters are active, the decision statistic γ given in equation (4.11) is no longer optimum. In the presence of multiple-access noise, which is not really Gaussian, the optimum receiver makes use of the information that the receiver knows about the structure of the multiple-access noise, regarding the knowledge of all the time hopping sequences. If the number of users is large and no such multi user detector is feasible, then, it is reasonable to approximate the combined effect of the other users de-hopped interfering signals as a Gaussian random process. Ergo the total noise in equation (4.10) is a spectrally white Gaussian random process and equation (4.11) is optimum [19].

By Substituting equation (4.10) in equation (4.9) and assuming that we are interested only in the reception of the first bit (i.e, i=0), then in equation (4.11), the decision statistic γ can be rewritten

$$\gamma = \sum_{j=0}^{N_s-1} \int_{\tau_1+jT_f}^{\tau_1+(j+1)T_f} \left[A_1 s^{(1)}(t-\tau_1) + n_{tot}(t)\right] v(t - jT_f - c_j^{(1)}T_c - \tau_1)dt$$

$$= \sum_{j=0}^{N_s-1} \int_{\tau_1+jT_f}^{\tau_1+(j+1)T_f} [A_1 s^{(1)}(t-\tau_1) v(t - jT_f - c_j^{(1)}T_c - \tau_1)$$

$$+ n_{tot}(t)\, v(t - jT_f - c_j^{(1)}T_c - \tau_1)]\, dt \tag{4.13}$$

Substituting equation (4.1) in equation (4.13) for the first user, and under the hypothesis that the first transmitted bit is a logic 1, the decision statistic γ can be rewritten as

$$\gamma = \sum_{j=0}^{N_s-1} \int_{\tau_1+jT_f}^{\tau_1+(j+1)T_f} \left[A_1 \sum_{l=0}^{N_s-1} p(t - jT_f - c_l^{(1)}T_c - \tau_1 - \delta)\, v(t - jT_f - c_j^{(1)}T_c - \tau_1) \right] dt$$

$$+ \sqrt{\frac{N_s}{E_b}} \sum_{j=0}^{N_s-1} \int_{\tau_1+jT_f}^{\tau_1+(j+1)T_f} \left[n_{tot}(t)\, v(t - jT_f - c_j^{(1)}T_c - \tau_1) \right] dt \qquad (4.14)$$

By substituting equation (4.10) into equation (4.14)

$$\gamma = \underbrace{\sum_{j=0}^{N_s-1} \int_{\tau_1+jT_f}^{\tau_1+(j+1)T_f} \left[A_1 \sum_{l=0}^{N_s-1} p(t - lT_f - c_l^{(1)}T_c - \tau_1 - \delta)\, v(t - jT_f - c_j^{(1)}T_c - \tau_1) \right] dt}_{m}$$

$$+ \underbrace{\sqrt{\frac{N_s}{E_b}} \sum_{j=0}^{N_s-1} \int_{\tau_1+jT_f}^{\tau_1+(j+1)T_f} \left[(\sum_{k=2}^{N_u} A_k s^{(k)}(t - \tau_k) + n((t)))\, (\, v(t - jT_f - c_j^{(1)}T_c - \tau_1)) \right] dt}_{n_d} \qquad (4.15)$$

Therefore, γ can be reduced to

$$\gamma = m + n_d \qquad (4.16)$$

The quantity m is evaluated by [19] as

$$m = N_s A_1 m_p \qquad (4.17)$$

Where

$$m_p = \int_{-\infty}^{+\infty} p(x - \delta)\, v(x) dx \qquad (4.18)$$

The quantity n_d can be rewritten as

$$n_d = \sqrt{\frac{N_s}{E_b}} \sum_{j=0}^{N_s-1} \int_{\tau_1+jT_f}^{\tau_1+(j+1)T_f} \sum_{k=2}^{N_u} A_k s^{(k)}(t-\tau_k)\, v(t - jT_f - c_j^{(1)} T_c - \tau_1)\, dt$$

$$+ \sqrt{\frac{N_s}{E_b}} \sum_{j=0}^{N_s-1} \int_{\tau_1+jT_f}^{\tau_1+(j+1)T_f} n(t)\, v(t - jT_f - c_j^{(1)} T_c - \tau_1)\, dt \qquad (4.19)$$

Therefore, n_d can be reduced to

$$n_d = \sum_{k=2}^{N_u} A_k n^{(k)} + n_{rec} \qquad (4.20)$$

Where $n^{(k)}$ is the component of n_d caused by the multiple access noise from the k^{th} transmitter for $k = 2,3,\ldots,N_u$, and n_{rec} is the component of n_d that is caused by receiver noise and the other sources of non-monocycle interference. It is assumed that the mean and variance of n_{rec} are given by *0* and σ_{rec}^2, respectively [19].

The average output signal-to-interference-plus-noise ratio of an impulse radio for randomly selected time-hopping sequences as a function of the number of users (N_u), under the assumption of the studied case of Gaussian approximation, is defined in [19] as

$$SNR_{out}(N_u) = \frac{m^2}{\mathrm{E}\{|n_d|^2\}} \qquad (4.21)$$

Since each of the random variables in the expression of n_d defined in equation (4.20) are independent with zero mean [19], the quantity $E\{|n_d|^2\}$ becomes

$$\mathrm{E}\{|n_d|^2\} = \sigma_{rec}^2 + N_s \sigma_a^2 \sum_{k=2}^{N_u} A_k^2 \qquad (4.22)$$

The quantity σ^2_{rec} is the variance of the receiver noise component at the pulse train integrator output. The parameter σ^2_a is defined in [19] as

$$\sigma_a^2 = \frac{1}{T_f} \int_{-\infty}^{+\infty} \left[\int_{-\infty}^{+\infty} p(x-s) v(x) dx \right] ds \qquad (4.23)$$

Therefore, when only the desired transmitter is on air, N_u=1, the single-user output SNR can be calculated by

$$SNR_{out}^{(1)} = \frac{(N_s A_1 m_p)^2}{\sigma_{rec}^2} \ . \tag{4.24a}$$

Thus, $SNR_{out}^{(1)}$ is equivalent to the output SNR that one might observe in single link experiments. This is a convenient parameter because it absorbs all of the scaling problems that one must confront in handling receiver noise and non-monocycle forms of interference [19].

On the other hand, when more than one monocycle transmitter is on air, then the $SNR_{out}(N_u)$ and by substituting equations (4.17) & (4.22) in equation (4.21), the $SNR_{out}(N_u)$ can be written as

$$SNR_{out}(N_u) = \frac{(N_s A_1 m_p)^2}{\sigma_{rec}^2 + N_s \sigma_a^2 \sum_{k=2}^{N_u} A_k^2}. \tag{4.24}$$

It can be observed from equation (4.24) that, the $SNR_{out}(N_u)$, is inversely proportional to the number of users; i.e., for a specific BER performance to be maintained constant, as the number of users increases, the $SNR_{out}(N_u)$ decreases.

We notice that when N_u = 1, the second term of the denominator is zero and (4.24) is reduced exactly to the expression (4.24a). It can be observed from (4.24) that, the $SNR_{out}(N_u)$ is inversely proportional to the number of users; i.e., for a specific BER performance to be maintained constant, as the number of users increases, the $SNR_{out}(N_u)$ decreases. One solution proposed in [18] is the introduction of the additional power increase in each user's signal. Therefore, the system can maintain a larger number of users for a specific BER performance by increasing the power of each user's signal. However, when the number of active users simultaneously using the system increases so much, then the receiver becomes saturated (i.e., cannot be able to hold much more users) since it

cannot maintain the specific level of performance regardless of the additional available power. A numerical example of such scenario is shown on the Figure 4-8.

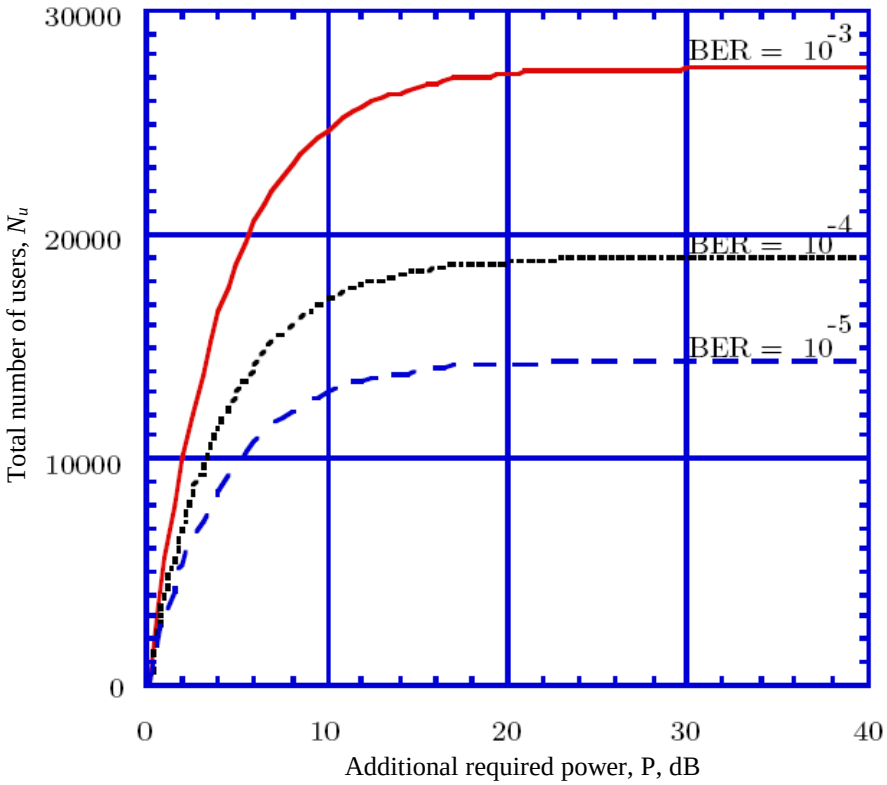

Figure 4-8 Total number of users versus additional power required in (dB) for the impulse radio UWB.

In order to analytically evaluate the effect of multi-access interference regarding the BER performance of TH-PPM UWB systems, one must take into consideration the combined effect of the reception process described by (4.9) and the effect of the overall interference described by (4.10), which is totally assumed to be a zero mean Gaussian random process in this analysis.

Under the hypothesis of the single user perfect synchronisation, and using steps and assumptions similar to the ones described in detail in [19], and with an analogue procedure to the one used to obtain equation (4.12), it is possible to evaluate the probability of error in the presence of multi-access interference as described in [110]

$$P_e = \frac{1}{2} erfc \sqrt{\left\{ (SNR)_1^{-1} + 2R_b P(\delta) \sum_{k=2}^{N_u} \left(\frac{A_k}{A_1} \right)^2 \right\}^{-1}} \tag{4.25}$$

Where

$$(SNR)_1 = A_1^2 \frac{N_s \; E_b}{2N_0} (1 - R(\delta)),$$

$$R_b = \frac{1}{T_b}, \;\; T_b = N_s T_f \,,$$

$$P(\delta) = \frac{\int_{-\infty}^{+\infty} [R(\alpha) - R(\alpha + \delta)]^2 \, d\alpha}{[1 - R(\alpha)]^2} = \frac{G(\delta)}{[1 - R(\alpha)]^2}$$

If perfect power control is assumed *($A_k = A_1$, for $k = 1, \ldots, N_u$)*, then

$$P_e = \frac{1}{2} erfc \; \sqrt{\left\{ (SNR)_1^{-1} + 2R_b P(\delta)(N_u - 1) \right\}^{-1}} \tag{4.26}$$

The theoretical multi access performances are analysed under perfect power control assumption. The parameter τ_p is set equal to 0.2877 ns; waveform width is then fixed to 0.7 ns. When only one transmitter is in function, the optimal value for δ is given by [110] as

$$\delta_{opt} = \arg\max_{\delta} (\sqrt{1 - R(\delta)}) = \arg\min_{\delta} R(\delta) = 0.156 \, ns \tag{4.27}$$

In case of multi access condition this value is still optimal when Gaussian noise is dominant. When multi user interference prevails:

$$\delta_{opt} = \arg\min_{\delta} p(\delta) = 0.144 \, ns \tag{4.28}$$

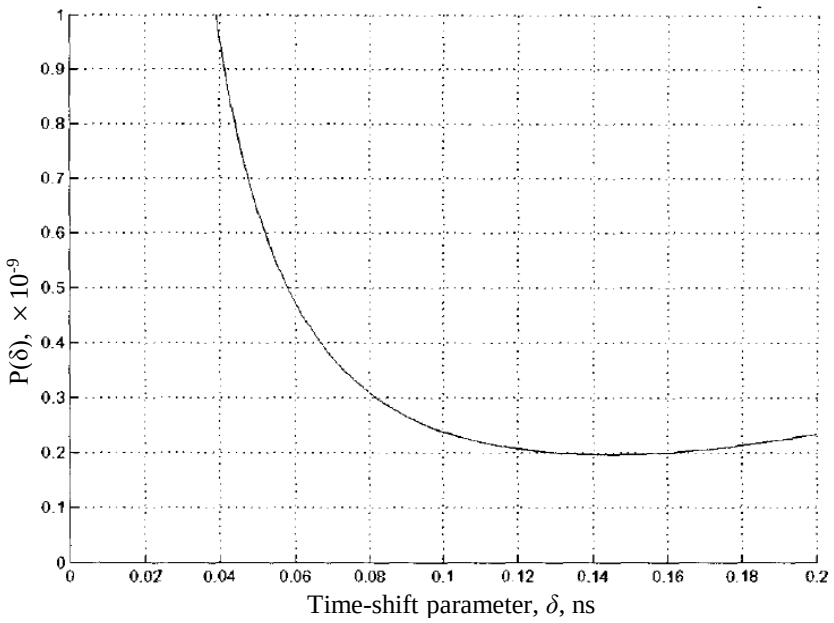

Figure 4-9 P(δ) Function [110].

From Figure 4-9 it is possible to note how small the variations of *p(δ)* are around its minimum. Therefore the first choice can be supposed optimal whatever type of interference is dominant. The repetition code is supposed to be absent and bit rate is fixed equal to 9.8 Mbit/s. Note that from equation (4.26), when $E_b / N_0 \to +\infty$, asymptotic performance of the system depends only on $R_b = \frac{1}{N_s T_f}$, i.e. it is function of the product of N_s and T_f and is not influenced by their single values.

4.6 Exact Multi Access Interference Model

A characteristic function method is proposed for precisely calculating the bit-error probability of time-hopping (TH) ultra-wideband (UWB) systems with multiple-access interference in an additive white Gaussian noise environment. The analytical expressions are used to assess the accuracy of the Gaussian approximation. The Gaussian approximation is shown to be inaccurate for predicting bit-error rates (BERs) for medium and large signal-to-noise ratio (SNR) values.

An exact BER calculation for a synchronous multiple access UWB system is usually unwieldy. The purpose in this section is to show an analytical method for calculating the average probability of the bit error rate of the TH-PPM UWB systems. A derivation is made to have exact average BER expressions for TH-PPM UWB systems in an additive white Gaussian noise (AWGN) environment based on the characteristic function (CF) technique [96], [17]. The AWGN channel model is important in its own right for some UWB applications [15], [19], and is a necessary intermediate step for future work for examining UWB on fading channel models. The performance evaluations show the sensitivity of TH-PPM UWB systems to various system and signal parameters. The results in Chapter 5 will show how greatly the performance of the system is enhanced by varying or perhaps optimising these parameters for a given environment for a certain application. Hence, these results, based on the precise analysis, provide important and valuable criteria for choosing the appropriate TH-PPM UWB system and signal parameters in practical applications.

The analytical method proposed here is based on the same system and signal models previously reported in section 4.5. This means that, the performance evaluation will be restricted on the analysis of the second-order monocycle in equation (4.4) with a time normalisation factor of τ_p = 0.2877 ns and hence, T_p = 0.7 ns, together with its corresponding autocorrelation properties given in equation (4.5). The analytical method, however, can be applied to UWB systems using arbitrary pulse shapes. Assuming N_u users are transmitting asynchronously on an AWGN channel, the received signal can be modelled as equation (4.8) and the correlator receiver takes its decision according to the decision statistic in equation (4.11), where the same template wave form *v(t)* in equation

(4.6) is contributed in this analysis. Also, considering the same example, therefore it will be considered that $s^{(1)}(t)$ is the desired signal and the reference distance $d_0^{(1)}$ to be transmitted. Without loss of generality, it will be further assumed that the signal of interest of the first user is not time-hopping, i.e., $c_j^{(1)} = 0$ for all values of j [15] and all the other N_u-1 signals are interference signals. Assuming perfect synchronisation with the reference signal, the single-user correlation receiver computed decision statistic can be given by

$$\gamma = \sqrt{\frac{N_s}{E_b}} \sum_{j=0}^{N_s-1} \int_{jT_f}^{(j+1)T_f} r(t)\, v(t - \tau_1 - jT_f)\, dt \tag{4.29}$$

Where $r(t)$ and $v(t)$ are given in equation (4.9), and equation (4.6), respectively. Define the correlation of the template waveform $v(t)$ with a time-shifted pulse $p(t)$ as

$$R_t(x) = \int_{-\infty}^{+\infty} p(t - x)\, v(t)\, dt \tag{4.30}$$

And from equation (4.5), equation (4.6), and equation (4.30), we obtain

$$R_t(x) = R(x) - R(x - \delta) \tag{4.31}$$

Case "1": $R_t(0)$ have a maximum positive value, if the received pulses and the template waveform pulses coincide over each other, then, their cross correlation (which calculates the area of intersection) will have a maximum positive value at x = 0 and hence $R_t(0)$ will be maximum positive, which indicates that these received pulses must be presenting a logical data bit which is "0".

Case "2": $R_t(0)$ will be zero, if the received pulses do not coincide with the template waveform pulses, therefore, their cross correlation $R_t(x)$ shown in Figure 4-10, will be zero at x = 0 (i.e. $R_t(0) = 0$) which indicates that these received pulses must be presenting a logic "1".

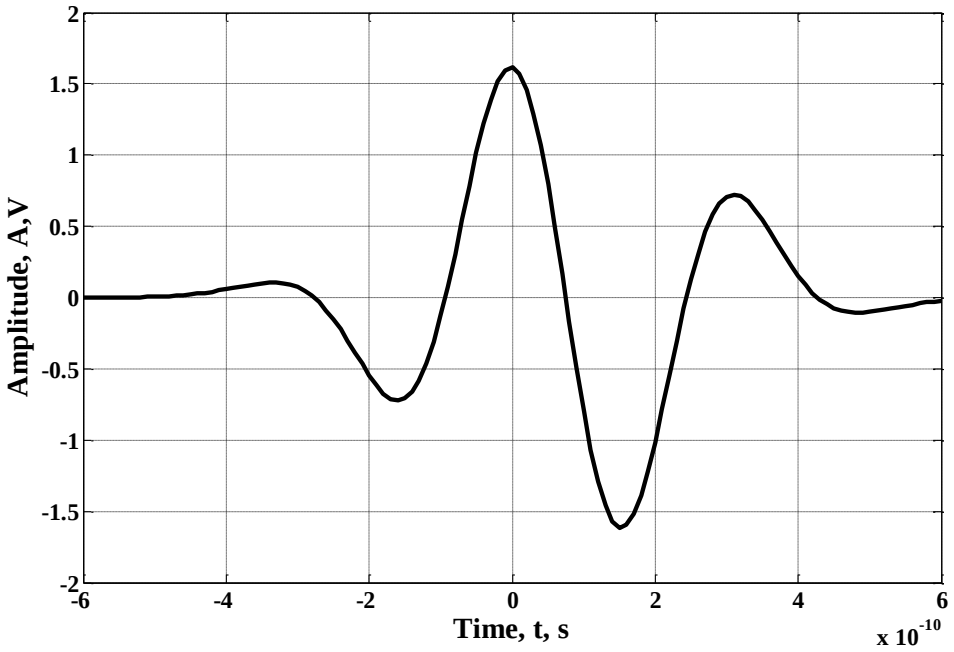

Figure 4-10 The Cross Correlation Function Rt(x).

Referring back to equation (4.7) and Substituting equation (4.8) into equation (4.29) yields

$$\gamma = \underbrace{\sum_{j=0}^{N_s-1}\int_{jT_f}^{(j+1)T_f} p(t-\tau_1-jT_f-d_0^{(1)}\delta)\,v(t-\tau_1-jT_f)\,dt}_{S}$$

$$\underbrace{+\sqrt{\frac{N_s}{E_b}}\sum_{j=0}^{N_s-1}\int_{jT_f}^{(j+1)T_f}\sum_{k=2}^{N_u} A_k s^{(k)}(t-\tau_k)\,v(t-\tau_1-jT_f)\,dt}_{I}$$

$$\underbrace{+\sqrt{\frac{N_s}{E_b}}\sum_{j=0}^{N_s-1}\int_{jT_f}^{(j+1)T_f} n(t)\,v(t-\tau_1-jT_f)\,dt}_{n} \qquad (4.32)$$

Therefore, equation (4.32) can be reduced to

$$\gamma = S + I + n \tag{4.33}$$

Where n is a Gaussian random variable (RV) with a zero mean and variance given by [20]

$$\sigma_n^2 = \frac{N_0 N_s^2 R_t(0)}{E_b} \tag{4.34}$$

The contribution of the decision statistic γ depending on user 1's useful signal bit $d_0^{(1)}$ S is given by [20]

$$S = \pm N_s R_t(0) \tag{4.35}$$

Referring back to equation (4.32), I is the total MAI due to all N_u-1 interfering signals, can be rewritten as

$$I = \sqrt{\frac{N_s}{E_b}} \sum_{k=2}^{N_u} \sum_{j=0}^{N_s-1} \int_{jT_f}^{(j+1)T_f} A_k s^{(k)}(t-\tau_k) \times v(t-\tau_1 - jT_f)\, dt \tag{4.36}$$

Again, the parameter "*S*" in *case "1"* must have a positive value. If there is no AWGN, and if there is no effect from the MAI, therefore, the decision statistic γ, together with I and n must indicate a positive value indicating that the received data bit must be logic "0". However, an error occurs if the effect of the MAI, parameter I, and the Gaussian noise, parameter n, make the decision statistic γ take a negative or zero value that will make the receiver decide that it is a logic "1", which is incorrect. On the other hand the parameter S in this *case "2"* must be less than or equal zero if there is no effect from the MAI and the Gaussian noise. Therefore, the receiver will decide correctly that the received bit is of logic "1". The error occurs here if, the parameters I and n make the decision statistic γ take a value greater than zero which will make the receiver decide that the received bit is logic "0", which is incorrect.

From equation (4.36), there are two time uncertainties that must be taken into consideration; namely, the transmission reference times τ_1 and τ_k. Since these are related to the times when the radios begin transmission in asynchronous operation, the uncertainty

concerning their differences may span many time frames (i.e., the difference between the two times τ_1 and τ_k can be more than one time frame T_f). This difference in the time shifts for user synchronism can be model as described in [19]

$$\tau_k - \tau_1 = j_k T_f + \alpha_k, \qquad -T_f/2 \le \alpha_k < T_f/2 \tag{4.37}$$

Where j_k is the value of the time difference τ_k- τ_1 rounded to the nearest frame time, and α_k is the error in this rounding process and it is uniformly distributed on [-$T_f/2$,$T_f/2$).

Based on the assumption for analytical convenience given in [19] that the time interval over which the monocycle can be time-hopped is less than half a frame time, so that

$$N_h T_c < \frac{T_f}{2} - 2T_p \tag{4.38}$$

Note that only one pulse from each interfering user in each frame contributes to the interference term, therefore equation (4.36) can be rewritten as:

$$I = \sum_{k=2}^{N_u} \sum_{j=0}^{N_s-1} \int_{-\infty}^{+\infty} A_k \, p(x - \alpha_k - c_j^{(k)} Tc - d_{\left\lfloor \frac{(j+j_k)}{N_s} \right\rfloor}^{(k)} \delta) \, v(x) \, dx \tag{4.39}$$

Considering the interfering signal $d_{\left\lfloor \frac{(j+j_k)}{N_s} \right\rfloor}^{(k)}$ may change sign during the transmission time of $d_o^{(1)}$, and referring back to the cross correlation function equation (4.30), therefore, equation (4.39) becomes

$$I = \sum_{k=2}^{N_u} A_k \left[\sum_{j=0}^{\beta_k - 1} R_t(\Theta_{0,j}^{(k)}) + \sum_{j=\beta_k}^{N_s-1} R_t(\Theta_{1,j}^{(k)}) \right] \tag{4.40}$$

Where

$$\left.\begin{aligned} \Theta_{0,j}^{(k)} &= \alpha_k + c_j^{(k)} T_c + d_0^{(k)} \delta \\ \Theta_{1,j}^{(k)} &= \alpha_k + c_j^{(k)} T_c + d_1^{(k)} \delta \end{aligned}\right\} \tag{4.41}$$

Where $d_0^{(k)}$ and $d_1^{(k)}$ represent the two adjacent bits for the k^{th} signal "user" that overlap with the transmission time of $d_0^{(1)}$, and β_k is uniformly distributed over [*0, N_s* - 1] according to the definition of j_k in equation (4.37).

$R_t(\Theta_{0,j}^{(k)})$, is the value of the cross correlation at the time when the first data bit of the k^{th} user is sent, for the j^{th} pulse, and

$$X^{(k)} = \sum_{j=0}^{\beta_k - 1} R_t(\Theta_{0,j}^{(k)}) \tag{4.42}$$

$R_t(\Theta_{1,j}^{(k)})$, is the value of the cross correlation at the time when the second data bit of the k^{th} user is sent, for the j^{th} pulse, and

$$Y^{(k)} = \sum_{j=\beta_k}^{N_s - 1} R_t(\Theta_{1,j}^{(k)}) \tag{4.43}$$

Substituting equation (4.42), equation (4.43) in equation (4.40) yields:

$$I = \sum_{k=2}^{N_u} A_k I^{(k)} = \sum_{k=2}^{N_u} A_k \left[X^{(k)} + Y^{(k)} \right] \tag{4.44}$$

The CF of $R_t(\Theta_{0,j}^{(k)})$ conditioned on $d_0^{(k)}$ and α_k can be written as [20]

$$\Phi_{R_{t0}|d,\alpha}(\omega) = E\left[e^{j\omega R_{t0}} \middle| d_0^{(k)} = d, \alpha_k = \alpha \right] = \frac{1}{N_h} \sum_{h=0}^{N_h - 1} e^{j\omega R_t(\alpha + hT_c + \delta d)} \tag{4.45}$$

Where E[.] denotes expectation. The conditional CF of $X^{(k)}$ is obtained as

$$\Phi_{x^{(k)}|d,\alpha,\beta}(\omega) = E\left[e^{j\omega \sum_{j=0}^{\beta_k - 1} R_t(\Theta_{0,j}^{(k)})} \middle| d_0^{(k)} = d, \alpha_k = \alpha, \beta_k = \beta \right]$$

$$= \left(\frac{1}{N_h} \sum_{h=0}^{N_h - 1} e^{j\omega R_t(\alpha + hT_c + \delta d)} \right)^{\beta} \tag{4.46}$$

Where the second equality follows from the fact that $R_t(\Theta_{0,j}^{(k)})$, $j = 0,\ldots,\beta_k - 1$, are independent when conditioned on $d_0^{(k)}$ and α_k. Note that when N_hT_c is small compared with T_f (when N_hT_c is not very large compared with the pulse duration T_p), the assumption that the interference is independent in different frames of the bit is not rigorously correct, and then equation (4.46) is an approximation. In the alternative, the analysis is valid under the assumption that the pseudorandom TH sequence is random rather than deterministic. Then, the CF of $X^{(k)}$ conditioned on α_k and β_k can be obtained using the theorem of total probability as

$$\Phi_{X^{(k)}|\alpha,\beta}(\omega) = \Phi_{X^{(k)}|0,\alpha,\beta}(\omega)\Pr(d=0) + \Phi_{X^{(k)}|1,\alpha,\beta}(\omega)\Pr(d=1)$$

$$= \frac{1}{2N_h^{\beta}}\left[\left(\sum_{h=0}^{N_h-1} e^{j\omega R_t(\alpha+hT_c)}\right)^{\beta} + \left(\sum_{h=0}^{N_h-1} e^{j\omega R_t(\alpha+hT_c+\delta)}\right)^{\beta}\right] \tag{4.47}$$

Similarly, the CF of $Y^{(k)}$ conditioned on α_k and β_k can be obtained as

$$\Phi_{Y^{(k)}|\alpha,\beta}(\omega) = \frac{1}{2N_h^{N_s-\beta}}\left[\left(\sum_{h=0}^{N_h-1} e^{j\omega R_t(\alpha+hT_c)}\right)^{N_s-\beta} + \left(\sum_{h=0}^{N_h-1} e^{j\omega R_t(\alpha+hT_c+\delta)}\right)^{N_s-\beta}\right] \tag{4.48}$$

For a given k, it can be shown that the random variables RVs $X^{(k)}$ and $Y^{(k)}$ are independent, which results from the independence of the data bits (d_0 and d_1), and the independence of the chip sequences (with distinct chip index j). Then the CF of $I^{(k)}$ conditioned on α_k and β_k is given by

$$\Phi_{I^{(k)}|\alpha,\beta}(\omega) = \Phi_{X^{(k)}|\alpha,\beta}(\omega)\Phi_{Y^{(k)}|\alpha,\beta}(\omega) \tag{4.49}$$

Considering the uniform distribution of β_k, the CF of $I^{(k)}$ conditioned on α_k can be obtained as

$$\Phi_{I^{(k)}|\alpha}(\omega) = \frac{1}{N_s}\sum_{i=0}^{N_s-1}\left[\Phi_{X^{(k)}|\alpha,i}(\omega)\Phi_{Y^{(k)}|\alpha,i}(\omega)\right] \tag{4.50}$$

Averaging out α_k, the CF of the k^{th} interferer can be obtained as

$$\Phi_{I^{(k)}}(\omega) = \frac{1}{T_f} \int_{\frac{-T_f}{2}}^{\frac{T_f}{2}} \Phi_{I^{(k)}|\alpha}(\omega) d\alpha \tag{4.51}$$

Owing to the independence of the interfering components, the CF of the total interference is

$$\Phi_I(\omega) = \prod_{k=2}^{N_u} \Phi_{I^{(k)}}(A_k \omega) \tag{4.52}$$

Last steps to determine expressions for the BERs of the TH-PPM UWB systems based on the previous analysis. Again, referring back to the decision statistic in section 4.4, the decision rule for the type-A TH-PPM system was described in [19] as:

$$\gamma > 0 \rightarrow d_i^{(1)} = 0$$

$$\gamma \leq 0 \rightarrow d_i^{(1)} = 1$$

Owing to the symmetry of the MAI and the noise, the average probability of error for the type-A TH-PPM UWB system is given in [19] as:

$$P_e = \Pr(\gamma \leq 0 | d = 0) \tag{4.53}$$

Defining the total noise-interference parameter as

$$\Lambda = I + n \tag{4.54}$$

Then, using the independence of the MAI and the background noise, the CF of Λ can be expressed as the product of the CF of the interfering signals I and the CF of the Gaussian noise as

$$\Phi_\Lambda(\omega) = \Phi_I(\omega)\Phi_n(\omega) \tag{4.55}$$

Where

$$\Phi_n(\omega) = e^{-\frac{\sigma_n^2 \omega^2}{2}} \tag{4.56}$$

Is the CF of the noise term *n*, and $\Phi_I(\omega)$ is the CF of the total interference in the TH-PPM system.

Taking the inverse transform of the CF in equation (4.55), the cumulative density function (cdf) of Λ can be expressed as [20]

$$F_\Lambda(\lambda) = \frac{1}{2} + \frac{1}{\pi}\int_0^\infty \frac{\sin(\lambda\omega)}{\omega}\Phi_\Lambda(\omega)\, d\omega \tag{4.57}$$

And the BER of the type-A TH-PPM UWB system can be further expressed as [20]

$$\begin{aligned} P_e &= P_r(I + n + A_1 N_s R_t(0) \le 0) \\ &= 1 - F_\Lambda(A_1 N_s R_t(0)) \end{aligned} \tag{4.58}$$

Substituting equation (4.57) into equation (4.58) yields

$$P_e = \frac{1}{2} - \frac{1}{\pi}\int_0^\infty \frac{\sin(A_1 N_s R_t(0)\omega)}{\omega}\Phi_\Lambda(\omega)d\omega \tag{4.59}$$

Substituting equation (4.55) into equation (4.59) yields

$$P_e = \frac{1}{2} - \frac{1}{\pi}\int_0^\infty \frac{\sin(A_1 N_s R_t(0)\omega)}{\omega}\Phi_I(\omega)\Phi_n(\omega)d\omega \tag{4.60}$$

And, substituting equation (4.52) and equation (4.56) into equation (4.60) yields

$$P_e = \frac{1}{2} - \frac{1}{\pi}\int_0^\infty \frac{\sin(A_1 N_s R_t(0)\omega)}{\omega} \times \left[\prod_{k=2}^{N_u}\Phi_{I^{(k)}}(A_k\omega)\right] \times \left[e^{-\sigma_n^2\omega^2/2}\right] d\omega. \tag{4.61}.$$

CHAPTER 5

5 RESULTS AND DISCUSSION

The theoretical performance of both single user and multiple-access is analysed under the perfect power control and Gaussian approximation (GA) assumptions. All of the numerical results presented in this chapter are based on the analysis using the second-order Gaussian monocycle. Results for the zero, first, third and fourth order monocycles are also provided to show the effect of changing the pulse shape. The parameters of the example UWB systems are listed in Table 5-1.

Parameter	Notation	Values
Frame Width	T_f	25, 50, or 100 ns
Impulse Width	T_p	0.7 ns
Time Hopping Chip Width	T_c	0.9 ns
Time Normalisation Factor	τ_p	0.2877, 0.4877, 0.6, 0.8 ns
Time Shift PPM	δ	0.05, 0.1, 0.14, 0.15, 0.2, 0.25, 0.3, 0.35, 0.4 ns
Bit Rate	$R_b = 1\backslash T_b$	2, 3.3, 8, 10, 16, 20, 32, or 40 Mbps
Number of Users	N_u	3, 5, 7, 8, 10, 15, 30, 32, 60, or 64
Number of Chips "hops" per Frame	N_h	4, 8, or 16
Repetition Code Length	N_s	2,6, or 10

Table 5-1 Parameters of the Example TH-PPM System.

5.1 Results of Gaussian Approximation

In this section, will analyse the performance of a single user link of TH-PPM UWB system in an AWGN environment and show the effect of the frame width on the performance of the BER. Also, show how the appropriate choice the modulation parameter δ can affect the performance of the receiver. In addition, the performance of the system is evaluated using different pulse and system parameters like repetition code length N_s and number of chips

"hops" per frame N_h, and number of users N_u. Moreover, the theoretical ability of TH-PPM techniques to provide multiple-access communications in a Gaussian channel is also shown using the multiple-access model. The response of the system for very large values of SNR together with the asymptotic performance of the system for variations in bit rate is observed. In Figure 5-1 the system performance is evaluated for different values of frame width (T_f= 25, 50, 100) ns, with the assumption of absent repetition code (i.e. N_s), therefore bit rates are (R_b = 40, 20, 10) Mbps, shows how the system is greatly influenced by the change in the frame width.

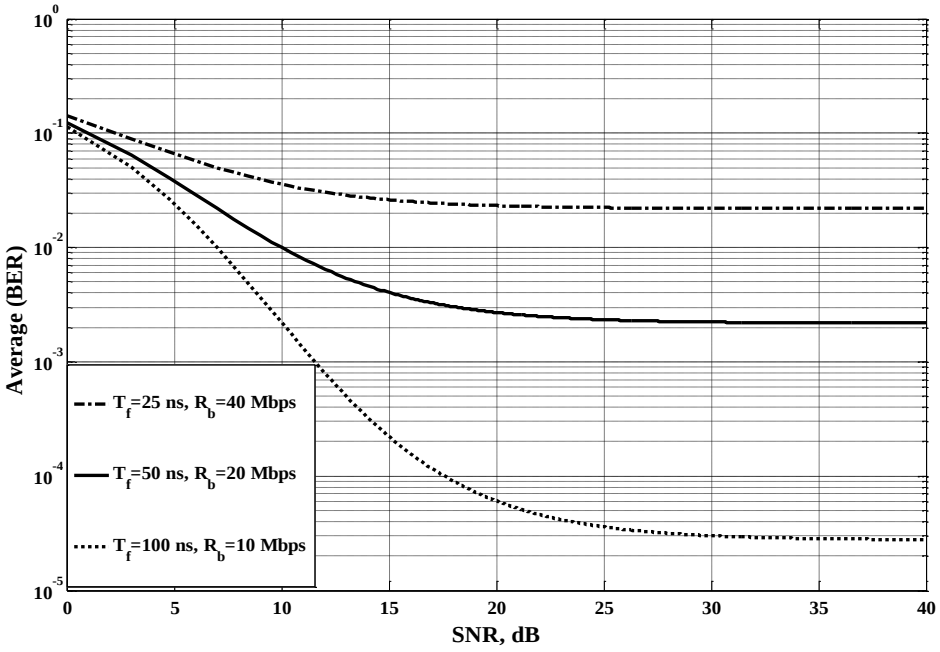

Figure 5-1 Average BER of the TH-PPM UWB system versus SNR for a repetition code Ns= 1, in terms of variations in T_f, R_b.

The curves show that the performance enhancement with increasing T_f, i.e with increasing in frame time T_f the BER is decrease, at the cost of a reduced user bit rate. For this we will choose the frame time at T_f = 50 ns.

In figure 5-2, we investigate the impact of the pulse shape on the average BER performance of the TH-PPM UWB systems for different Gaussian monocycles. Example

of the zero, first, second, third, and fourth order Gaussian monocycles with τ_p=0.2877 ns are examined for the purpose of comparison. The corresponding autocorrelation properties of each are previously shown in Figure 4-3, and in Figure 4-4, from which the minimum autocorrelation value and the corresponding δ of each can easily be calculated It is noted that, as the order increases, minimum values of autocorrelation are obtained at smaller values of time shift. With a close investigation of Figure 5-2, it can be observed that, each higher order outperforms its adjacent lower order for all SNR values. For that, it seems that the higher order Gaussian monocycles can provide lower multiple-access bit error rates when the pulse width is fixed. Such observation is reported in [13].

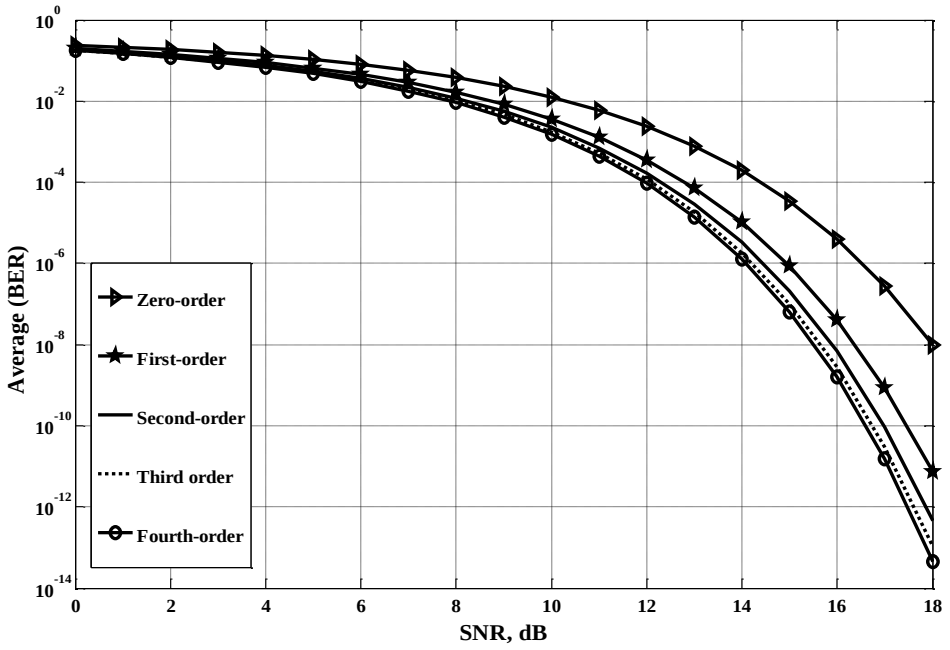

Figure 5-2 Average BER of the TH-PPM UWB system versus SNR for different order Gaussian monocycles, in case of no MAI.

For this reason, Figure 5-3 shows how the system is greatly influenced by the change in the modulation parameter δ. Based on equation (4.12), when only one transmitter is in function. The depicted curves show that the bit error rate (BER) values are in continuous change with a tracing relationship to the autocorrelation properties of the chosen pulse.

Different autocorrelation values, corresponding to the increasing values of δ examined for each curve, can easily be calculated from the autocorrelation function of equation (4.5).

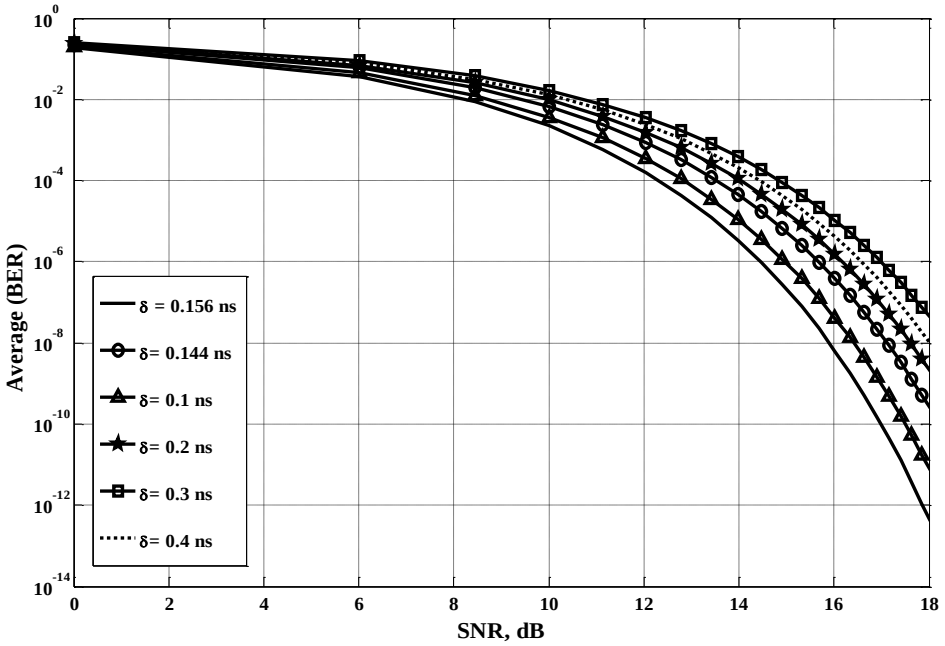

Figure 5-3 Average BER of the TH-PPM UWB system versus SNR for different values of time shift δ, in case of no MAI.

By referring back to equation (4.27), and Figure 4-8, together with Figure 5-3 it can be shown that the best performance is obtained when the choice of δ is optimum at 0.156 ns for the second order Gaussian monocycle of τ_p=0.2877 ns. This because the probability of error is observed to be directly affected by the autocorrelation value at a certain time shift δ of a specific pulse shape with a specific pulse width. For the probability of error to have minimum value, the argument of the *erfc*(.) function must be maximised corresponding to a minimum autocorrelation value for a specific optimum δ. One must refer back to equation (4.25), and equation (4.28) to investigate its minimum conditions.

When multi access user interference prevails, it can be shown in this case that the probability of error can yield minimum values from the $P(\delta)$ function depicted in Figure 4-8 it can be shown that it's minimum occur when δ_{opt} is chosen to be 0.144 ns. According

to the operating environment for the second order Gaussian monocycle waveform used in the analysis, these considerations imply that δ should be chosen either 0.156 ns or 0.144 ns. However, it can also be observed from Figure 4-8 how small the variations of $P(\delta)$ are around its minimum, which indicates that a little is lost in choosing either of these values. Therefore, the first choice of δ_{opt}=0.156 ns can be supposed optimum for whatever type of interference is dominant. Note that, δ_{opt} is determined according to the pulse shape and the pulse-width normalisation factor τ_p. Due to the sensitivity of the TH-PPM UWB systems to the choice of the time-shift, a suitable value for δ should be chosen according to the specific pulse shape and the pulse width employed in a practical UWB application. In addition, the choice of Gaussian monocycle with their special autocorrelation properties of positive and negative values, permit the use of non-orthogonal pulses with δ values < T_p. Hence, we are not restricted to orthogonal pulses where δ should be > T_p to prevent overlapping of pulses.

From Figures 5-2 and 5-3, it is clear that, the BER curves are in a continuous sharp decrease with an increase in the SNR. This is because we are studying the effect of AWGN only which is completely eliminated by the increase in SNR without any MAI effect. This observation, however, will not be shown in the following case of MAI where the system reaches saturation at BER floors for whatever SNR increase is imposed.

In Figure 5-4, and Figure 5-5, the system performance is evaluated for different values of N_u regarding the operation is in indoor and outdoor environments, all with the assumption of constant repetition code at N_s= 2, and a fixed frame time T_f= 50 ns (therefore bit rate at R_b = 10 Mbps).

To investigate the operation of the system in indoor environments where the system is supposed to provide access to a small number of users, Figure 5-4 is depicted to show the performance for different small number of users (N_u = 5, 7, 10) as assumption an average. As expected, it is clear, that the increase in the number of users simultaneously using the system degrades the system performance. When observing the results depicted in Figure 5-4, one should immediately record the imaginable decrease in the BER reached for smaller values of N_u.

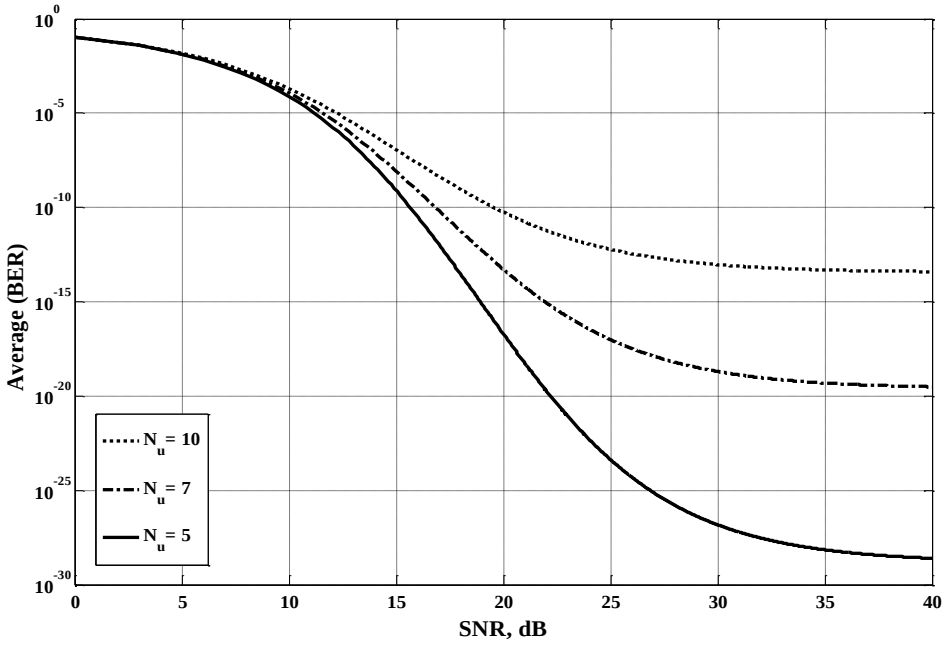

Figure 5-4 Average BER of the TH-PPM UWB system in indoor environments for small and high values of SNR, with a repetition code Ns= 2, and different small number of users.

Similar results, showing the effect of varying the number of users, are shown in Figure 5-5 for environments simulating outdoor conditions where the number of users is supposed to be larger in magnitude and is much being reduced. Three different larger values are depicted for comparison (N_u = 15, 30, 60). By comparing Figures 5-4 and 5-5 for the same system parameters, one can also note the very different performance results, regarding the BER values, between indoor and outdoor environments.

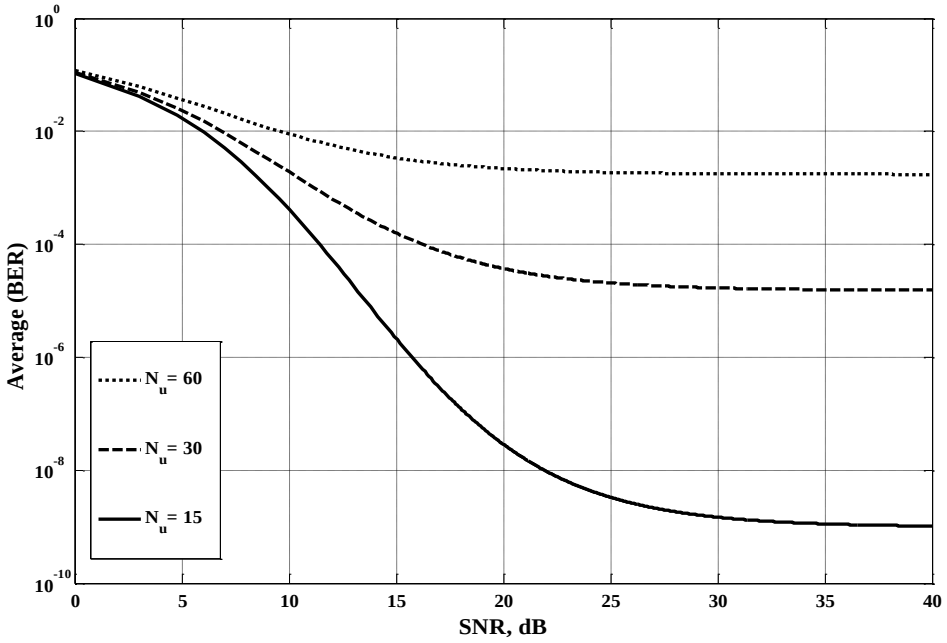

Figure 5-5 Average BER of the TH-PPM UWB system in outdoor environments for small and high values of SNR, with a repetition code Ns= 2, and different large number of users.

From Figure 5-5, we can note that the performance of the system operating for small values of the SNR in which a predicted decrease in BER is accompanied by an increase in the SNR. This is because the effect of the AWGN is gradually being eliminated by the increase in the SNR. However, there is the effect of MAI that has nothing to do with the increase in the SNR. Also, it must be noted that whatever the randomness of the TH sequences are, this does not guarantee that collisions are totally eliminated. It is clearly shown, for the same number of users that the system reaches saturation for high values of SNR where the effect of AWGN is eliminated and the MAI is dominant. This observation can also be explained by referring to equation (4.26), when $E_b / N_0 \rightarrow \infty$, the asymptotic performance of the system depends only on the constant values of N_u and R_b, correspondingly making the system takes saturated constant values of bit error rates.

The depicted curves in Figures 5-4 and 5-5 show the theoretical ability of TH-PPM techniques to provide multiple-access communications in a Gaussian channel. For completeness, it must be noted that these results totally neglect the effect of multi-path fading environments which greatly introduces performance degradation especially in indoor environments.

As previously mentioned, N_s is the number of pulses required to present a single bit of information. The receiver collects these pulses to be able to recover the original transmitted bit. During the transmission (or perhaps the reception) process, if one or more of these pulses are lost, the receiver can still recover the original transmitted bit from the other pulses. Therefore, extra repetition of the pulses is important for the receiver to be able to precisely recover the transmitted bit with a minimum probability of error.

Hence, the effect of increasing the number of pulses per bit (N_s) for the same system parameters and T_f, is analysed in Figure 5-6 and is used to determine how the system responds to these variations. Figure 5-6 investigate the effect of different values of repetition code (N_s = 2, 6, 10) on the performance of TH-PPM UWB system for N_u = 48 and T_f = 50 ns, therefore bit rates are (R_b = 10, 3.3, 2) Mbps.

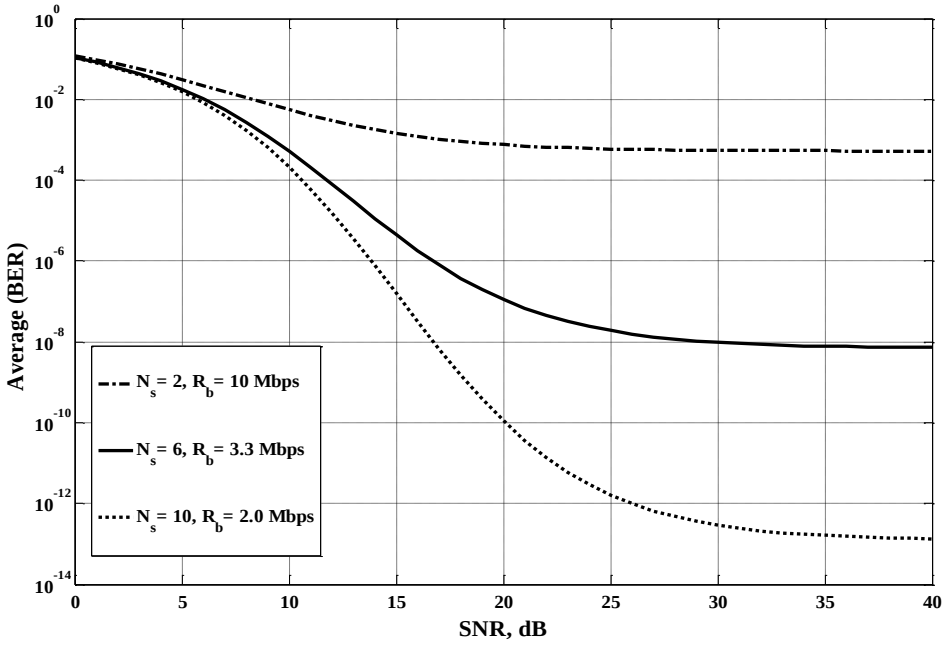

Figure 5-6 Average BER of the TH-PPM UWB system versus SNR assuming number of users Nu = 48 for a repetition code with Ns= 2, Ns= 6, and Ns= 10.

From Figure 5-6 it is clearly shown that, the BER performance greatly improves when a longer repetition code N_s is used, as expected, reaching saturation asymptotic values for

high values of SNR similar to that in Figures 5-4 and 5-5. Another observation is that since the frame time is constant at T_f = 50 ns. Therefore, an increase in the repetition code *(N_s)* imposes a similar increase in the bit duration *(T_b)* that results in a corresponding decrease in the bit rate. Since this is the case for most of the communication systems, a compromise must be made between the specified level of probability of error and the bit rate required for a certain application. It is clearly shown in Figure 5-6 that, although an increase in N_s decreases the BER, however, it reduces the bit rate. This requires system developers to make an appropriate decision, that is, application dependent.

Figure 5-7 is insuring the result came in Figures 5-4, 5-5, and 5-6 together.

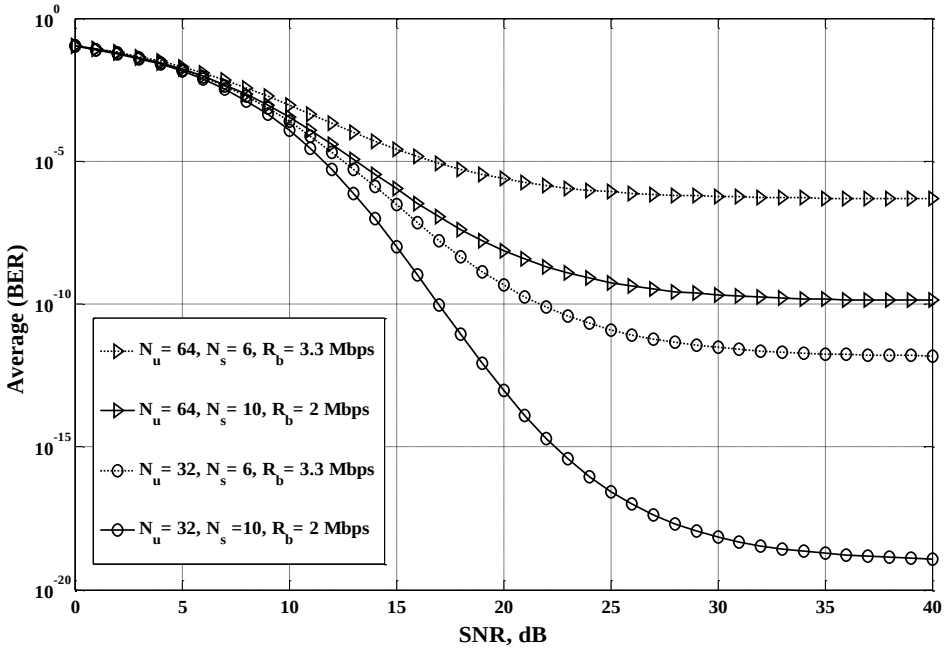

Figure 5-7 Average BER of the TH-PPM UWB system versus SNR comparison between two cases Nu= 64 and Nu= 32 for a repetition code with Ns= 6, and Ns= 10.

In Figure 5-7 The solid and dotted lines with triangle markers represent the BER curves at N_u= 64, and the bit rate R_b=3.3 Mbps, 2 Mbps, with repetition code N_s= 6, and N_s= 10, while the solid and dotted lines with circle markers represent the BER curves at N_u= 32, and the same bit rate R_b=3.3 Mbps, 2 Mbps, with repetition code N_s= 6, and N_s= 10. This Figure clearly indicates that the BER performance greatly improves as expected when:

* A longer repetition code N_s is used

* A lower number of users N_u

When the other system parameters like (δ, T_f) are kept constant.

5.2 Results of Exact BER

The results in this section are analysed and discussed, based on the exact numerical analysis of TH-PPM, mentioned in Chapter 4. These numerical results are also evaluated based on the analysis of the second order Gaussian monocycle, with its associated autocorrelation properties, assuming that, a multiple access scenario in indoor environments is operated in an AWGN channel. Similar to the GA results, the exact results are also evaluated for different system and signal parameters, such as δ, N_u, and N_s. and new parameters, which are extracted from the exact expression, such as τ_p, and N_h. All the numerical calculations in this section are performed using the composite Simpson's rule and are programmed using Matlab.

From the point of view of the signal characteristics, it is noticed from Figure 5-8 that, the BERs of the TH-PPM system of the second order monocycle with smaller $\boldsymbol{\tau_p}$, corresponding to a smaller pulse width, performs better when other system parameters are kept constant.

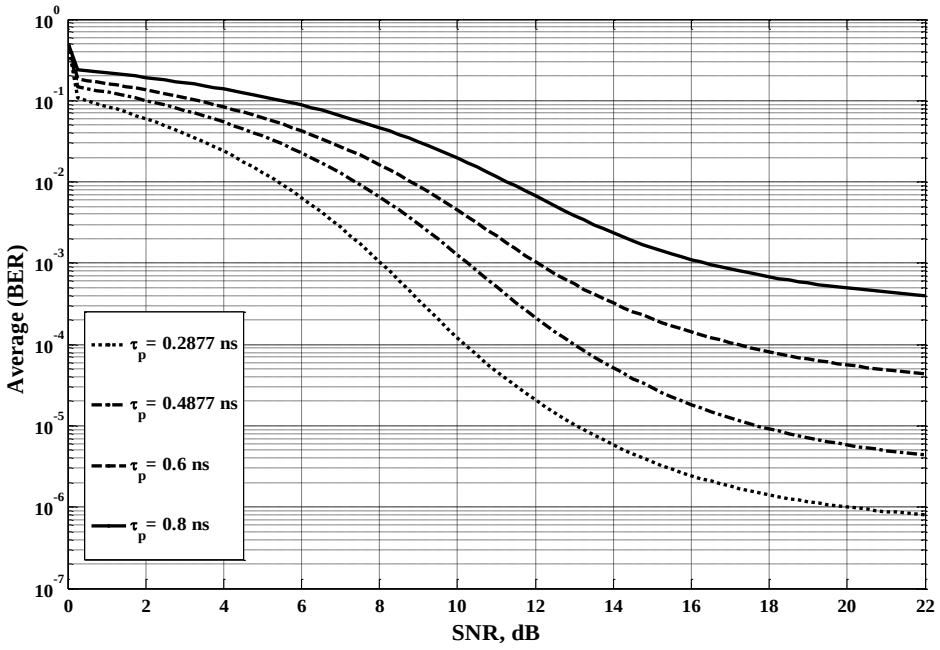

Figure 5-8 Average BER of the TH-PPM UWB system versus SNR for Ns=8, assuming seven asynchronous interferers showing the effect of different pulse widths τp.

All the depicted curves are drawn with 8 users operating in an asynchronous environment. The same value is set to N_h and N_s. It is concluded that, the performance in an asynchronous environment using the second order monocycle with a smaller τ_p is better than that when using the same order with a larger τ_p.

Figure 5-9 shows how the system performs best when δ = 0.15 ns which is the optimum value obtained from the autocorrelation function *R(x)* of equation (4.5) of the second order Gaussian monocycle. Different curves are plotted at different increasing values of δ from 0.05 ns to 0.35 ns. Referring back to Figure 4-3 it can be shown that the BER curves trace the increase and decrease in the autocorrelation value at each δ, where the best performance denoted by stars is recorded at the value of δ that corresponds to the minimum autocorrelation. This is used to confirm the previous results of Figure 5-3 where the multiple access interference is modeled as a Gaussian random process.

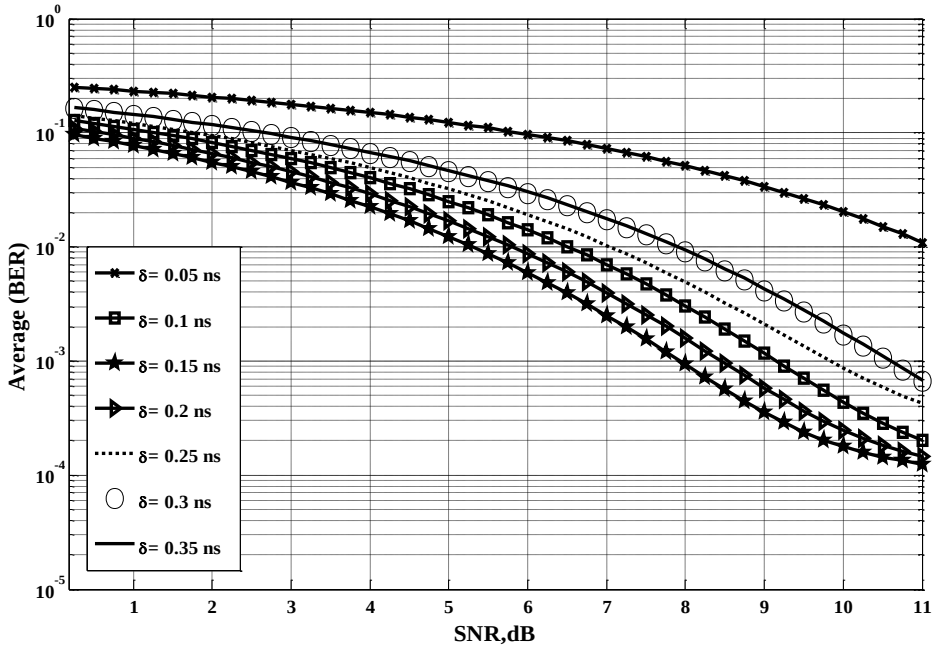

Figure 5-9 Average BER of the TH-PPM UWB system versus SNR for Ns= 2, showing the effect of different values of the time shift δ.

To reach better values of BER while still maintaining the same bit rate, for the same number of users operating in a specific environment, simply increase the number of hopping compartments, N_h, within the time frame. Since the TH sequence is based on PN random code, therefore, this approach greatly reduces the collision between the time-hopping pulses of different users resulting in an equivalent decrease in the BER.

Figure 5-10 show the effect of different values of time hopping on the performance of the system. It must be noted that although an increase in N_h is required to decrease the BER, or perhaps to make the system support a great number of users, however, this increase is limited by the chip duration time T_c which in turn is limited by the pulse width of the pulse under investigation. This limitation must be taken into consideration to prevent overlapping of pulses.

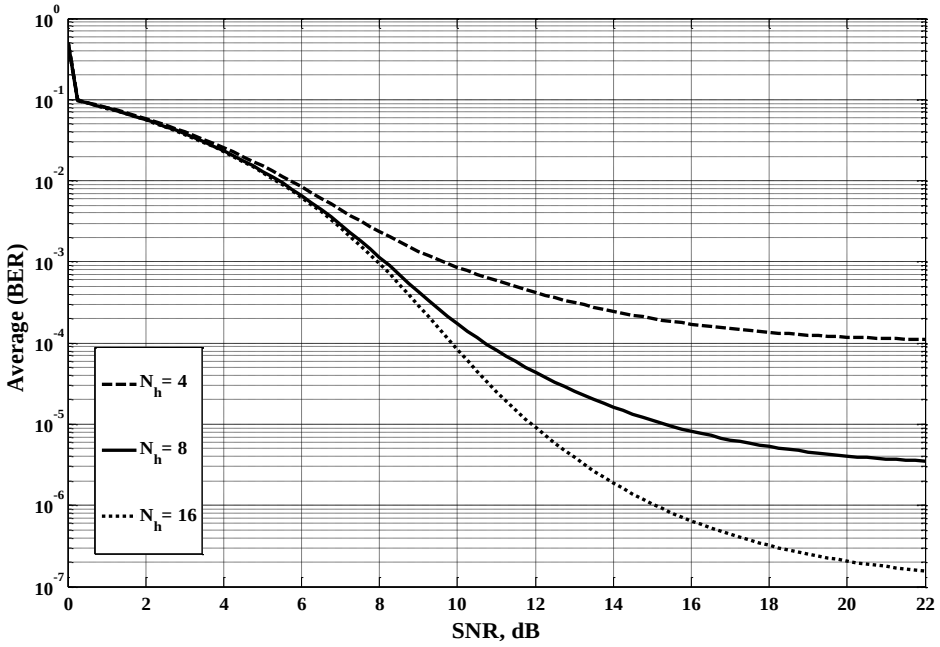

Figure 5-10 Average BER of the TH-PPM UWB system versus SNR for a repetition code with Ns = 6 showing the effect of different number of time hopping compartments Nh on the performance of the system.

Figure 5-10 clearly shows how the increase in the number of N_h greatly influence the performance of the TH-PPM system in a multiple access environment of 7-asynchronous interferers pulsing at a repetition code rate of N_s = 6.

The effect of different number of users operating the system, in AWGN indoor environments, on the BER performance of TH-PPM systems is shown in Figure 5-11, as well. Both Figures 5-10 and 5-11 are evaluated using the second order Gaussian monocycle with T_f = 50 ns, τ_p= 0.2877 ns, δ_{opt} = 0.15 ns where its minimum autocorrelation properties is obtained, the repetition code used here is N_s= 6.

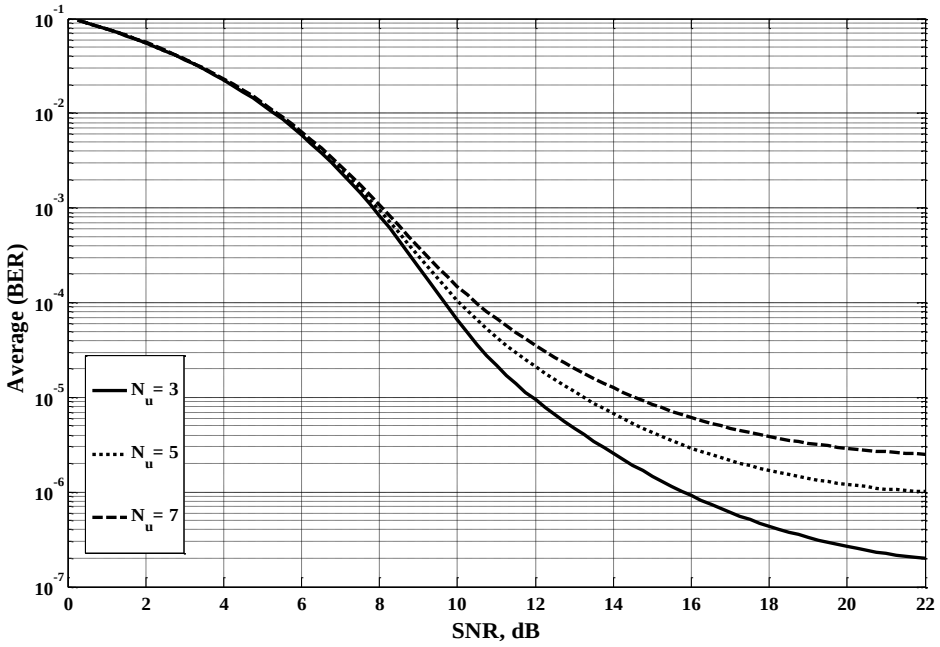

Figure 5-11 Average BER of the TH-PPM UWB system versus SNR for a repetition code with Ns = 6 showing the effect of different number of users on the performance of the system operating the system in an indoor environment.

From Figure 5-11 as expected we observe from the numerical results that a continuous increase in the number of users degrades the system performance.

On the other hand, as previously mentioned, the SNR in the analytical results is defined as E_b / N_0. Figure 5-12 shows the accurate BER performance of TH-PPM system computed using equation (4.61) for different values of the repetition code parameter, as expected Figure 5-12 indicates that the BER improves when a longer repetition code is used. It must be mentioned that the depicted curves are drawn for a constant frame duration time at T_f = 50 ns where a variation in the repetition code is accompanied by a variation in the bit duration time, T_b, resulting in variations in the bit rate, as indicated. As previously mentioned, although the increase in N_s results in better BER values, the bit rate decreases. Hence, a compromise between both criteria has to be accomplished for a specific application.

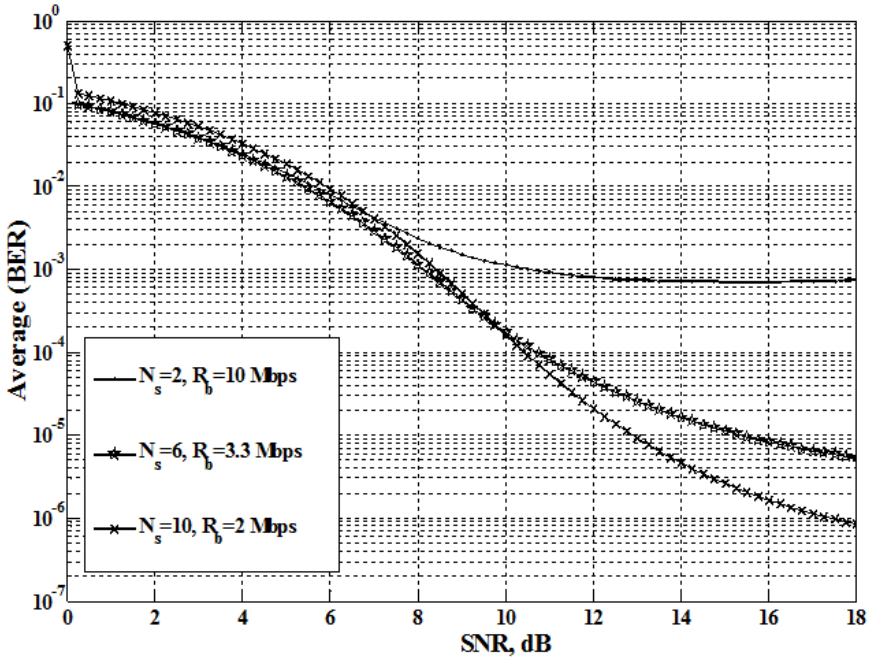

Figure 5-12 Average BER of the TH-PPM UWB system versus SNR for a repetition code with Ns = 2, Ns = 6, and Ns = 10 assuming seven asynchronous interferers.

The methods of varying the bit rate are a system, or perhaps an application, dependent. This means that, if T_b itself is changed while N_s, is constant, it will also result in a variation in the bit rate. In this case, similar variations also take place for the chip duration time, as long as N_h is constant ($T_f = T_b / N_s$ and $T_c = T_f / N_h$). This effect is shown in Figure 5-13 for two different constant values of the repetition code N_s = 2 and N_s = 8. Three different values of T_b are examined for comparison: T_b = 31.25 ns, 62.5 ns, and 125 ns. The

equivalent bit rate value of each is R_b= 32 Mbps, 16 Mbps, and 8 Mbps. Both Figures 5-12 and 5-13 are evaluated using the second order Gaussian monocycle with τ_p = 0.2877 ns, δ_{opt} = 0.15 ns, and number of hops N_h = 8.

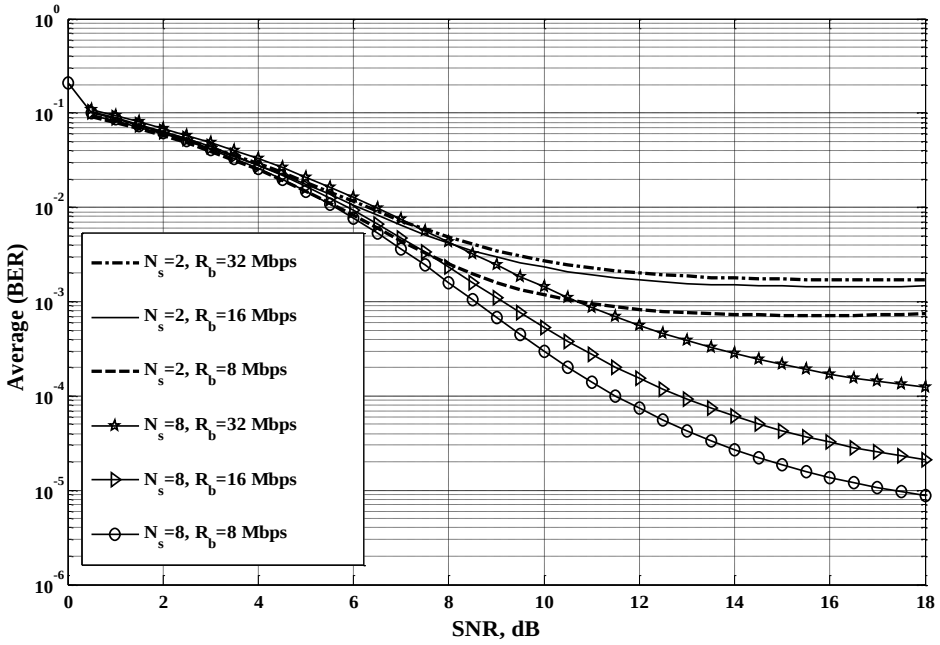

Figure 5-13 Average BER of the TH-PPM UWB system versus SNR assuming seven asynchronous interferers, showing the effect of changing the bit rate for a repetition code with Ns = 2 and Ns = 8.

From Figure 5-13, the effect of increasing the repetition code on the BER performance can be noticed, together with this new criterion of varying the bit rate. The solid and dotted lines represent the BER rate curves at N_s = 2, while the solid lines with star, triangle, or circle markers represent the BER curves at N_s = 8.

5.3 Comparison Between the GA and the Exact Numerical Results

By equating the parameters of both the GA and the exact models, regarding the use of the same pulse parameters and the same number of chips "hops" per frame (N_h = 8). The following results are based on the analytical method presented in Chapter 4 and are used to assess the validity of the GA model used for simulating environments operating in multiple access interference.

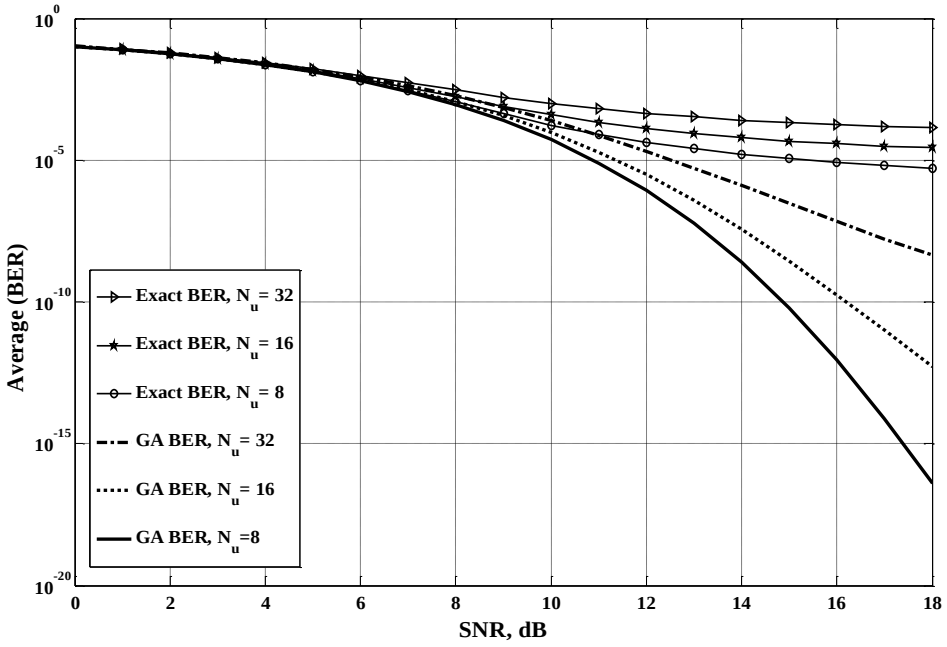

Figure 5-14 Comparison between the exact MAI and GA models, in terms of different accessing number of users in Nu, in evaluating the performance of TH-PPM UWB systems in an asynchronous multiple access environments.

Figure 5-14 is used to compare between the two models from the point of view of different accessing number of users (N_u = 8, 16, 32). The solid lines with triangle, star or circle markers represent the exact analytical results of BERs, while the solid and dashed lines represent the BERs obtained from the GA model. Apart from the fact of performance degradation, easily shown in Figure 5-14, when the number of users increase, Figure 5-14

also shows that, the GA fails to predict the error-rate floor caused by the interference for large values of SNR, and that the models do not agree.

Figure 5-15 further confirms the results obtained in Figure 5-14 by comparing the two models from the view point of three different values of the repetition code (N_s = 2, 6, 10). The solid lines with triangle, circle or star markers represent the exact analytical results of BERs, while the solid and dashed lines represent the BERs obtained from the GA model.

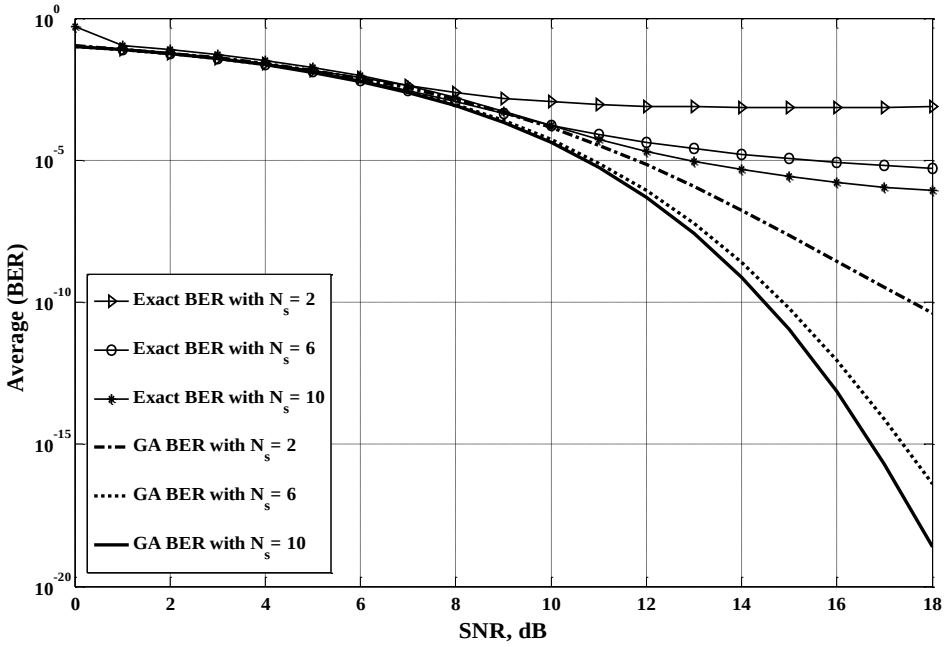

Figure 5-15 Comparison between the exact MAI and GA models, in terms of variations in Ns, in evaluating the performance of TH-PPM UWB systems in an asynchronous multiple access environments.

Apart from the clearly shown performance enhancement when a larger repetition code is used, it is clearly shown that the GA is in a good agreement with the exact analysis only for small values of SNR, say SNR < 7 dB. However, the GA fails to predict the error rate floor of the TH-PPM UWB system (caused by interference) for medium and large values of SNR.

Thus, the GA is not a reliable approximation. Actually, when the SNR equals 18 dB, the exact BER is approximately 7.45×10^{-4} with N_s = 2 and the BER predicted from the GA is 4.06×10^{-11}, which underestimates the actual BER performance by over seven orders of magnitude. We can observe that the amount of the actual improvement can be less or more than the improvement predicted by the GA. For example, when the SNR = 9 dB, the amount of improvement (between N_s = 2 and N_s = 6), due to the longer repetition code predicted by the GA, is less than the actual improvement. When SNR = 18 dB, the amount of improvement predicted by the GA is more than the actual improvement. Therefore, the GA can underestimate or overestimate the improvement obtained by using longer repetition codes.

Actually, in the GA, the BERs are obtained by modelling the total MAI as a Gaussian-distributed RV. Indeed, it can be shown that the MAI is not Gaussian distributed. Referring back to equation (4.54), for small values of SNR, the background Gaussian noise "n" is dominant in the term $\Lambda=I+n$, and therefore, Λ can be approximated as a Gaussian-distributed RV. Hence, the GA can provide good BER estimates of BERs for small SNR. On the other hand, when SNR is large, the interference "I" is dominant in the term Λ, and Λ cannot be approximated as a Gaussian-distributed RV. Thus, the GA fails to predict the actual BERs for large values of SNR.

CHAPTER 6

6 CONCLUSION AND FUTURE WORK

In order to transmit digital data containing a large spectrum from near DC to few Giga Hertz, Ultra-wideband (UWB) in an approaching latest wireless technology. Its prompt bandwidth is many times larger than the least needed to convey specific data, an additional bandwidth that is the chief feature of UWB. The skill of UWB technology is dependent on the usage and partaking of previously engaged spectrum resources without making any damaging interference to the operating systems previously engaged by the spectrum, instead of finding the still offered but perhaps inappropriate latest bands; therefore, allowing infrequent spectrum resources to be utilised more proficiently. The primary theory of UWB is to convey and get an exceptionally short duration RF energy pulses (in the order of nanoseconds) over a very broad band of frequencies. The important benefits of this technology are low-power operation, moderated multipath fading outcomes, high bit rates, low budget execution, exclusive exact arrangement and situation capability, capability to conduct signals among hindrances, highly protected, carrier-free modulation, and simple design for the wireless transceiver systems.

For UWB signals, a number of modulation methods have been suggested, such as PPM and a broad range of PAMs consisting BPSK and OOK. Time hopping and direct sequence are the two spread spectrum methods recommended for UWB, which are fundamental for multiple access operation and interference resistance to conventional radio systems previously engaged by the spectrum.

This thesis presents, analysis of asynchronous multiple access performance for TH combined with PPM method, based on BER, and is assessed for transmission through an additive white Gaussian noise (AWGN) channel. Multiple access interference (MAI) is initially exhibited as a Gaussian random variable to mimic the outcome of functioning a various number of users in an indoor environment.

A precise systematic expression, yet, for the average BER of TH-PPM system is concluded depending on the characteristic function (CF) technique. Equated with other techniques

utilised in the performance analysis of UWB systems, the current assessment gives a strong tool for measuring the BER to any preferred precision with a very minimum complication.

Furthermore, the gathered systematic outcomes are utilised to evaluate the GA of the MAI model, initially supposed. They point towards that the GA substantially overestimates the performance of UWB systems at medium and large values of SNR. The contrast between the two methodologies demonstrates the non-validity of the Gaussian model to portray the multi access interference in TH binary PPM system. To be precise, the BER floor because the interference level is entirely dissimilar with the two methodologies and the Gaussian model causes more positive estimation.

Besides, this theory also demonstrates a number of methodologies by which the performance of TH-PPM UWB systems could be enhanced on large extent, despite preserving the similar bit rate. This is in opposition to other greater multi-levels such as M-ary PPM or N-ary PAM, where small values of BER are achieved at the price of a decreased user bit rate, R_b, and an up rise in the transceiver intricacy. The critical outcomes demonstrate that by changing or possibly augmenting, some system and/or signal factors the performance of the system can be improved to a great extent.

The outcomes of changing the pulse shape and the equivalent pulse constraints on the performance of TH-PPM systems have been assessed initially. According to an instance the ideal value of the time shift 'δ' related with the binary TH-PPM should be cautiously selected to make sure the finest performance of the TH-PPM system for a given pulse shape utilised in a specific submission. In addition it has been demonstrated that the ideal choice of the time shift parameter 'δ' denotes back to the autocorrelation characteristics of the pulse shape under examination. The finest BER performance is attained when the autocorrelation of a particular pulse shape is of least value. According to the samples, among Gaussian monocycles of the similar pulse width, higher order has better performance in comparison to the lower order ones. Furthermore, it has been also demonstrated that for Gaussian monocycles of the similar order, ones with a smaller pulse width, have better multiple access performance.

Secondly, the outcomes of altering few system frameworks on the performance of TH-PPM systems has been also inspected and assessed. The achieved outcomes demonstrate

that the increase in the repetition code, *Ns*, enhances the system performance to a great extent, as predicted, permitting a lower BER floor. Though, this is at the cost of a decreased user bit rate. This is due to the number of pulses per bit increases; the receiver is more approved regarding its bit verdict of logic 1s or 0s. Alternatively, it has been revealed that the continuous rise in the number of users worsens the system performance for either indoor or outdoor settings. Raising the number of time slots per frame, N_h, is the way out recommended to resolve this issue. It has been made known that as N_h per frame rises, while the number of users is fixed; the system performance is enhanced to a great extent.

Utilising the estimated examination, it has to be taken into account that most of the systematic outcomes verify the consequences achieved in prior experiments of other writers. The assessment of various UWB systems, grounded on the accurate investigation, gives consistent statistics in order to select the appropriate signal, system, or possibly modulation patterns in the framework of UWB systems.

The comparison between the two approaches shows the non-validity of the Gaussian model to characterise the multi access interference in TH binary PPM system. In particular, the BER floor due to the interference level is totally different with the two approaches and the Gaussian model results in a more optimistic prediction.

Suggestions for Future Work:

In accordance to the conclusions extracted from the present work, suggestions for future work are:

1. The effect of using other pulses waveform on the system performance.
2. The effect of using higher levels (M-ary PPM) or other different modulation techniques on the system performance.
3. The application of the analytical method to UWB systems using arbitrary pulse shapes.
4. Investigation of the performance TH-PPM in presence of Narrow Band (NB) interference.

5. The effect of using other channels on the system performance.

REFERENCES

[1] H. H. H. Mosa and M. Hope, "The Effects of Varying System Parameters on the Performance of TH-PPM UWB Systems," presented at the PGNET 2014, 2014.

[2] V. Sipal, B. Allen, D. Edwards, and B. Honary, "Ultrawideband: the superstar of wireless communication," *IET Communications*, 2011.

[3] P. Cheolhee and T. S. Rappaport, "Short-Range Wireless Communications for Next-Generation Networks: UWB, 60 GHz Millimeter-Wave WPAN, And ZigBee," *Wireless Communications, IEEE*, vol. 14, pp. 70-78, 2007.

[4] D. Porcino and W. Hirt, "Ultra-wideband radio technology: potential and challenges ahead," *IEEE Communications Magazine*, vol. 41, pp. 66-74, 2003.

[5] FCC, "Federal Communications Commission Revision of Part 15 of the commission's Rules Regarding Ultra-Wideband Transmission System from 3.1 to 10.6 GHz, ET-Docket, 98-153," Washington, DC. adopted/released Feb. 14/Apr. 22, 2002.

[6] D. Cabric, M. S. Chen, D. A. Sobel, S. Wang, J. Yang, and R. W. Brodersen, "Novel radio architectures for UWB, 60 GHz, and cognitive wireless systems," *EURASIP Journal on Wireless Communications and Networking*, vol. 2006, pp. 1-18, 2006.

[7] D. Cabric, M. S. W. Chen, D. A. Sobel, Y. Jing, and R. W. Brodersen, "Future wireless systems: UWB, 60GHz, and cognitive radios," in *Custom Integrated Circuits Conference, 2005. Proceedings of the IEEE 2005*, 2005, pp. 793-796.

[8] L. Jin-Shyan, C. Chun-Chieh, and S. Chung-Chou, "Applications of Short-Range Wireless Technologies to Industrial Automation: A ZigBee Approach," in *Telecommunications, 2009. AICT '09. Fifth Advanced International Conference on*, 2009, pp. 15-20.

[9] B. Kumbhani, T. S. Reddy, K. S. Sastry, and R. S. Kshetrimayum, "Narrow Band Interference (NBI) mitigation technique for TH-PPM UWB systems in IEEE

802.15.3a channel using wavelet packet transform," in *Emerging Trends and Applications in Computer Science (ICETACS), 2013 1st International Conference on*, 2013, pp. 38-42.

[10] K. Eun Cheol and K. Jin Young, "Performance analysis of space time block coded PPM-TH UWB systems in indoor wireless channels," in *Advanced Communication Technology, 2009. ICACT 2009. 11th International Conference on*, 2009, pp. 2329-2332.

[11] G. Lijia, Y. Guangrong, and S. Affes, "On the BER performance of pulse-position-modulation UWB radio in multipath channels," in *2002 IEEE Conference on Ultra Wideband Systems and Technologies (IEEE Cat. No.02EX580)*, May 2002, pp. 231-234.

[12] S. Gezici, H. Kobayashi, H. V. Poor, and A. F. Molisch, "Performance evaluation of impulse radio UWB systems with pulse-based polarity randomization in asynchronous multiuser environments," in *2004 IEEE Wireless Communications and Networking Conference (IEEE Cat. No.04TH8733)*, 2004, pp. 908-913 Vol.2.

[13] J. Zhang, T. D. Abhayapala, and R. A. Kennedy, "Performance of ultra-wideband correlator receiver using Gaussian monocycles," in *Communications, 2003. ICC '03. IEEE International Conference on*, 2003, pp. 2192-2196.

[14] V. S. Somayazulu, "Multiple access performance in UWB systems using time hopping vs. direct sequence spreading," in *Wireless Communications and Networking Conference, 2002. WCNC2002. 2002 IEEE*, 2002, pp. 522-525.

[15] G. Durisi and S. Benedetto, "Performance evaluation of TH-PPM UWB systems in the presence of multiuser interference," *Communications Letters, IEEE*, vol. 7, pp. 224-226, May 2003.

[16] G. Durisi and S. Benedetto, "Performance evaluation and comparison of different modulation schemes for UWB multiaccess systems," in *Communications, 2003. ICC '03. IEEE International Conference on*, 2003, pp. 2187-2191.

[17] J. Cheng and N. C. Beaulieu, "Accurate DS-CDMA bit-error probability calculation in Rayleigh fading," *Wireless Communications, IEEE Transactions on,* vol. 1, pp. 3-15, Jan 2002.

[18] M. Z. Win and R. A. Scholtz, "Impulse radio: how it works," *Communications Letters, IEEE,* vol. 2, pp. 36-38, 1998.

[19] M. Z. Win and R. A. Scholtz, "Ultra-wide bandwidth time-hopping spread-spectrum impulse radio for wireless multiple-access communications," *Communications, IEEE Transactions on,* vol. 48, pp. 679-689, April 2000.

[20] H. Bo and N. C. Beaulieu, "Exact bit error rate analysis of TH-PPM UWB systems in the presence of multiple-access interference," *Communications Letters, IEEE,* vol. 7, pp. 572-574, Dec 2003.

[21] M. Crepaldi and P. R. Kinget, "Error ratio model for synchronised-OOK IR-UWB receivers in AWGN channels," *Electronics Letters,* vol. 49, pp. 25-27, 2013.

[22] M. Uzzafer, "Single correlator receiver for wideband multipath channel," in *Emerging Technologies: Frontiers of Mobile and Wireless Communication, 2004. Proceedings of the IEEE 6th Circuits and Systems Symposium on*, 2004, pp. 421-424 Vol.2.

[23] S. M. Ekome, G. Baudoin, M. Villegas, and J. Schwoerer, "Estimation of the energy detector performances on UWB channel based on the analysis with AWGN channel," in *2012 IEEE International Conference on Ultra-Wideband,* 2012, pp. 150-154.

[24] M. Kheir, T. Kroger, and M. Hoft, "A New Class of Highly-Miniaturized Reconfigurable UWB Filters for Multi-Band Multi-Standard Transceiver Architectures," *IEEE Access,* vol. PP, pp. 1-1, 2017.

[25] J. H. Reed, *An Introduction to Ultra Wideband Communication Systems*. Upper Saddle River, NJ: Prentice Hall PTR, 2005.

[26] T. W. Barrett, "History of ultrawideband (UWB) radar & communications: pioneers and innovators," in *Proc. Progress in Electromagnetics Symposium*, 2000, pp. 1-42.

[27] W. Webb, "Ultrawideband: an electronic free lunch," *Dec*, vol. 21, pp. 85-92, 2000.

[28] K. Siwiak and D. McKeown, *Ultra-wideband Radio Technology*. England: John Wiley, Chichester, West Sussex PO19 8SQ, , 2004.

[29] K. Mandke, H. Nam, L. Yerramneni, C. Zuniga, and T. Rappaport, "The evolution of ultra wide band radio for wireless personal area networks," *High Frequency Electronics Magazine*, vol. 3, pp. 22-32, Sep. 2003.

[30] G. R. Aiello and G. D. Rogerson, "Ultra-wideband wireless systems," *IEEE Microwave Magazine*, vol. 4, pp. 36-47, Jun. 2003.

[31] H. Alam, "Design of Rectangular Microstrip Patch Antenna for IEEE 802.15. 3a (WPAN) with MB-OFDM Ultra Wide Band Communication System," *International Journal of Scientific and Research Publications*, vol. 4, 2014.

[32] A. Batra, J. Balakrishnan, G. R. Aiello, J. R. Foerster, and A. Dabak, "Design of a multiband OFDM system for realistic UWB channel environments," *IEEE Transactions on Microwave theory and techniques*, vol. 52, pp. 2123-2138, 2004.

[33] A. Batra, "Multi-band OFDM physical layer proposal for IEEE 802.15 task group 3a," *IEEE P802. 15-03/268r3*, 2004.

[34] R. Yang and R. S. Sherratt, "Multiband OFDM modulation and demodulation for ultra wideband communications," in *novel applications of the UWB technologies*, ed: InTech, 2011.

[35] N. Bradai, L. Chaari, and L. Kamoun, "A comprehensive overview of wireless body area networks (WBAn)," *Digital Advances in Medicine, E-Health, and Communication Technologies*, vol. 1, 2013.

[36] Jeff Foerster, Evan Green , Srinivasa Somayazulu , and D. Leeper, "Ultra-wideband technology for short-or medium-range wireless communications," *Intel Technology Journal,* 2001.

[37] D. G. Leeper, "A long-term view of short-range wireless," *IEEE Computer Magazine,* vol. 34, pp. 39-44, 2001.

[38] B. Kelland. (10/12/2002). *Ultra-Wideband Wireless Technology*. Available: http://mms.ecs.soton.ac.uk/mms2003/papers/32.pdf

[39] H.-W. Wu and Y.-F. Chen, "Ultra wideband bandpass filter with dual-notched bands using stub-loaded rectangular ring multi-mode resonator," *Microelectronics Journal,* vol. 43, pp. 257-262, 4// 2012.

[40] D. C. Laney, *Modulation, coding and RF components for ultra-wideband impulse radio*: Ph.D., University of California, San Diego, 2003.

[41] D. Cabric, M. S. W. Chen, D. A. Sobel, Y. Jing, and R. W. Brodersen, "Future wireless systems: UWB, 60GHz, and cognitive radios," in *Proceedings of the IEEE 2005 Custom Integrated Circuits Conference, 2005.*, 2005, pp. 793-796.

[42] D. Cabric, M. S. Chen, D. A. Sobel, S. Wang, J. Yang, and R. W. Brodersen, "Novel radio architectures for UWB, 60 GHz, and cognitive wireless systems," *EURASIP Journal on Wireless Communications and Networking,* vol. 2006, pp. 22-22, 2006.

[43] C. Park and T. S. Rappaport, "Short-Range Wireless Communications for Next-Generation Networks: UWB, 60 GHz Millimeter-Wave WPAN, And ZigBee," *IEEE Wireless Communications,* vol. 14, pp. 70-78, 2007.

[44] J. Zhang, P. V. Orlik, Z. Sahinoglu, A. F. Molisch, and P. Kinney, "UWB Systems for Wireless Sensor Networks," *Proceedings of the IEEE,* vol. 97, pp. 313-331, 2009.

[45] C. Xiaoli and R. D. Murch, "The effect of NBI on UWB time-hopping systems," *Wireless Communications, IEEE Transactions on,* vol. 3, pp. 1431-1436, 2004.

[46] S. Stroh, "Ultra-Wideband: multimedia unplugged," *Spectrum, IEEE,* vol. 40, pp. 23-27, 2003.

[47] N. Cravotta. (Oct. 2002) Ultra wideband: the next wireless panacea? *Techtrends Magazine*. 51-58.

[48] M. Hamalainen, R. Tesi, and J. Iinatti, "On the UWB system performance studies in AWGN channel with interference in UMTS band," in *2002 IEEE Conference on Ultra Wideband Systems and Technologies (IEEE Cat. No.02EX580)*, 2002, pp. 321-325.

[49] S. P. Team, "Ultra Wideband (UWB) A Background Brief," pp. 1-16.

[50] S. Lee, "Design and analysis of ultra-wide bandwidth impulse radio receiver," UNIVERSITY OF SOUTHERN CALIFORNIA, Aug. 2002.

[51] L. E. Miller, "Why UWB? A review of ultrawideband technology," *National Institute of Standards and Technology, DARPA,* pp. 1-72, April 2003.

[52] I. Oppermann, M. Hämäläinen, and J. Iinatti, *UWB: Theory and Applications*. England: John Wiley, 2004.

[53] M. Hamalainen, V. Hovinen, R. Tesi, J. H. J. Iinatti, and M. Latva-aho, "On the UWB system coexistence with GSM900, UMTS/WCDMA, and GPS," *Selected Areas in Communications, IEEE Journal on,* vol. 20, pp. 1712-1721, 2002.

[54] R. Tesi, "Ultra wideband system performance in the presence of interference," *Licentiate Thesis, Department of Electrical and Information Engineering, University of Oulu, Oulu, Finland,* 2004.

[55] H. Hashemi, "Impulse response modeling of indoor radio propagation channels," *Selected Areas in Communications, IEEE Journal on,* vol. 11, pp. 967-978, 1993.

[56] J. R. Foerster, M. Pendergrass, and A. F. Molisch, "A channel model for ultrawideband indoor communication," in *International Symposium on Wireless Personal Multimedia Communication*, 2003.

[57] A. F. Molisch, "Ultra-Wide-Band Propagation Channels," *Proceedings of the IEEE*, vol. 97, pp. 353-371, 2009.

[58] S. Soonyong, Y. Kunmin, K. Youngil, and R. Won, "Symbol detection under multi-path fading environments for ZigBee receiver," in *2013 International Conference on ICT Convergence (ICTC)*, 2013, pp. 84-85.

[59] M. D. Lin, L. Fansheng, and S. Jie, "Simulation on Multi-path Fading in Wireless Channel," in *2012 International Conference on Computer Science and Electronics Engineering*, 2012, pp. 427-429.

[60] H. El-Sallabi, M. Abdallah, and K. Qaraqe, "Modelling of parameters of Rician fading distribution as a function of polarization parameter in reconfigurable antenna," in *2014 IEEE/CIC International Conference on Communications in China (ICCC)*, 2014, pp. 534-538.

[61] S. Sar, imath, taş, B. Dulek, A. D. Sezer, S. Gezici, *et al.*, "Optimal Power Allocation for Average Detection Probability Criterion Over Flat Fading Channels," *IEEE Transactions on Signal Processing*, vol. 65, pp. 1383-1398, 2017.

[62] H. Bai and M. Atiquzzaman, "Error modeling schemes for fading channels in wireless communications: A survey," *Communications Surveys & Tutorials, IEEE*, vol. 5, pp. 2-9, 2003.

[63] T. S. Rappaport, *Wireless communications: principles and practice* vol. 2: prentice hall PTR New Jersey, 1996.

[64] L. Agba, F. Gagnon, and A. Kouki, "Small-scale fading modeling for tactical ad hoc networks," in *2006 12th International Symposium on Antenna Technology and Applied Electromagnetics and Canadian Radio Sciences Conference*, 2006, pp. 1-5.

[65] T. S. Rappaport, *Wireless communications: principles and practice* vol. 2: prentice hall PTR New Jersey, 2002.

[66] T. S. Rappaport, K. Blankenship, and H. Xu, "Propagation and radio system design issues in mobile radio systems for the glomo project," *Mobile and portable radio research group, Virginia Polytechnic Institute and State University,* vol. 31, 1997.

[67] T. Staff, "Propagation Overview for TM-UWB System," 2005.

[68] K. Guan, Z. Zhong, B. Ai, C. Briso-Rodríguez, and L. Zhang, "Large scale fading characteristics in rail traffic scenarios," in *2015 IEEE International Symposium on Antennas and Propagation & USNC/URSI National Radio Science Meeting*, 2015, pp. 83-84.

[69] M. B. Hcine and R. Bouallegue, "Exact evaluation of outage probability in correlated lognormal shadowing environment," in *2015 13th International Symposium on Modeling and Optimization in Mobile, Ad Hoc, and Wireless Networks (WiOpt)*, 2015, pp. 545-552.

[70] W. Zhuang, X. Shen, and Q. Bi, "Ultra-wideband wireless communications," *Wireless Communications and Mobile Computing*, vol. 3, pp. 663-685, 2003.

[71] J. G. Proakis, "Digital Communications," 4 ed: McGraw-Hill Companies, Inc., New York, NY, 2001.

[72] G. S. Prabhu and P. Mohana Shankar, "Simulation of flat fading using MATLAB for classroom instruction," *Education, IEEE Transactions on*, vol. 45, pp. 19-25, 2002.

[73] P. S. Bithas, K. Maliatsos, and A. G. Kanatas, "The Bivariate Double Rayleigh Distribution for Multichannel Time-Varying Systems," *IEEE Wireless Communications Letters*, vol. 5, pp. 524-527, 2016.

[74] X. Jian, X. Zeng, A. Yu, C. Ye, and J. Yang, "Finite series representation of Rician shadowed channel with integral fading parameter and the associated exact performance analysis," *China Communications*, vol. 12, pp. 62-70, 2015.

[75] W. Wu, H. Guo, and X. Li, "Nonstationary target detection method based on Rician distribution," in *2012 IEEE International Geoscience and Remote Sensing Symposium*, 2012, pp. 6841-6843.

[76] P. M. Shankar, "A compound scattering pdf for the ultrasonic echo envelope and its relationship to K and Nakagami distributions," *IEEE Transactions on Ultrasonics, Ferroelectrics, and Frequency Control*, vol. 50, pp. 339-343, 2003.

[77] P. M. Shankar, "A model for ultrasonic scattering from tissues based on the K distribution," *Physics in medicine and biology*, vol. 40, p. 1633, 1995.

[78] P. M. Shankar, "A general statistical model for ultrasonic backscattering from tissues," *IEEE Transactions on Ultrasonics, Ferroelectrics, and Frequency Control*, vol. 47, pp. 727-736, 2000.

[79] R. Mitra, A. K. Mishra, and T. Choubisa, "Maximum likelihood estimate of parameters of Nakagami-m distribution," in *2012 International Conference on Communications, Devices and Intelligent Systems (CODIS)*, 2012, pp. 9-12.

[80] S. Singh and Y. M. Tripathi, "Bayesian Estimation and Prediction for a Hybrid Censored Lognormal Distribution," *IEEE Transactions on Reliability*, vol. 65, pp. 782-795, 2016.

[81] S. Kotz, N. Balakrishnan, and N. L. Johnson, *Continuous multivariate distributions*, 2 ed.: John Wiley & Sons, 2000.

[82] J. Zhilong, Y. Junyi, Z. Ran, K. Yang, and C. Wei, "Experimental multipath delay spread and path loss analysis for the indoor environment at 5.9 GHz," in *2016 International Conference on Wireless Communications, Signal Processing and Networking (WiSPNET)*, 2016, pp. 1859-1863.

[83] D. Cassioli, W. Ciccognani, and A. Durantini, "Uwb channel model report," *ULTRAWAVES (IST-2001-35189), Document D*, vol. 3, p. 2003, 2003.

[84] K. Jong Ho, "The multipath delay spread model for the LOS case in urban areas," in *2007 6th International Conference on Information, Communications & Signal Processing*, 2007, pp. 1-4.

[85] E. M. Shaheen and M. El-Tanany, "The impact of narrowband interference on the performance of UWB systems in the IEEE802.15.3a channel models," in *CCECE 2010*, 2010, pp. 1-6.

[86] A. F. Molisch, J. R. Foerster, and M. Pendergrass, "Channel models for ultrawideband personal area networks," *IEEE Wireless Communications*, vol. 10, pp. 14-21, 2003.

[87] J. Foerster and Q. Li, "UWB channel modeling contribution from intel IEEE P802. 15 wireless personal area networks," *IEEE P802*, pp. 15-02, 2002.

[88] M. Pendergrass, "Empirically based statistical ultra-wideband channel model," *IEEE P802. 15-02/240-SG3a*, 2002.

[89] J. Kunisch and J. Pamp, "Radio channel model for indoor UWB WPAN environments," *IEEE P802. 15-02/281-SG3a*, 2002.

[90] D. Cassioli, M. Z. Win, and A. F. Molisch, "The ultra-wide bandwidth indoor channel: from statistical model to simulations," *Selected Areas in Communications, IEEE Journal on*, vol. 20, pp. 1247-1257, 2002.

[91] R. Hidayat and Y. Miyanaga, "IR-UWB Pulse Position Modulation and Pulse Shape Modulation Through S-V Channel Model," in *2010 Second International Conference on Communication Software and Networks*, 2010, pp. 214-217.

[92] I. Bergel, E. Fishler, and H. Messer, "Narrowband interference suppression in time-hopping impulse-radio systems," in *2002 IEEE Conference on Ultra Wideband Systems and Technologies (IEEE Cat. No.02EX580)*, 2002, pp. 303-307.

[93] L. Qinghua and L. A. Rusch, "Hybrid RAKE/multiuser receivers for UWB," in *Radio and Wireless Conference, 2003. RAWCON '03. Proceedings*, 2003, pp. 203-206.

[94] K. Mandke, H. Nam, L. Yerramneni, and C. Zuniga, "The evolution of UWB and IEEE 802.15. 3a for very high data rate WPAN," *EE 381K-11 Wireless Communications UWB Group, The University of Texas at Austin*, 2003.

[95] S. Kazimierz and M. Debra, *Ultra-wideband Radio Technology*: Wiley, 2005.

[96] N. C. Beauliea, "The evaluation of error probabilities for intersymbol and cochannel interference," *Communications, IEEE Transactions on*, vol. 39, pp. 1740-1749, 1991.

[97] R. L. Pickholtz, D. L. Schilling, and L. B. Milstein, "Theory of Spread-Spectrum Communications--A Tutorial," *Communications, IEEE Transactions on*, vol. 30, pp. 855-884, 1982.

[98] I. J. Meel. (Oct. 1999). *Spread Spectrum (SS) Introduction, (DE NAYER institute, Belgium 6th*

ed.). Available: http://www.sss-mag.com/pdf/Ss_jme_denayer_intro_print.pdf

[99] R. L. Peterson, R. E. Ziemer, and D. E. Borth, *Introduction to Spread-spectrum Communications*: Prentice Hall, 1995.

[100] Y. P. Nakache and A. F. Molisch, "Spectral Shape of UWB Signals - Influence of Modulation Format, Multiple Access Scheme and Pulse Shape," in *The 57th IEEE Semiannual Vehicular Technology Conference, 2003. VTC 2003-Spring.*, 2003, pp. 2510-2514 vol.4.

[101] B. Mihai. *Ultra Wide Band Technology*. Available: http://www.tml.tkk.fi/Studies/T-110.557/2002/papers/burlacu_mihai.pdf

[102] A. F. Molisch, J. Zhang, and M. Miyake, "Time hopping and frequency hopping in ultrawideband systems," in *2003 IEEE Pacific Rim Conference on Communications Computers and Signal Processing (PACRIM 2003) (Cat. No.03CH37490)*, 2003, pp. 541-544 vol.2.

[103] (Nov, 2005). *Time Modulated Ultra-Wideband Technology*. Available: http://www.timedomain.com

[104] P. C. Li. (2003) Challenges for A/V Streaming Over Wireless LAN. [ECN].

[105] J. Ibrahim, "Notes on Ultra Wideband Receiver Design," ed: April, April. 2004.

[106] A. TALESARA, "SIMULATION/ANALYSIS OF MODULATION SCHEMES FOR UWB IN PRESENCE OF MULTIPATH AND MUI," MSc, Electronic Thesis or Dissertation, May, 2003.

[107] H. Mei, "Modeling and Performance Evaluation of a BPPM UWB System," MSc, July 2003.

[108] A. M. Orndorff, "Transceiver Design for Ultra-Wideband Communications," MSc, May 2004.

[109] C. Xiaomin and S. Kiaei, "Monocycle shapes for ultra wideband system," in *Circuits and Systems, 2002. ISCAS 2002. IEEE International Symposium on*, 2002, pp. I-597-I-600 vol.1.

[110] G. Durisi and G. Romano, "On the validity of Gaussian approximation to characterize the multiuser capacity of UWB TH PPM," in *Ultra Wideband Systems and Technologies, 2002. Digest of Papers. 2002 IEEE Conference on*, 2002, pp. 157-161.

PUBLICATIONS

[1] H. Mosa, M. Hope, "The Effects of Varying System Parameters on the Performance of TH-PPM UWB Systems", 15th Postgraduate Symposium on the Convergence of Telecommunication, Networking and Broadcasting, June 2014.

[2] H. Mosa, M. Hope, "Optimising Time-Hopping Pulse Position Modulation in Ultra wide Band Systems", 'Poster', Dean's Research showcase conferences 2015. Salford, UK.

[3] Hasan Mosa, Martin Hope, "PERFORMANCE OF PULSE POSITION MODULATION FOR ULTRA WIDE BAND SYSTEM USING TIME-HOPPING TECHNIQUES IN MULTIPLE ACCESS ENVIRONMENTS", SPARC 2016, Salford, UK.

[4] Hasan Mosa, Martin Hope, "A POWERFUL ANALYSIS FOR CALCULATING BER OF TH-PPM SYSTEM", 2017.

APPENDICES

APPENDIX-A [2] : UWB Spectrum Emission Limits

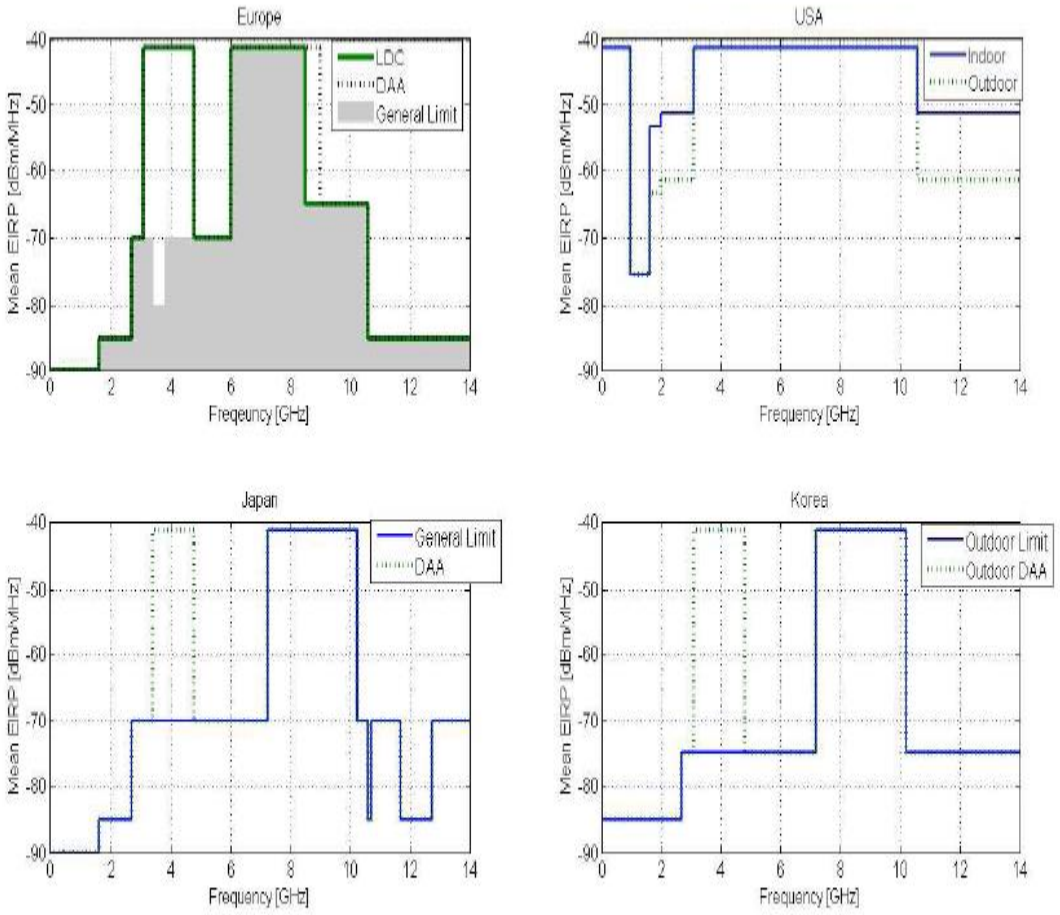

UWB spectrum emission limits
331x188mm (96 x 96 DPI)

APPENDIX-B : IEEE 802 Standards

Standard	Description
802.1	LAN (Architecture, Bridging, High Level, Interface
802.2	LAN (LLC) Local Link Control Sub Layer
802.3	LAN (CSMA/CD Ethernet) Carrier Sense Multiple Access with Collision Detection
802.4	Token Bus Arcnet (Ethernet) LAN
802.5	Token Ring (IBM Ring) LAN
802.6	Queued Packet Synchronous Exchange (QPSX) MAN
802.7	Broad Band NW
802.8	Optical Fiber Technology LAN, MAN
802.9	Integrated voice and data LAN working group ISDN
802.10	LAN Security group
802.11	Wireless LAN, Wi-Fi
802.12	Demand Priority
802.14	Cable Modem (Through Cable TV)
802.15	Short Range Radio WPAN (UWB, Blue Tooth)
802.16	WMAN Wi-MAX or HIPERMAN
802.17	Resilient Packet Ring (RPR)
802.18	Radio Regulatory Technical Advisory Group (RR-TAG)
802.20	Mobile Broad Band Wireless Access

APPENDIX-C : DIFFERENT UWB MONOCYCLE SHAPES

The frequency-domain spectral content of a UWB signal depends on the pulse waveform shape and the pulse width. Typical pulse waveforms used in research include rectangular, Gaussian, Gaussian doublet, and Rayleigh monocycles, etc. A monocycle should have zero DC component to allow it to radiate effectively. In fact, to satisfy the UWB emission constraint specified in FCC regulation, the desired frequency spectrum of the monocycle waveform should be flat over a target bandwidth not including the zero frequency. A rectangular monocycle with width τ_p and unity energy can be represented by:

$$\sqrt{\frac{1}{\tau_p}}\left[U(t)-U(t-\tau_p)\right]$$

Where $U(.)$ denotes the unit step function. The rectangular pulse has a large DC component, which is not a desired property. Even so, the rectangular monocycle has often been used in academic research because of its simplicity. A generic Gaussian pulse is given by:

$$p_g(t)=\frac{1}{\sqrt{2\pi}\sigma}\exp\left[-\frac{1}{2}\left(\frac{t-\mu}{\sigma}\right)^2\right]$$

Where μ defines the center of the pulse and σ determines the width of the pulse. Some popular monocycles are derived from the Gaussian pulse. The Gaussian monocycle is the second derivative of a Gaussian pulse, and is given by:

$$p_G(t) = A_G\left[1-\left(\frac{t-\mu}{\sigma}\right)^2\right]\exp\left[-\frac{1}{2}\left(\frac{t-\mu}{\sigma}\right)^2\right]$$

Where the parameter σ determines the monocycle width τ_p. The effective time duration of the waveform that contains 99.99% of the total monocycle energy is $\tau_p = 7\sigma$ centered at $\mu = 3.5\sigma$. The factor A_G is introduced so that the total energy of the monocycle is normalised to unity, i.e. $\int p_G^2(t)dt = 1$. The frequency spectrum of the Gaussian monocycle is:

$$P_G(f) = A_G\sqrt{2\pi}\sigma(2\pi\sigma f)^2\exp\left[-\frac{1}{2}(2\pi\sigma f)^2\right]\times\exp(-j2\pi f\mu)$$

The Gaussian doublet is a bipolar signal, consisting of two amplitude reversed Gaussian pulses with a time gap of T_w between the two pulses. The mathematical expression for the monocycle is:

$$p_{GD}(t) = A_{GD}\left\{\exp\left[-\frac{1}{2}\left(\frac{t-\mu}{\sigma}\right)^2\right]-\exp\left[-\frac{1}{2}\left(\frac{t-\mu-T_w}{\sigma}\right)^2\right]\right\}$$

which has a Fourier transform given by

$$P_{GD}(f) = 2A_{GD}\sqrt{2\pi}\sigma \sin(\pi f T_w)\exp\left[-\frac{1}{2}(2\pi\sigma f)^2\right] \times \exp\{-j[2\pi f(\mu + 0.5T_w - 0.5\pi)]\}$$

The pulse width is determined by the parameters μ, σ *and* T_w. The truncated pulse with $T_p = 14\sigma$ for $T_w = 7\sigma$ contains 99.99% of the total monocycle energy.

The Rayleigh monocycle is derived from the first derivative of the Gaussian pulse and is given by:

$$p_R(t) = A_R\left[\frac{t-\mu}{\sigma^2}\right]\exp\left[-\frac{1}{2}\left(\frac{t-\mu}{\sigma}\right)^2\right]$$

With the Fourier transform

$$P_R(f) = A_R\sqrt{2\pi}(2\pi\sigma f)\exp\left[-\frac{1}{2}(2\pi\sigma f)^2\right] \times \exp[-j(2\pi f\mu + 0.5\pi)]$$

The effective time duration of the waveform that contains 99.99% of the total monocycle energy is $T_p = 7\sigma$ centered at $\mu = 3.5\sigma$, which is the same as that of the Gaussian monocycle.

Different from the rectangular waveform, an important feature of the above monocycles is that they do not have a DC component, which makes the radiation of the monocycles more efficient. Figure C-1 shows the UWB monocycles and their frequency spectra in dB, where the maximum magnitudes of the monocycles and spectra are normalised to unity and 0 dB

respectively. Define the 10-dB bandwidth of the monocycles as $B_{10dB} = f_H - f_L$, where f_H and f_L are the frequencies at which the magnitude spectrum attains $1/\sqrt{10}$ of its peak value, and the nominal center frequency $f_C = (f_H + f_L)/2$. Table 1 lists the 10-dB bandwidth and center frequency for the monocycles, where $T_w = \tau_p = 2$ for the Gaussian doublet. Note that the Gaussian doublet has a larger out-band radiation than the other two monocycles, even though it has a smaller 10-dB bandwidth. Important criteria in designing the monocycle waveform include (a) simplicity of the monocycle generator and (b) minimal interference between the UWB system and other narrowband systems coexisting in the same frequency band.

Table C-1 The 10-dB bandwidth and center frequency of the monocycles

Monocycle	B_{10dB}	f_C
Gaussian	$1.11/T_p$	$1.61/T_p$
Rayleigh	$1.11/T_p$	$1.16/T_p$
Gaussian doublet	$0.83/T_p$	$0.94/T_p$

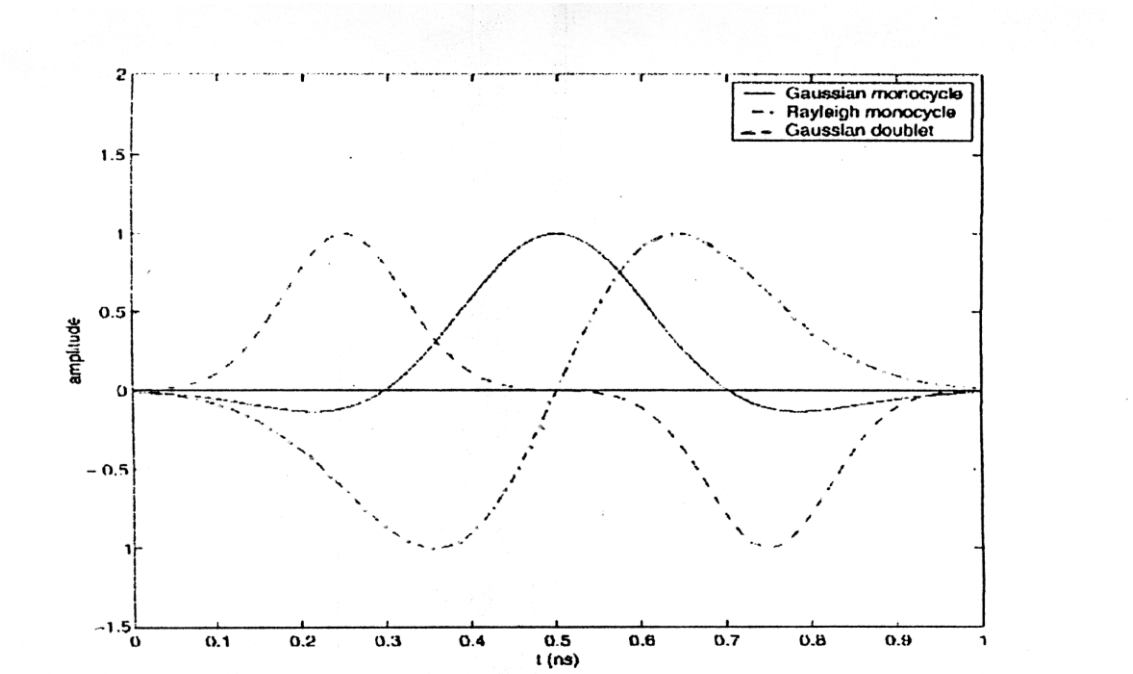

(a) Monocycle waveforms

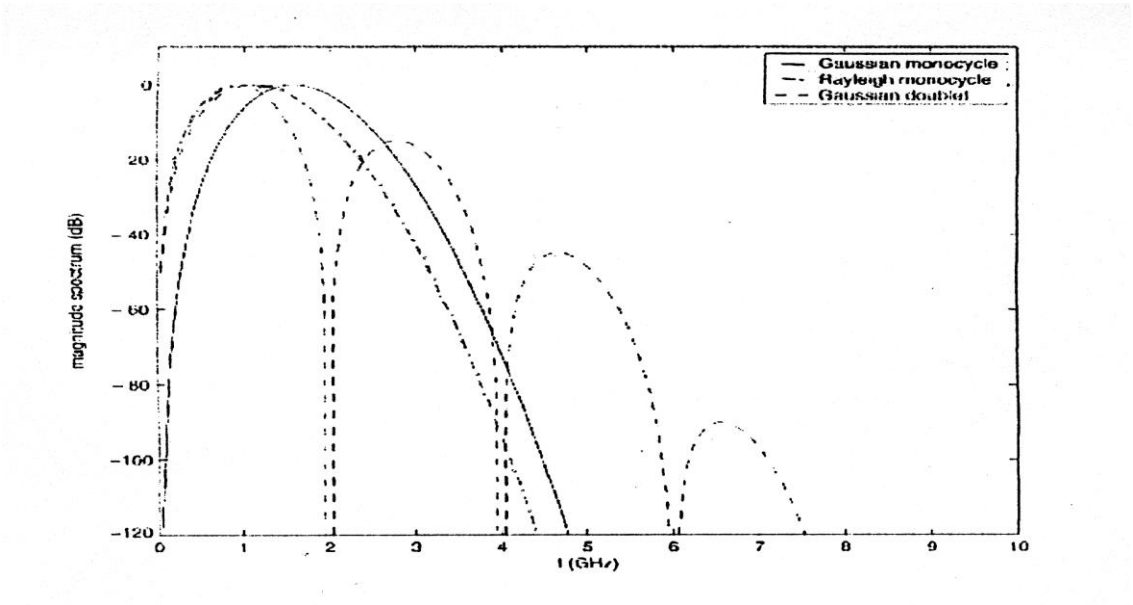

(b) Magnitude spectra

Figure C-1 The waveforms and magnitude spectra of Gaussian monocycle, Rayleigh monocycle and Gaussian doublet with $T_p = 1\,ns$ and $T_w = 0.5\,ns$